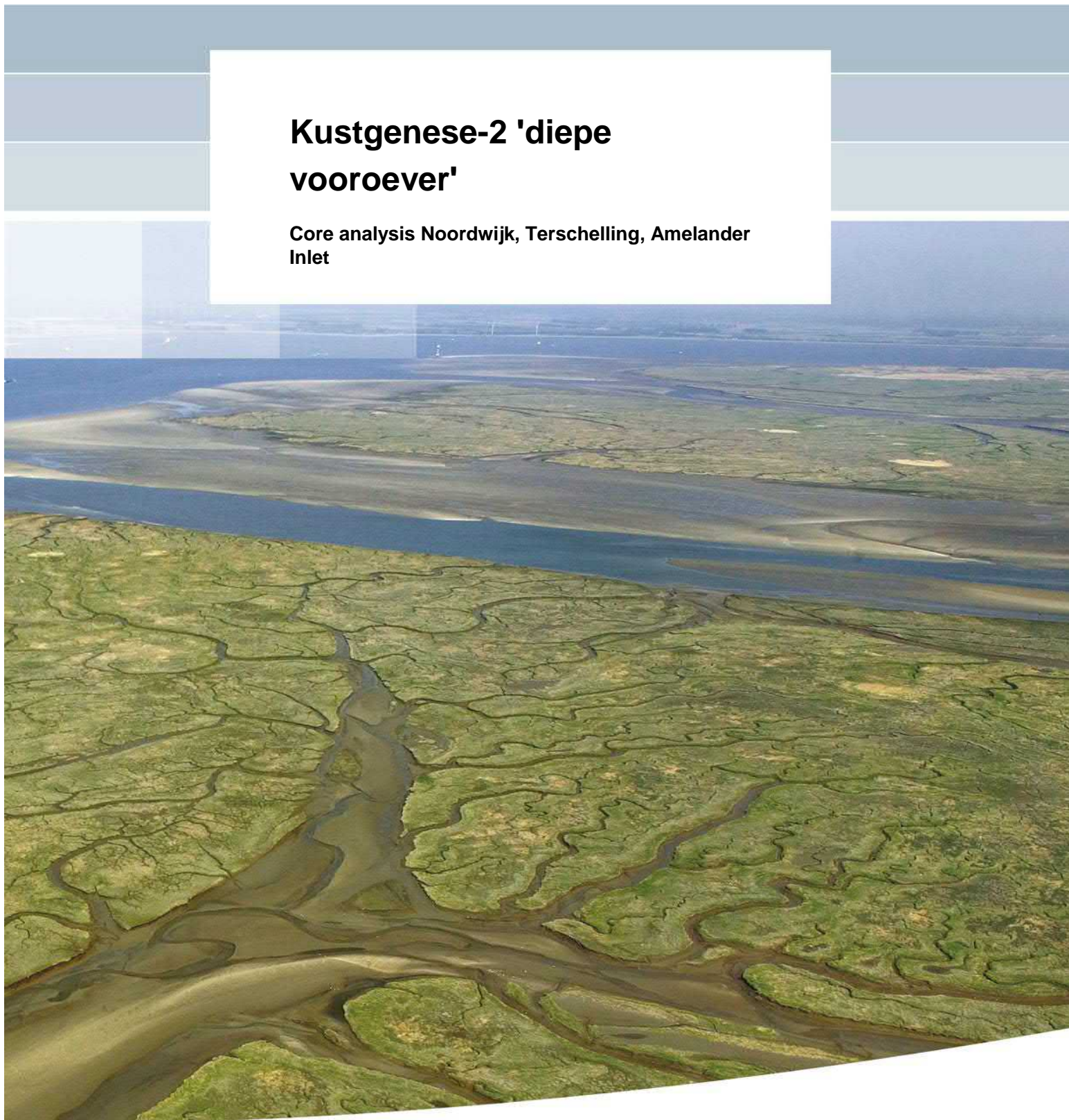


## **Kustgenese-2 'diepe vooroever'**

**Core analysis Noordwijk, Terschelling, Ameland  
Inlet**





## **Kustgenese-2 'diepe vooroever'**

**Core analysis Noordwijk, Terschelling, Ameland Inlet**

Albert Oost  
Andrea Forzoni  
Ad van der Spek  
Tommer Vermaas



## Title

Kustgenese-2 'diepe vooroever'

Client	Project	Attribute	Pages
Rijkswaterstaat Water Verkeer en Leefomgeving	1220339-004	1220339-004-ZKS-0008	82

## Keywords

Kustgenese-2, lower shoreface, diepe vooroever, sedimentology, geology

## Summary

This report is part of the Kustgenese-2 programme “Diepere Vooroever”, which focuses on understanding the morphodynamics and sedimentology of the Dutch lower shoreface in order to sustainably manage the Dutch coastal system and keeping the coast safe. The goal of this research project is gaining insight into the sedimentary built-up of the coast and which processes determine the exchange of sediment between the upper shoreface and the lower shoreface.

To this end, sediment cores (vibrocores and box cores) were collected in three different areas of the Dutch lower shoreface: Noordwijk, Terschelling and Ameland Inlet in 2017 and 2018. The lower shoreface (here taken to be between -6 and -20m) predominantly exists of older Holocene deposits. We interpreted the sediments in terms of facies/depositional environment: lower shoreface deposits, tidal channel deposits, ebb-shield deposits and fluvial deposits.

On top of the older deposits we could distinguish an active layer, based on the higher abundance of shells, the lighter colour and the absence of clay layers and laminae. These features indicate recent, periodical sediment transport on the seabed. From box cores it appears that bioturbation is more dominant over physical reworking during quiet phases and that the reverse is true during periods with higher shear stresses. At all water depths the various sediment layers within the active layer are often separated by an irregular surface, which indicates reworking of the sediments below it. These signify higher energy events and could in a few cases be interpreted as storm events and in at least one case likely as bottom trawling fishery. Next to that, the possibility exists that the surfaces are partially generated during the passage of the troughs of large-scale ripples.

Sand grain size is medium-coarse in the area of Noordwijk and fine-medium in the other two areas, most likely due to different origin of the sands. Grain size analysis shows that in each area there is a zone where the grain size decreases with decreasing depth. This is probably partially determined by the duration of the winnowing processes during the coastal erosion over centuries. The winnowing process itself is probably determined by the tidal forces which decrease with decreasing depth and perhaps a coastward directed bottom residual current which may explain the observed decrease in grain size.

In order to understand the role of the lower shoreface in the (development of the) coastal foundation it is necessary to take into account geological inheritance, selective transport and annual energy fluctuations.

## Title

Kustgenese-2 'diepe vooroever'

Client	Project	Attribute	Pages
Rijkswaterstaat Water Verkeer en Leefomgeving	1220339-004	1220339-004-ZKS-0008	82

## Samenvatting

Dit rapport is een bijdrage aan het Kustgenese 2 project, deelproject “Diepere Vooroever” dat zich richt op het begrijpen van de morfodynamica en sedimentologie van de diepe onderwateroever van de Nederlandse kust. Deze kennis vormt de basis voor duurzaam beheer van de kust en voor het handhaven van de kustveiligheid. Het doel van dit onderzoek is meer inzicht verwerven in de sedimentaire opbouw van de kust en te bepalen welke processen de uitwisseling van sediment tussen de diepe en ondiepe vooroever bepalen.

Hiertoe is de dieper onderwateroever (ca. -6 tot -20m) bemonsterd op drie verschillende locaties langs de Nederlandse kust, te weten Noordwijk, Terschelling en het Amelanders Zeegat, met behulp van vibro- en box cores in 2017/2018. De aangetroffen afzettingen zijn overwegend oudere Holocene afzettingen. Ze zijn ingedeeld op afzettingmilieu: onderwateroever-, getijgeul-, ebschild- en rivier-afzettingen.

Op de oudere afzettingen ligt een dunne actieve laag die kan worden onderscheiden op basis van een hoger percentage schelpen, een lichtere kleur en de afwezigheid van kleilagen en –laagjes. Deze kenmerken wijzen op recent, periodiek transport over de zeebodem. Uit box cores blijkt dat bioturbatie belangrijker wordt tijdens rustige perioden. De fysieke structuren worden vooral gevormd tijdens de perioden welke gekenmerkt worden door hogere schuifspanningen. Op alle waterdiepten worden de verschillende sedimentlagen binnen de actieve laag vaak gescheiden door onregelmatig vlakken, die gepaard gaan met een gedeeltelijke omwerking van de afzettingen. Deze duiden op energierijke gebeurtenissen en konden in een aantal gevallen worden geïdentificeerd als stormen en bodemberoerende visserij. Daarnaast wordt ook rekening gehouden met de mogelijkheid dat deze vlakken worden veroorzaakt door de passage van grootschalige ribbel-troggen.

De gemiddelde korrelgrootte is matig grof bij Noordwijk en matig fijn in de twee andere gebieden, waarschijnlijk door de verschillende herkomst van het zand. Uit de korrelgrootte analyse blijkt dat er in elk gebied sprake is van een zone waar de korrelgrootte afneemt naar ondieper water. Dit wordt waarschijnlijk deels bepaald door de duur van de uitwassingsprocessen gedurende de kust terugtrekking over eeuwen (hoe dieper, hoe langer). Daarnaast zal het uitwassingsproces waarschijnlijk met name bepaald worden door de getijdekrachten die afnemen met afnemende diepte, mogelijk in combinatie met een residuele kustwaartse bodemstroming, waardoor in dieper water alleen de grofste korrels kunnen blijven liggen.

Om de rol van de diepere vooroever voor (ontwikkeling van) het Kustfundament te kunnen begrijpen is het noodzakelijk om de geologische opbouw en ontwikkeling mee te nemen evenals selectief transport en jaarlijkse variaties in energie.

**Title**  
Kustgenese-2 'diepe vooroever'

<b>Client</b>	<b>Project</b>	<b>Attribute</b>	<b>Pages</b>
Rijkswaterstaat Water Verkeer en Leefomgeving	1220339-004	1220339-004-ZKS-0008	82

Version	Date	Author	Initials	Review	Initials	Approval	Initials
0.1	jul. 2019	Albert Oost Andrea Forzoni Ad van der Spek Tommer Vermaas		Bob Hoogendoorn		Frank Hoozemans	

**Status**  
final



## Contents

<b>1</b>	<b>Introduction</b>	<b>1</b>
1.1	Kustgenese-2	1
1.2	The Dutch lower shoreface	1
1.3	Objectives	2
1.4	Research areas	3
<b>2</b>	<b>Methods</b>	<b>5</b>
2.1	Data collection	5
2.2	Core and laquer profile analyses	8
2.2.1	Vibrocores collected in 2017	8
2.2.2	Round box cores collected in 2017	8
2.2.3	Rectangular box cores collected in 2018	8
<b>3</b>	<b>Vibrocores- sedimentology and geology</b>	<b>11</b>
3.1	Geological units	11
3.2	Borehole description	11
3.2.1	Ameland Inlet research area	11
3.2.2	Terschelling research area	15
3.2.3	Noordwijk	17
3.3	Geological cross-sections	21
3.3.1	Ameland Inlet research area	21
3.3.2	Terschelling research area	23
3.3.3	Noordwijk research area	25
3.4	Thickness analysis of the shoreface deposits active layer	27
<b>4</b>	<b>Box core descriptions</b>	<b>31</b>
4.1	Introduction	31
4.2	Box cores Ameland area	31
4.2.1	Introduction	31
4.2.2	Description of the observations on round box cores 2017	31
4.2.3	Description of the observations box cores 2018	34
4.2.4	Interpretation	43
4.3	Box cores Terschelling research area	44
4.3.1	Introduction	44
4.3.2	Description of the observations round box cores 2017	44
4.3.3	Description of the observations rectangular box cores 2018	46
4.3.4	Interpretation	54
4.4	Box cores Noordwijk research area	54
4.4.1	Introduction	54
4.4.2	Description of the observations on round box cores 2017	54
4.4.3	Description of the observations of the rectangular box cores of 2018	58
4.4.4	Interpretation	66
<b>5</b>	<b>Discussion: integration of observations</b>	<b>69</b>
5.1	Introduction	69
5.2	Ameland area	69
5.3	Terschelling research area	70

5.4	Noordwijk research area	71
5.5	Comparing the various study areas	72
5.6	An answer to research questions	74
<b>6</b>	<b>Conclusions</b>	<b>77</b>
<b>7</b>	<b>Recommendations</b>	<b>79</b>
<b>8</b>	<b>References</b>	<b>81</b>
	<b>Appendices</b>	
<b>A</b>	<b>Appendix A</b>	<b>A-1</b>
<b>B</b>	<b>Appendix B</b>	<b>B-1</b>

# 1 Introduction

## 1.1 Kustgenese-2

The Dutch coastal policy aims for a safe, economically strong and attractive coast. In order to achieve this, the coast and the shoreface are maintained with sand nourishments. The nourished maintenance zone is called 'coastal foundation'. The offshore boundary of the coastal foundation is set at the -20m depth contour, while the onshore limit is formed by the landward boundary of the coastal dune area and by the shortest line through the tidal inlets (open coast).

In 2020 the Dutch Ministry of Infrastructure and Water Management will decide on the future annual nourishment volume, considering the impact of climate change. The Kustgenese-2 (KG2) programme is aimed to generate knowledge to support this decision process. The subproject "Diepere Vooroever" (DV, i.e., lower shoreface) of the KG2 programme, commissioned by Rijkswaterstaat to Deltares, focuses on two main questions:

- What are possibilities for an alternative offshore boundary of the coastal foundation?
- And more generic: How much sediment is required for the coastal foundation to grow with sea level rise?

These questions have been translated into several more detailed, research questions. The present report studies the sedimentology of the Dutch lower shoreface and as such contributes to the following research questions underlying main question 1:

*Which part of the coastal profile below MSL actively contributes to the stability of the coast?*

With underlying research questions:

- a) What is the sedimentary built-up of the coast, in terms of bed forms, sedimentary structures, bottom profiles and grain-size distributions?
- b) Which processes determine the exchange of sediment between the shoreface and the North Sea bed and what is their frequency of occurrence and their contribution?
- c) In which subareas (or zones) can the coastal profile be subdivided, which are similar in (stability) of the profile, sedimentary built up and dynamics?

More background information and a detailed description of definitions can be found in the literature study report of the "Diepe Vooroever" subproject (Van der Werf et al. 2017). All depths are given with reference to NAP (Dutch Ordinance Level), which is approximately mean sea level.

## 1.2 The Dutch lower shoreface

The shoreface is the area seawards of the low water line that is affected by wave and tidal currents. Along the Dutch coast the lower shoreface is defined as the zone between approx. the -8m and -20m depth contours, with typical bed slopes between 1:200 and 1:1000. The lower shoreface is the zone below fair-weather wave base, where tidal currents and storm waves are predominant. The knowledge about the Dutch lower shoreface is limited. It remains unclear what the relative importance is of the different marine processes such as tides and waves. This knowledge gap is mainly caused by lack of observations.

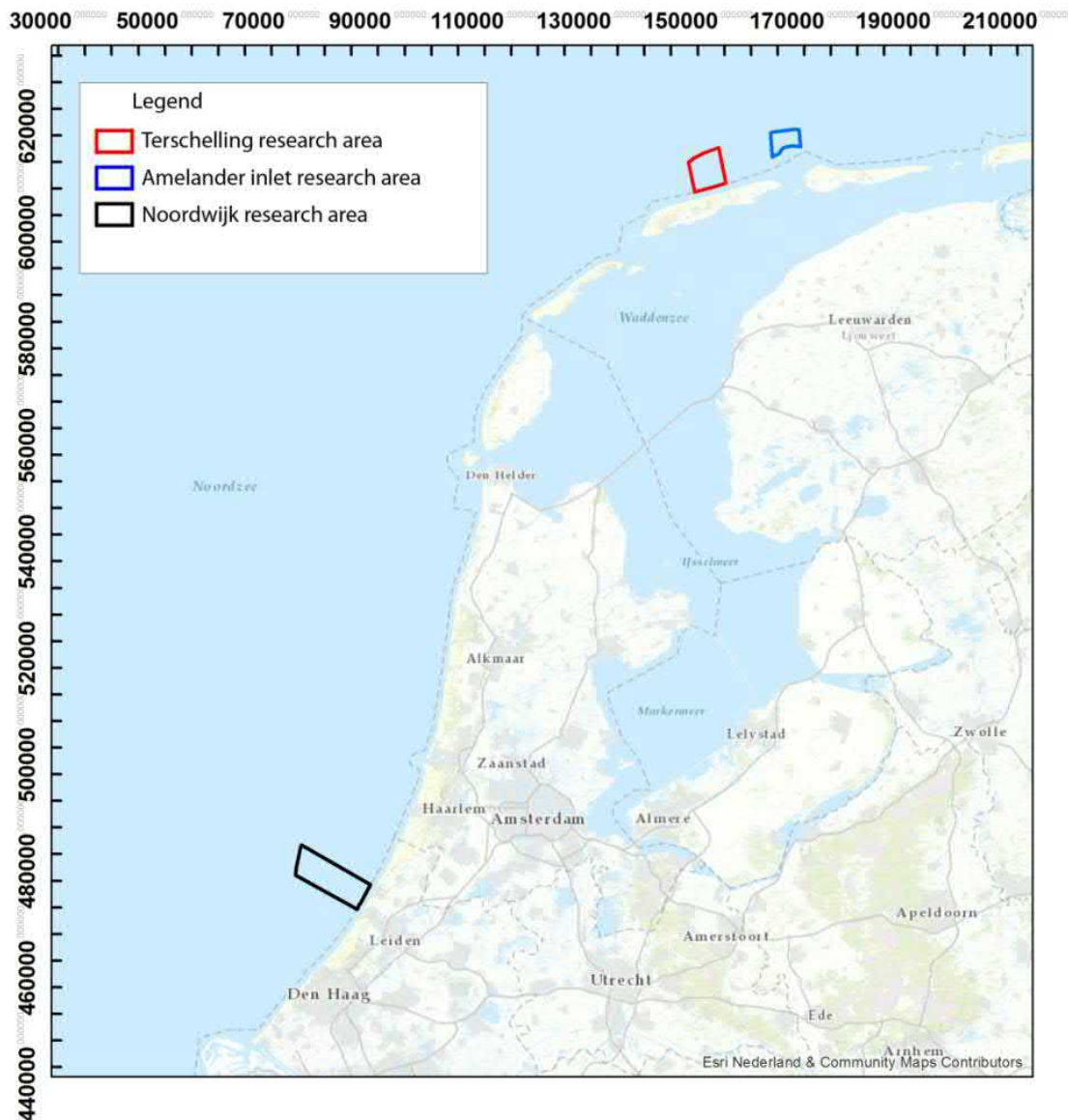


Figure 1.1 Overview map with the three research areas

The impact of marine processes on the seabed can be studied by analysing sediment cores. Onshore sediment cores, preserving Holocene lower shoreface deposits, show sedimentary structures and properties indicating a large impact of storm-generated waves on the lower shoreface at the time of deposition. Borehole data from the present seabed will help to improve our understanding of the dominant marine processes and their relative effect on the erosion, deposition and preservation of the sedimentary deposits on the lower shoreface.

### 1.3 Objectives

Better understanding the role of different (hydrodynamic) processes on the lower shoreface is one of the main objectives for the subproject 'Diepe Vooroever'. This knowledge will help defining the offshore boundary of the coastal foundation and the nourishment volume.

The goal of this study is to determine the physical processes that occur on the lower shoreface, e.g. the relative importance of (storm) wave action for sediment transport in the lower

shoreface, as well as gaining insight in the sedimentary built-up of the Dutch lower shoreface. By analysing the properties and the structures of the sediments on and below the present seabed it is possible to understand the dominant marine processes during deposition.

#### 1.4 Research areas

This report presents the data and description of the vibrocores and box cores from the three research areas along the Dutch coast (Figure 1.1), their analysis, interpretation and integration with existing data. In this report only some results of the multibeam observations of both 2017 and 2018 are discussed. For a full description the reader is referred to the report on the multibeam observations (Oost et al., 2019).

##### **Amelander Inlet research area**

The barrier chain of the Dutch Wadden Sea is considered to have retreated landward over a distance of several km during the past 5000 years (Sha, 1990). The Ameland inlet between Ameland and Terschelling has existed since at least the early middle ages, but probably since Roman times or earlier onwards. Since the 19<sup>th</sup> century it has shifted over more than 1 km to the east. Given the long-time span of known existence, it may be stated that the ebb-tidal delta lobe is a constant feature. On the ebb-tidal delta, erosion and sedimentation alternate due to the lateral shifting of channels and bars and shifts of the delta lobe. The ebb-tidal delta lobe forms a relatively steep slope locally going down from -8 to -16m with a slope of about 1:100. The ebb-tidal delta lobe and the inlet are active morphological features which determine to a large extent the sedimentary development of the area. Only for deeper water (-18 to -20m) their influence is limited. Multibeam observations show that on such depths large tidal ripples are the dominant sedimentary feature.

##### **Terschelling research area**

The coast of Terschelling is part of the barrier island chain of the Wadden Sea. There are many indications from geological observations (e.g. Sha, 1990) that during the Holocene the barrier chain has retreated in a landward direction. At the specific location of the Terschelling research area, nautical maps and historic information indicate that at least since 800 AD the area was part of the shoreface of Terschelling (Oost, 1995). Since at least 1900 the coastal position has been rather stable. The slope of the Terschelling shoreface is gradual; going down only some 7m over a distance of 5 km.

##### **Noordwijk research area**

The Noordwijk area is part of the closed barrier coast of Holland. The sediments present originate to a large extent from earlier fluvial deposits of the river Rhine and tidal channel deposits. The coast at Noordwijk has probably been eroding since Medieval times and retreated over 200-1000m since 1600 AD (Van der Spek et al., 1999). In the lower part of the shoreface connected ridges are present, which, given the above described erosion, also (partially) be formed via erosion.



## 2 Methods

### 2.1 Data collection

Sediment cores have been collected in three areas of the Dutch lower shoreface: Noordwijk, Terschelling and Ameland Inlet (Figure 1.1). The three research areas were selected to get a complete insight of the shoreface and where data from previous measurement campaigns are available (see Van der Werf et al. 2017 for details on the areas).

In 2017 Marine Sampling Holland acquired box cores and vibrocores in the lower shoreface of these areas, at locations indicated by Deltares (Figure 2.1 to Figure 2.3). The sampling was executed during calm weather conditions (which started half-way May) on 3 July 2017 (Noordwijk), 4 July 2017 (Ameland and Terschelling) and 5 July 2017 (Terschelling). Box cores were taken with a round box corer with a maximum penetration depth of 0.6m, the actual sampled depth depends on sediment properties. The box cores were photographed on board, after which three sub cores were taken using pvc liner tube. Moreover, sediment samples were taken of the surface sediment to be analysed in the laboratory. The vibrocores had a maximum length of 5.5m and were divided in 1m pieces, drained and stored vertically. At some locations due to a limited water depth no vibrocore samples were acquired, therefore not all indicated locations were sampled (in total 8 locations were not sampled, of which 2 at Noordwijk, 2 at Terschelling and 4 at Ameland).

Rijkswaterstaat acquired a second batch of 16 rectangular box cores on the following locations (Figure 2.1 to Figure 2.3): Terschelling (4 September 2018), Ameland (5 September 2018) and Noordwijk (6 September 2018). Many of the box cores are situated along shore perpendicular lines at the centre of the research areas. A few were collected in areas of special interest, as identified by analysing the multibeam sonar observations of 2017. The samples were collected after a long quiet period, i.e. no storms, between February and September. Rectangular box cores can be opened at one side, allowing the study of the sedimentary structures in detail (Figure 2.34). Furthermore, lacquer peels were made from these cross-sections, which show even more details. The goal of it was to obtain insight in the sediments and sedimentary structures present. Both are the resultant of the sedimentary built-up, the hydro-morphodynamics and the influence of biota on the sediments. As such, they provide insight in sedimentary development of the shoreface.

In the Ameland inlet research area two rows of rectangular box cores were collected between -8 and -20m water depth, namely AM01 to AM09 and AM10 to AM16 (Figure 2.1).

In the Terschelling research area one row of rectangular box cores was collected, between -12.4 and -19.4m, namely TS01 to TS10. The remainder of the samples (TS11 to TS16) are concentrated in the NW of the area. This is an area of special interest due to the observation on multibeam sonar that large sediment-starved ripples seem to be present there (Figure 2.2).

At Noordwijk, most of the samples (NW01 to NW13) were collected along one profile in the centre of the area, from -11.9m to -18.1m (Figure 2.3). Three other samples (NW14 to NW16) were collected somewhat to the south at water depths of -11.8m to -13.9m. This is an area of special interest where erosional patterns were observed in the area on the multibeam survey data collected in 2017.

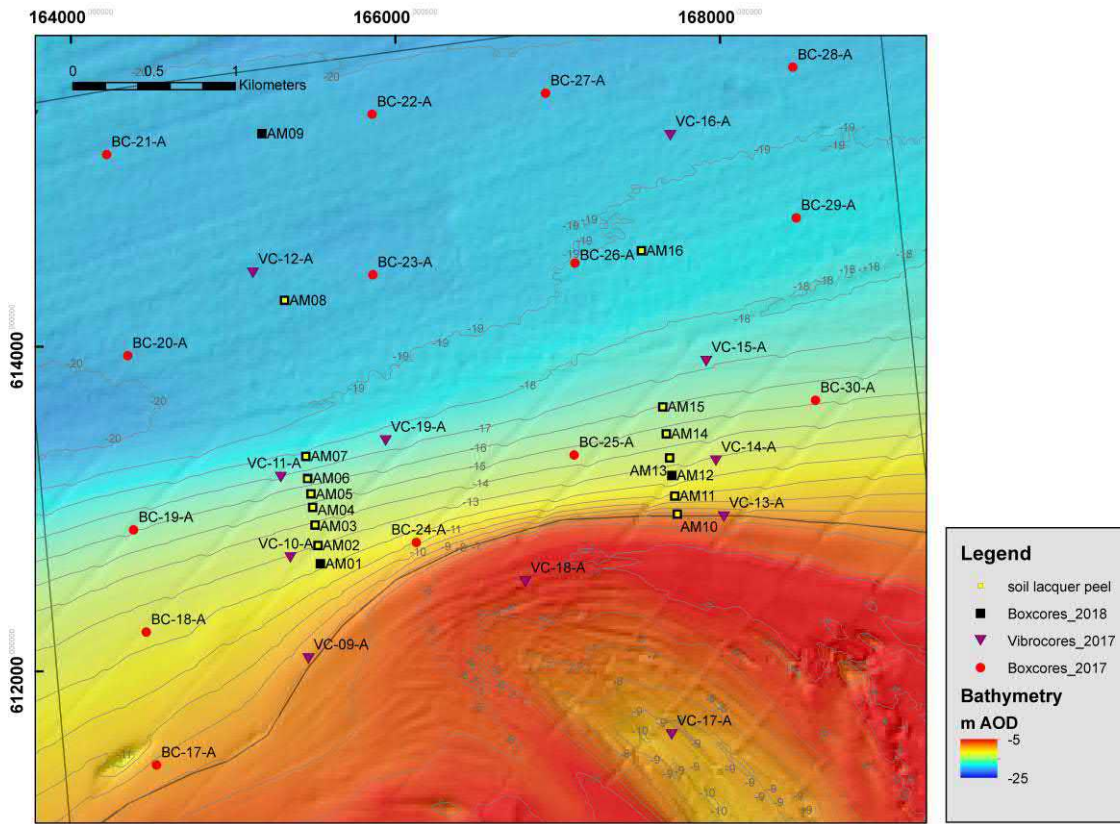


Figure 2.1 Map showing locations for box cores and vibrocores at Ameland Inlet area (bathymetry compilation of depth soundings in the period 2009- 2014).

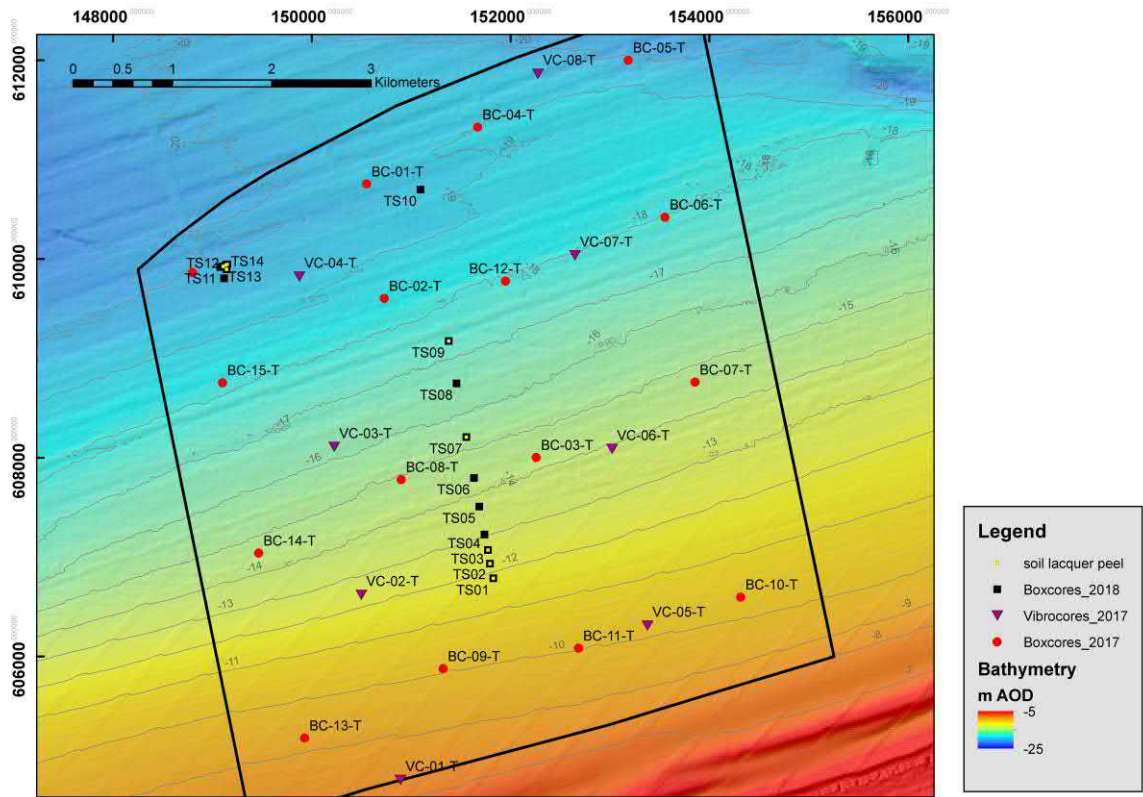


Figure 2.2 Map showing locations for box cores and vibrocores at the Terschelling area (bathymetry compilation of depth soundings in the period 2009- 2014).

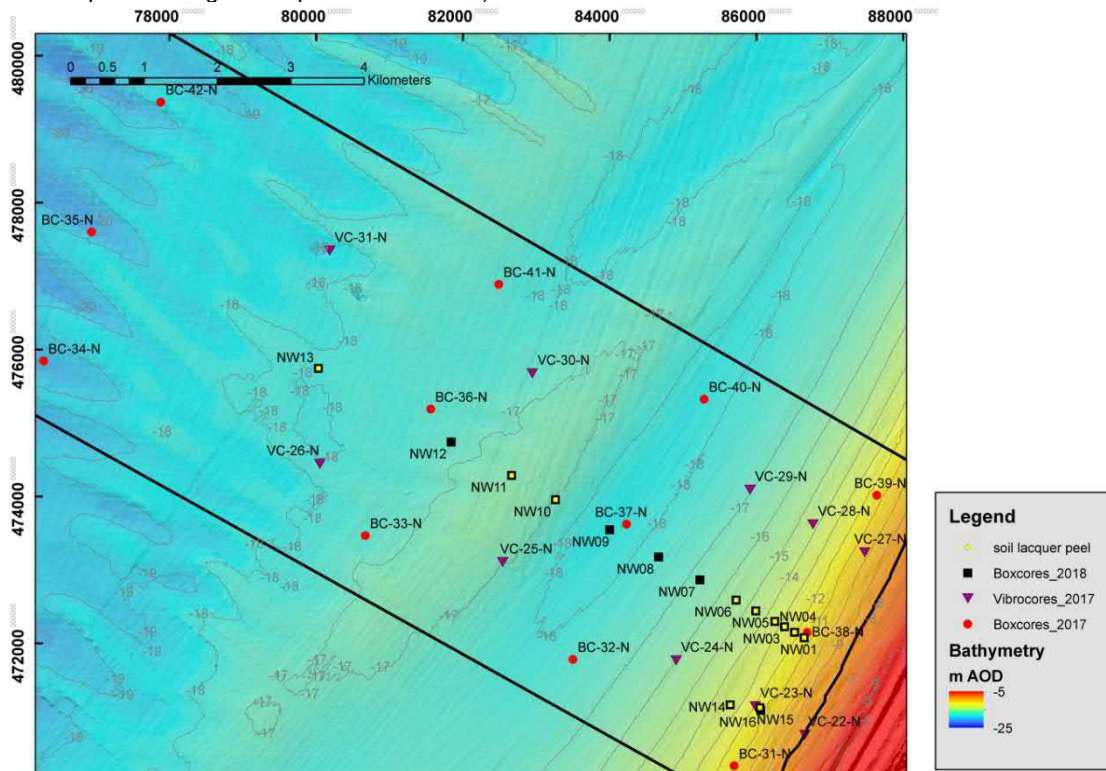


Figure 2.3 Map showing locations for box cores and vibrocores at Noordwijk area (bathymetry compilation of depth soundings in the period 2009- 2014).

## 2.2 Core and laquer profile analyses

### 2.2.1 Vibrocores collected in 2017

The vibrocores were transported to the laboratories of Deltares/TNO -Geological Survey of the Netherlands, where they were opened, photographed and described. Consequently, they were interpreted based on lithology, faunal assemblage of the living and dead shell content, and depositional environment. Grain sizes were visually estimated using a microscope and a sand ruler. This information was used to build geological cross-sections. Analysis and description of sedimentary structures within the active layer, like cross-bedding laminae, was unfortunately not possible, since none were preserved in the cores. In addition to this, we integrated the new data with existing boreholes information from DINOloket (Appendix A). Additional geological cross-sections including both the DINOloket and the new boreholes (Appendix A) were assembled to present the general stratigraphic setting.

### 2.2.2 Round box cores collected in 2017

The sampled subcores of the round box cores were transported to the laboratories of Deltares/TNO -Geological Survey of the Netherlands, where they were opened, photographed and described. Consequently, they were interpreted based on lithology, faunal assemblage of the living and dead shell content, and depositional environment. For the maps of Chapter 3, grain sizes were visually estimated using a microscope and a sand ruler. As this was also done for the vibrocores it was decided to use these data in Chapter 3. A more detailed volumetric grain size analysis of the fraction <2000 microns of the sediment samples taken from the round box cores was made in 2018 with a Malvern laser particle size analyser () and will be presented in Chapter 4. Samples were measured including CaCO<sub>3</sub> and organic matter: no pretreatment using acid and hydrogen peroxide were used. As it appeared that mud showed a different behavior than the sand fraction, it was decided to look separately at the mud fraction and at the sand fraction (63-2000 microns).

### 2.2.3 Rectangular box cores collected in 2018

All rectangular box cores were photographed and described on board of the research vessel and the surface sediments were sampled and analysed. A selection of the box cores was sampled with a small-diameter core (PVC liner), for later checks on grain size and structures, if needed. After opening of the sides of the box cores, lacquer peels of the sediment cross-sectional area were made. The selection criteria for making lacquer peels were representativeness of a certain facies (for instance: heavily bioturbated by sea urchins; Figure 2.4), well-developed sedimentary profile, unique sedimentary profile and position along the cross section. For analysis the lacquer profiles were drawn by hand on a scale 0.5x and photographed (all lacquer peels are presented in Appendix B). The descriptions given below are mainly based on the lacquer profiles. If lacquer profiles were not made the initial description made aboard was used. In the description a short interpretation is given of what the observations indicate. For full details the reader is referred to Chapter 4.



Figure 2.4 Opened rectangular box core Ameland A8, showing bioturbation trace of sea urchin (sea potato) in great detail.

Parameters which are registered for each sample location are: coordinates, water depth, boundary depth of layers, grain-size distribution, and presence of clay layers, erosional boundaries, presence of angular, wavy or parallel bedding, and presence of bioturbation. The presence of living American jack-knife clams (*Ensis leei*; former name: *Ensis directus*), which can survive fast vertical sediment movements, was registered. Also, the presence of a sea urchin which can be quite abundant (up to 20/m<sup>2</sup>), the so-called sea potato (*Echinocardium cordatum*), characteristically found in morphological more quiet areas, were also registered.

The grain-size distribution of the fraction <2000 microns of the sediment samples taken from the rectangular box cores (sampled 2018) was determined with a Malvern laser particle size analysis. The same procedures were followed as for the round box cores. The results of the grain-size analyses are presented in volumetric grain-size distribution curves. As it appeared that mud showed a different behavior than the sand fraction, it was decided to look separately at the mud fraction and at the sand fraction (63-2000 microns).

As stated above, the characteristics of recent sediments (sediment types, size and structures) are the result of local reworking of older sediments deposited in the geological past and supply of sediment from other areas. The sediments show characteristic lateral and vertical alternations of grain sizes that are representative for the formative morphodynamics. The following formative morphodynamics may be important, of which the first 3 mentioned bring about physical structures<sup>1</sup> in the sediments:

- Tide-, wind- and density-gradient driven or wave-induced currents. Depending on grain size and current velocities, physical structures may be anything between parallel bedding (upper or lower stage plane beds), small-scale ripples, large-scale ripples, megaripples, sand waves and shoreface-connected ridges, erosional lags. Characteristics are parallel and large- to small-scale angular laminae (mono- to

<sup>1</sup> The sedimentological term "physical structures" is used to indicate sedimentary structures formed by physical processes, such as currents and wave-action.

multidirectional), erosion surfaces and –if currents decrease enough- layers consisting of finer sediments such as silts and clays.

- Wave-related sediment transport due to the orbital motion under a non-linear wave. Such movements may lead to (asymmetric) wave ripples and to larger scale hummocky cross stratification which is slightly convex over a length of 2-5 m.
- Turbidity-like currents which move down along a slope. Deposits thus formed have been observed in the inner German Bight (Aigner, 1985). Depending on the velocity the following structures may form on top of each other: 1) erosional lower surface, 2) coarser sediments with an upward decrease of grain size (graded layering), 3) parallel laminae (upper stage plane bed), 4) layers with current ripples and cross-bedding, parallel laminae of finer sediments (lower stage plane beds) and unsorted fine sediments on top. However, it should be noted that similar sequences can be formed by sediment gradually settling from suspension after erosional reworking of the sea bed, particularly by storm waves.
- Bioturbation which is disturbance of the sediments by burrowing animals thus forming biogene structures<sup>2</sup>. This can be either at the surface or in the sediment itself. The most important burrowers are: 1) American jack-knife clams, which forms vertical or almost vertical burrows up to a depth of up to several dm, and 2) the sea potato which migrates sideways through the sediments leaving sand filled tubes which shows as concentric rings in cross-section.

Disturbance by fishery using ground disturbing methods. For fish this may be beam-trawling disturbing the upper surface with chains etc. For catching shell fish a bottom slicer is used. Both may leave a disturbed trail on the seabed which has an irregular erosional surface.

---

<sup>2</sup> The sedimentological term: “biogene structures” is used to indicate structures brought about by the action of animals which may disturb the original bedding structures.

### 3 Vibrocores- sedimentology and geology

#### 3.1 Geological units

Based on the vibrocores description we recognized the following four geological units/facies: lower shoreface deposits, tidal channel deposits, ebb-shield deposits and fluvial deposits. In the shoreface deposits a subunit was recognized: the active layer. This section provides a general description of these units. Section 3.2 provides a detailed description of the boreholes in the three areas.

##### *Lower shoreface deposits*

Shoreface deposits consist of fine to coarse sand, varying in colour between yellow, brown and grey. They typically contain many shells and shell fragments and in some cores some clay laminae. The base of these deposits is often sharp, indicating its erosive nature. These deposits were formed by wave-reworking of the underlying Pleistocene fluvial and deltaic deposits and belong to the Southern Bight Formation. The three areas have characteristic faunal assemblage: in the Noordwijk area *Spisula* and *Ensis leei*, in the Amelander Inlet *Donax vittatus* and *Ensis leei*, and in the Terschelling area *Donax vittatus*, *Spisula* and *Ensis leei*.

Within the shoreface deposits we could distinguish an active layer, based on the higher abundance of shells, the lighter colour and the absence of clay layers and laminae. These features indicate recent reworking of the seabed sediment.

##### *Tidal channel deposits*

Tidal channel deposits consist of brown-grey and grey sand with clay laminae and layers and sometimes with peat clasts and organic material. The base of these deposits is often sharp. In the Terschelling and Amelander Inlet areas the shell content is low. These deposits formed during the periodical transport and deposition in tidal channels and belong to the Naaldwijk Formation. Characteristic species in the Amelander Inlet area are *Donax*, *Spisula*, *Cerastodema* and *Macoma*. In the Noordwijk area they are *Spisula*, *Macoma*, *Donax* and *Mytilus*.

##### *Ebb-shield deposits*

Ebb-shield deposits consist of brown-grey and grey sand with clay clasts, often showing a chaotic arrangement. *Cerastodema* and *Macoma* are typical shells in this facies. These deposits formed due to the transport and fast deposition in the tidal delta of the Amelander Inlet and were interpreted as part of the Naaldwijk Formation.

##### *Fluvial deposits*

Fluvial deposits, found only in the Noordwijk area, consist of brown-grey to red cross-laminated sand without shells. These deposits were formed by transport and deposition by Pleistocene braided rivers and belong to the Kreftenheye Formation.

#### 3.2 Borehole description

A full description of all boreholes and high-resolution photographs of the vibrocores is available as an Appendix A to this report.

##### 3.2.1 Amelander Inlet research area

In the Amelander inlet research area all the cores display an upper layer of yellow-brown lower shoreface sand and the lower layer of tidal channel grey sand with clay laminae. In two of the

boreholes the chaotic-arranged layer with sand and clay bands/clasts was interpreted as part of ebb-shield deposits. Table 3.1 provides an overview of the vibrocore characteristics in the Amelander Inlet research area. Figure 3.1 gives two examples of boreholes in this area.

Table 3.1 Schematic description of the vibrocores in the Amelander Inlet research area. WD=water depth in m below NAP. Formations (Fm): SB=Southern Bight, Na=Naaldwijk. Q= level of certainty of the description, with 1=uncertain and 3=certain. See figure 2.1 for locations.

	<b>WD</b> <b>(m)</b>	<b>top</b> <b>(m)</b>	<b>Bottom</b> <b>(m)</b>	<b>facies</b>	<b>Q</b>	<b>Fm.</b>	<b>description</b>
VC-10-A	13.70	0.00	0.16	Shoreface-active layer	2	SB	Brown-yellow sand
		0.16	5.35	Tidal channel/ebb-shield	2	Na	Grey sand, traces of clay layers
VC-11-A	17.30	0.00	0.42	Shoreface-active layer	3	SB	Beige-brown sand
		0.42	1.60	Ebb-shield	1	Na	Grey and beige sand, convoluted, with clay balls
		1.60	5.40	Tidal channel	3	Na	Grey sand, clay layers
VC-12-A	20.30	0.00	0.29	Shoreface-active layer	3	SB	Brown-yellow sand
		0.29	4.18	Tidal channel	3	Na	Sand, clay laminae, clay layer at the top, peat clasts
VC-14-A	12.70	0.00	0.20	Shoreface-active layer	3	SB	Beige sand
		0.20	3.70	Tidal channel/ebb-shield	2	Na/ SB	Grey-brown sand, patchy structure, clay layers
VC-15-A	17.50	0.00	0.40	Shoreface-active layer	3	SB	Brown-yellow sand
		0.40	4.00	Ebb-shield	1	Na	Grey sand, unstructured
		4.00	4.55	Tidal channel	3	Na	Grey sand, clay laminae
VC-16-A	20.20	0.00	0.20	Shoreface-active layer	3	SB	Brown-yellow sand
		0.20	2.45	Tidal channel	3	Na	Grey sand with traces of clay layers
VC-19-A	18.10	0.00	0.50	Shoreface-active layer	3	SB	Light grey-brown sand
		0.50	0.70	Shoreface/ebb-shield	2	Na	Brown sand
		0.70	4.00	Tidal channel	3	Na	Grey sand, clay layers
VC-20-A	19.90	0.00	0.43	Shoreface-active layer	3	SB	Brown-yellow sand
		0.43	1.40	Shoreface	3	SB	Grey sand, small clay layer
		1.40	3.30	Tidal channel	3	Na	Grey sand, clay layers
VC-21-A	19.00	0.00	0.60	Shoreface-active layer	3	SB	Brown-yellow sand
		0.60	2.40	Shoreface	2	SB	Grey-brown sand
		2.40	4.55	Tidal channel	3	Na	Grey sand, clay laminae

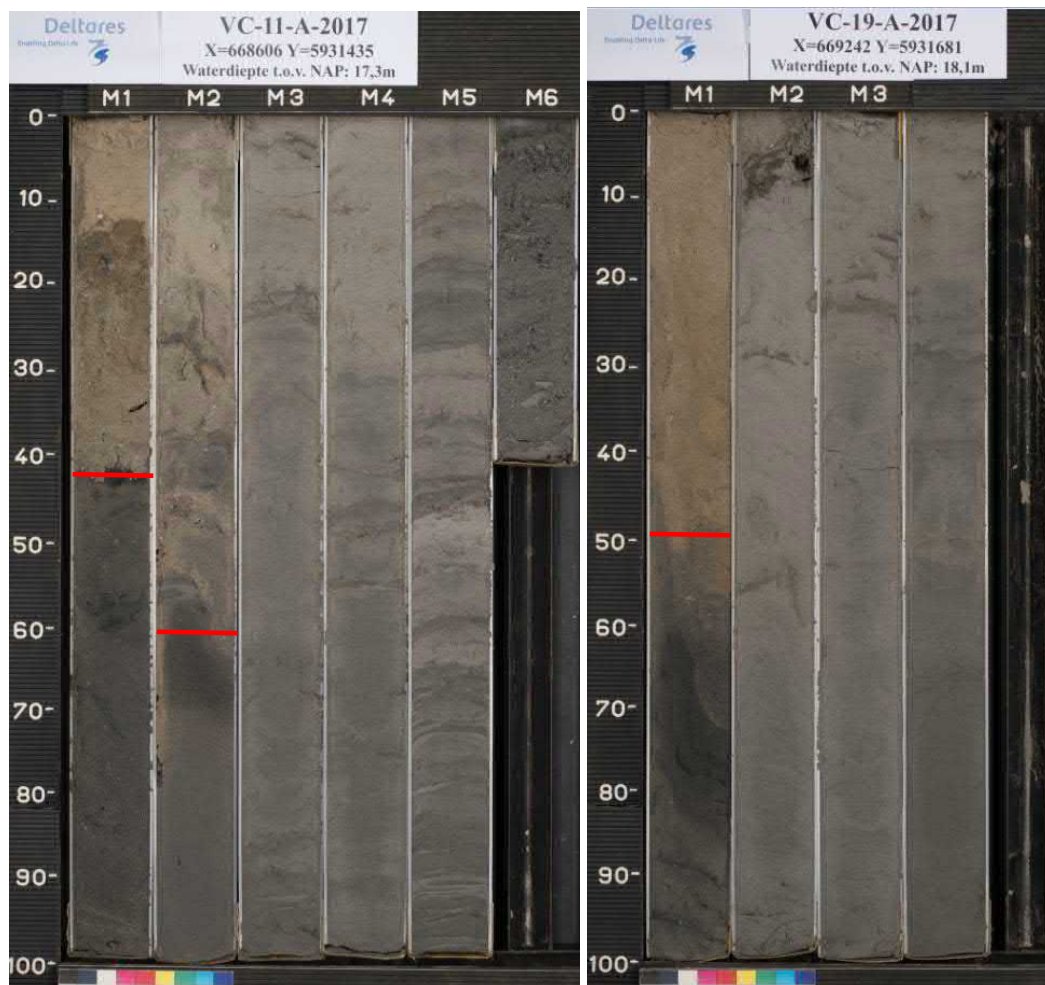


Figure 3.1 Picture of the boreholes VC-11-A (left) and VC-19-A (right) in the Ameland research area. In VC-11-A 40 cm of yellow-brown shoreface sand overlies ebb-shield deposits with convoluted sand and clay layers. Below 1.60m depth the core is formed by tidal channel deposits with sand and intercalated clay laminae. In VC-19-A lower shoreface sandy deposits directly overlie tidal channel deposits (boundary at 50 cm depth).

### Fauna

Table 3.2 and Figure 3.2 present faunal assemblage and visually estimated median grain size of the lower shoreface deposits of the round box cores and the vibrocores. In the lower shoreface deposits the shell abundance is higher closer to the inlet and very low further offshore. *Donax* and *Ensis* are the most abundant species found within the lower shoreface deposits.

Table 3.2 Detailed analyses of the lower shoreface deposits in the Ameland Inlet research area based on vibrocores description. BN=Borehole number. SA=shell abundance: 0=absent, 1=traces, 2=few, 3=many. Shell species: Spi=Spisula, Car=Cardium, Don=Donax, Ens=Ensis, Myt=Mytilus, Mac=Macoma, Ang=Angulus. WD=Water Depth in m with reference to NAP. d50=50 percentile sand grains diameter as visually determined. GS=visually estimated grain size: vf=very-fine sand, mf=medium-fine sand, mc=medium-coarse sand.

BN	SA	Spi	Car	Don	Ens	Myt	Mac	Ang	WD	d50	GS
Vibrocores											
10	1	0	0	0	0	0	0	0	-13.7	140	vf
11	2	2	0	3	1	0	0	0	-17.3	140	vf
12	1	0	0	0	0	0	0	0	-20.3	210	mc
14	1	1	1	1	1	1	0	0	-12.7	180	mf
15	2	1	1	2	3	0	0	1	-17.5	185	mf
16	1	1	1	3	0	0	0	0	-20.2	180	mf
19	1	1	1	0	0	0	0	0	-18.1	185	mf
20	1	1	1	1	0	0	0	1	-19.9	160	mf
21	1	1	0	1	0	0	0	0	-19.0	185	mf

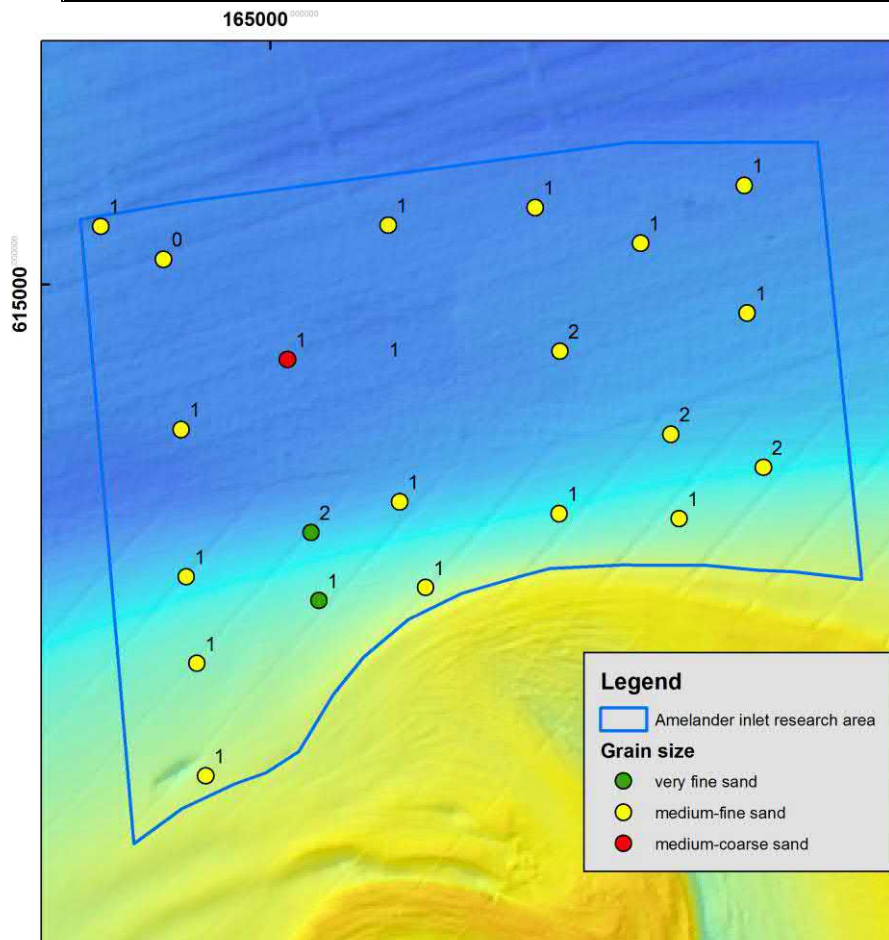


Figure 3.2 Grain size as visually estimated and shell abundance of lower shoreface sediments in the Ameland Inlet research area. The total shell abundance is shown as a number (0-3) in the upper right corner of each borehole. Note that the 2017 round box cores will be dealt with in detail in Chapter 4. (bathymetry compilation of depth soundings in the period 2009- 2014).

### 3.2.2 Terschelling research area

In the Terschelling research area all the cores display a thin upper layer of yellow-brown lower shoreface sand and a thick lower layer of tidal channel grey sand with clay laminae. These tidal channel deposits are very poor in shell content, with exception of deposits in borehole VC-07-T that contain abundant shells. Table 3.3 provides an overview of the vibrocore characteristics in this area. Figure 3.3 shows an example of a core from the Terschelling area.

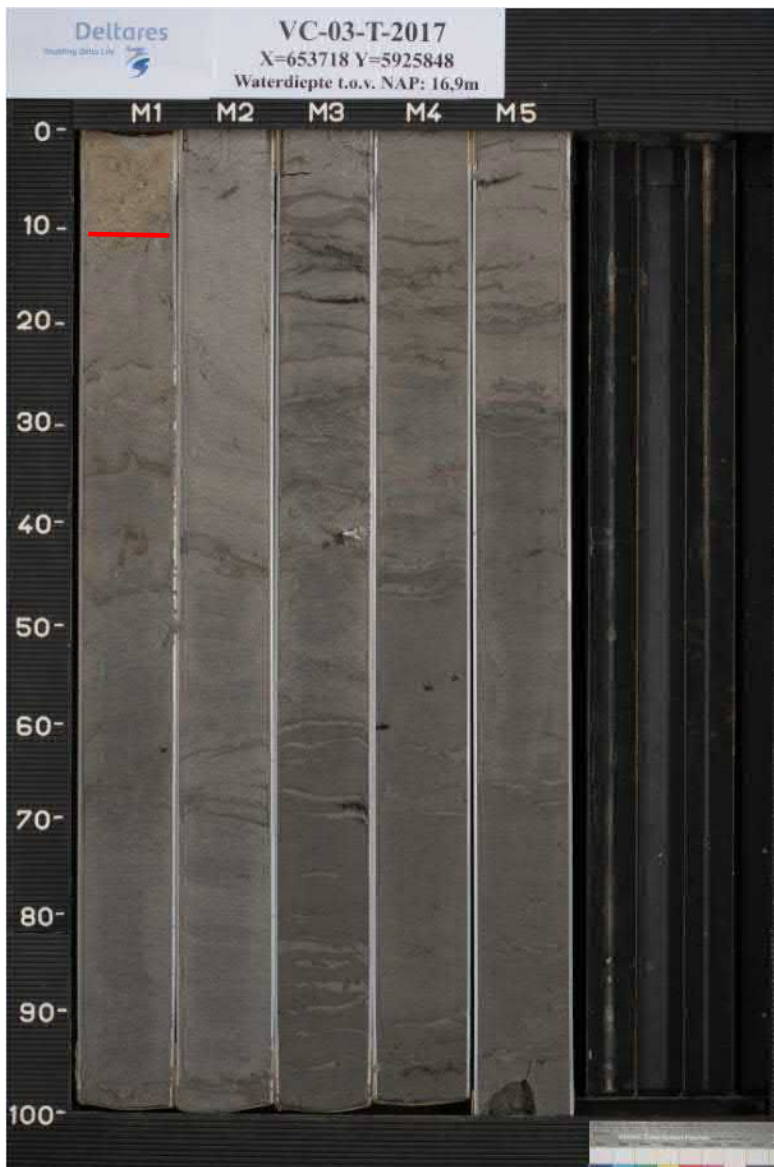


Figure 3.3 Photo of borehole VC-03-T in the Terschelling research area. A thin layer (0.1 m) of shoreface sand (yellow-brown) overlies tidal channel sand with clay layers.

Table 3.3 Schematic description of the vibrocores in the Terschelling research area. WD=water depth. Formations: SB=Southern Bight, Na=Naaldwijk. Q= level of certainty of the description, with 1=uncertain and 3=certain. See Figure 2.2 for locations.

	WD (m)	top (m)	Bottom (m)	facies	B	Fm	Description
VC-02-T	12.80	0.00	0.20	Shoreface-active layer	3	SB	beige sand
		0.20	4.45	Tidal channel	3	Na	Grey sand, clay laminae
VC-03-T	16.90	0.00	0.12	Shoreface-active layer	3	SB	beige sand
		0.12	5.10	Tidal channel	3	Na	Grey sand, clay laminae
VC-04-T	19.50	0.00	0.08	Shoreface-active layer	3	SB	Brown-grey sand
		0.08	4.50	Tidal channel	3	Na	Grey sand, clay laminae
VC-06-T	14.40	0.00	0.50	Shoreface-active layer	3	SB	Light brown-yellow sand
		0.50	4.04	Tidal channel	3	Na	Grey sand, clay laminae
VC-07-T	18.50	0.00	0.35	Shoreface-active layer	3	SB	Light brown-yellow sand
		0.35	4.35	Tidal channel	3	Na	Grey sand, clay laminae and pieces of peat
VC-08-T	19.50	0.00	0.60	Shoreface-active layer	3	SB	Light brown-yellow sand
		0.60	3.17	Tidal channel	3	Na	Grey sand, clay laminae

Fauna

Table 3.4 and Figure 3.4 present the faunal assemblage and median grain size of the lower shoreface deposits as sampled with the vibrocores and round box cores in 2017. In the lower shoreface the visually estimated sediment grain size is typically fine-medium (d50: 160-180 mu) with some coarser outliers (210-240 mu). Shell abundance is low to very high across the area with no clear spatial pattern. *Donax*, *Spisula*, *Angulus* and *Macoma* are the most abundant species found.

Table 3.4 Detailed analyses of the lower shoreface deposits in the Terschelling research area based on vibrocores description. BN=Borehole number. SA=shell abundance: 0=absent, 1=traces, 2=few, 3=many. Shell species: Spi=Spisula, Car=Cardium, Don=Donax, Ens=Ensis, Myt=Mytilus, Mac=Macoma, Ang=Angulus. WD=Water Depth. d50=50 percentile sand grains diameter. GS=grain size: vf=very-fine sand, mf=medium-fine sand, mc=medium-coarse sand.

BN	SA	Spi	Car	Don	Ens	Myt	Mac	Ang	WD	d50	GS
Vibrocores											
2	3	3	0	3	0	1	0	0	-12.8	170	mf
3	2	1	1	0	1	0	3	0	-16.9	170	mf
4	2	0	1	2	0	1	2	1	-19.5	210	mc
6	1	0	0	2	1	0	0	0	-14.4	180	mf
7	2	0	0	2	0	1	1	0	-18.5	185	mf
8	2	3	1	3	0	0	0	0	-19.5	240	mc

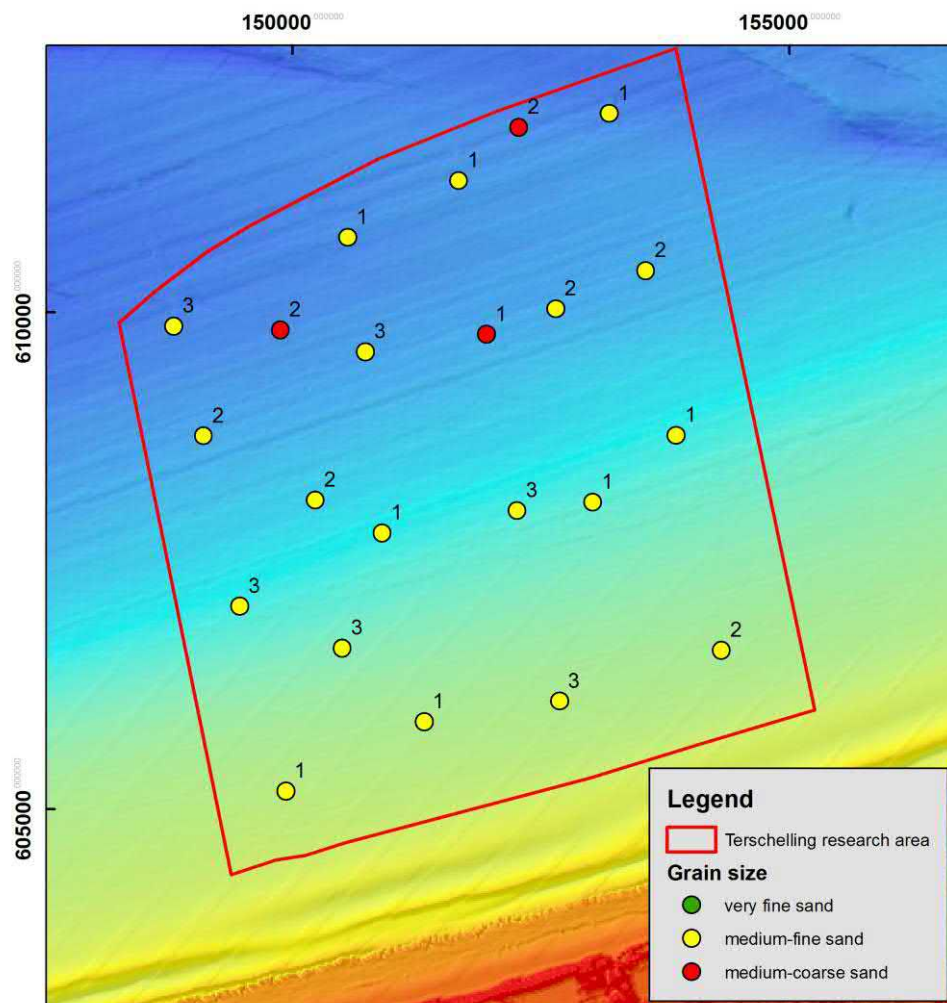


Figure 3.4 Grain size as visually estimated and shell abundance of lower shoreface sediments in the Terschelling research area. The total shell abundance is shown as a number (0-3) in the upper right corner of each borehole. Note that the 2017 round box cores will be dealt with in detail in Chapter 4 (bathymetry compilation of depth soundings in the period 2009- 2014).

### 3.2.3 Noordwijk

In the Noordwijk research area all the cores display a thin upper layer of brown lower shoreface sandy deposits, above a layer of tidal channel grey sand with clay laminae and a lowest layer of laminated red-brown fluvial sands. Table 3.5 provides an overview of the vibrocore characteristics in this area. Figure 3.5 shows two examples of cores from the Noordwijk site.

Table 3.5 Schematic description of the vibrocores in the Noordwijk research area. WD=water depth. Formations: SB=Southern Bight, Na=Naaldwijk. Q= level of certainty of the description, with 1=uncertain and 3=certain. See figure 2.3 for locations.

	<b>WD (m)</b>	<b>top (m)</b>	<b>bottom (m)</b>	<b>facies</b>	<b>B</b>	<b>Fm.</b>	<b>Description</b>
VC-23-N	12.40	0.00	0.36	Shoreface-Active layer	3	SB	Grey-brown sand
		0.36	0.78	Shoreface	3	SB	Brown sand
		0.78	3.75	Tidal channel	2	Na	Grey and sand, clay laminae and layers
VC-24-N	16.40	0.00	0.60	Shoreface-Active layer	3	SB	Grey-brown sand
		0.60	2.15	Tidal channel	1	Na/SB	Grey sand, silty
		2.15	3.33	Fluvial	1	Kr/Na	Grey-brown sandy silt, silty sand
VC-25-N	17.10	0.00	0.69	Shoreface-Active layer	3	SB	Brown gravelly sand
		0.69	3.81	Shoreface	3	SB	Grey-brown sand with clay laminae
		3.81	4.50	Fluvial	3	Kr/Na	Grey, laminated sand
VC-26-N	18.10	0.00	0.76	Shoreface-Active layer	3	SB	Grey-brown sand
		0.76	1.40	Seabed	3	SB	Grey sand
		1.40	4.05	Tidal channel	3	Na	Grey sand, clay laminae
VC-28-N	15.00	0.00	AL	Shoreface-Active layer	3	SB	Yellow-brown sand
		0.27	2.45	Seabed	3	SB	Grey-brown coarse sand
		2.45	4.20	Tidal channel	3	Na	Grey and brown sand, organic material
VC-29-N	17.30	0.00	0.41	Shoreface-Active layer	3	SB	Grey-brown sand
		0.41	1.05	Tidal channel	3	Na	Grey sand, clay laminae, organic material
		1.05	5.30	Fluvial	3	Kr	Brown-red sand,
VC-30-N	17.80	0.00	0.48	Shoreface-Active layer	3	SB	yellow-brown sand
		0.48	1.14	Seabed	3	SB	grey sand
		1.14	4.40	Tidal channel	3	Na	grey sand, clay laminae, pieces of peat
VC-31-N	19.30	0.00	0.62	Shoreface-Active layer	3	SB	yellow-brown sand
		0.62	0.72	Tidal channel	2	Na	Grey sand, clay laminae
		0.72	4.80	Fluvial	3	Kr	Grey, laminated sand

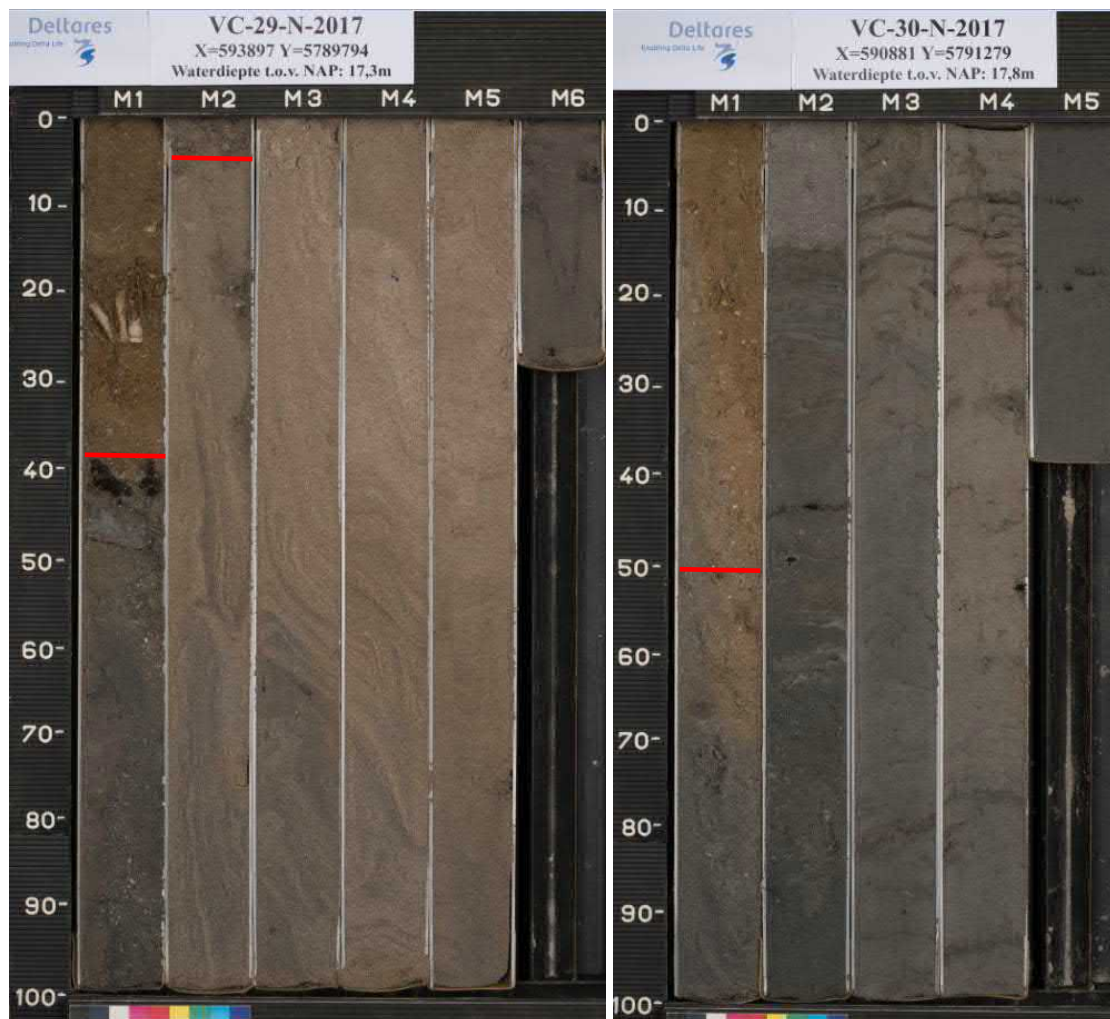


Figure 3.5 Pictures of the boreholes VC-29-N (left) and VC-30-N (right) in the Noordwijk research area. In VC-29-N 40 cm of yellow-brown shoreface sand with abundant shells overlies 65 cm of grey tidal channel deposits with sand and intercalated clay laminae. A thick package of reddish fluvial laminated sands underlies the tidal deposits. In VC-30-N lower shoreface sandy deposits overlie tidal channel deposits (boundary at 50 cm depth).

### Fauna

Table 3.6 and Figure 3.6 present the faunal assemblage and grain size of the lower shoreface deposits. In the lower shoreface deposits the visually estimated sediment grain size is typically medium coarse ( $d_{50}$ : 220-280  $\mu$ ), finer closer to the coast (160-200  $\mu$ ) with a very fine outlier (130  $\mu$ ). Shell abundance is very different across the area varying from none to very high. *Spisula* is the dominant species in the faunal assemblage.

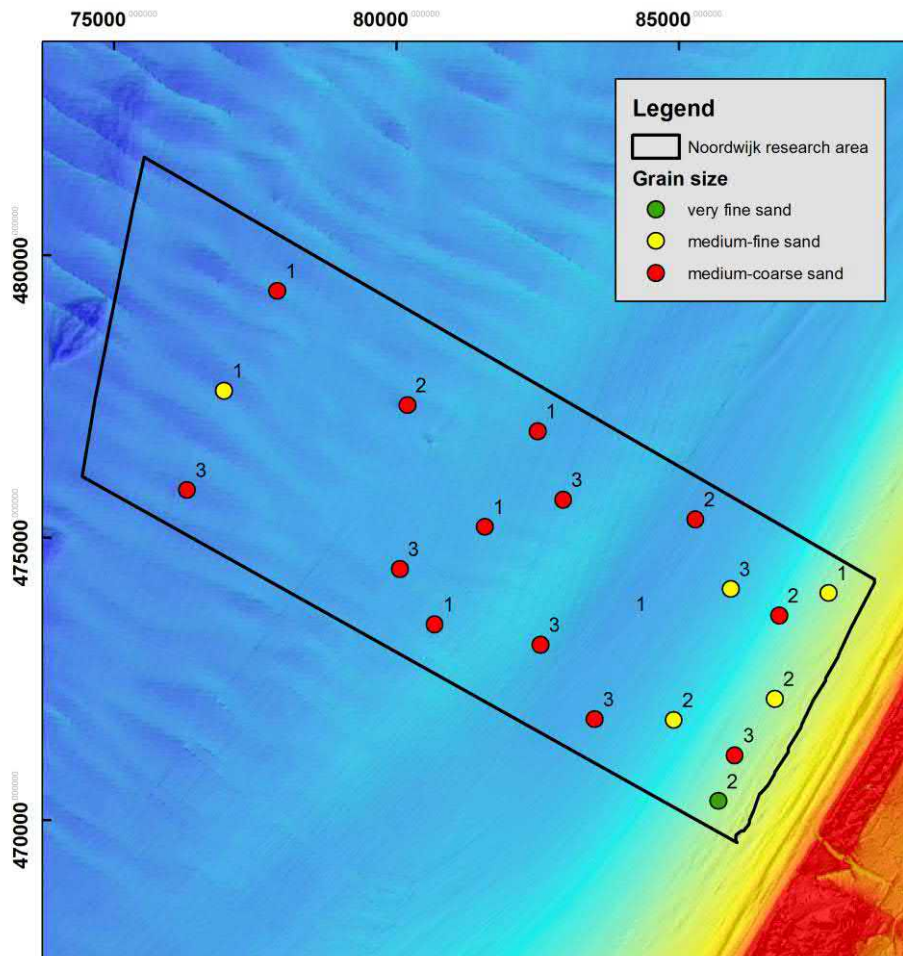


Figure 3.6 Grain size as visually estimated and shell abundance of lower shoreface sediments in the Noordwijk research area. The total shell abundance is shown as a number (0-3) in the upper right corner. Note that the 2017 round box cores will be dealt with in detail in Chapter 4 (bathymetry compilation of depth soundings in the period 2009- 2014).

Table 3.6 detailed analysis of the lower shoreface deposits in the Noordwijk research area based on vibrocores and box cores description. BN=Borehole number. SA=shell abundance: 0=absent, 1=traces, 2=few, 3=many. Shell species: Spi=Spisula, Car=Cardium, Don=Donax, Ens=Ensis, Myt=Mytilus, Mac=Macoma, Ang=Angulus. WD=Water Depth. d50=50 percentile visually estimated sediment grain size diameter. GS=grain size: vf=very-fine sand, mf=medium-fine sand, mc=medium-coarse sand.

BNN	SA	Spi	Car	Don	Ens	Myt	Mac	Ang	WD	d50	GS
Vibrocores											
23	3	3	2	1	1	0	3	1	-12.4	230	mc
24	2	3	0	0	1	0	0	1	-16.4	170	mf
25	3	3	1	0	2	0	0	1	-17.1	280	mc
26	3	3	0	1	1	1	0	1	-18.1	260	mc
28	2	3	0	0	0	0	0	0	-15.0	230	mc
29	3	3	0	0	3	0	0	2	-17.3	160	mf
30	3	3	1	0	0	1	0	3	-17.8	260	mc
31	2	3	0	0	1	0	2	1	-19.3	220	mc

### 3.3 Geological cross-sections

Boreholes were correlated using the facies interpretation to build two geological cross sections per research area, roughly perpendicular to the shoreline. In the cross-sections the position of the top of the boreholes in some cases does not coincide with the bathymetric profile. This is caused by the fact that the bathymetry was not surveyed simultaneously with the coring, which allows for bed level changes in the intervening period, and, possibly, to measurement errors.

#### 3.3.1 Amelander Inlet research area

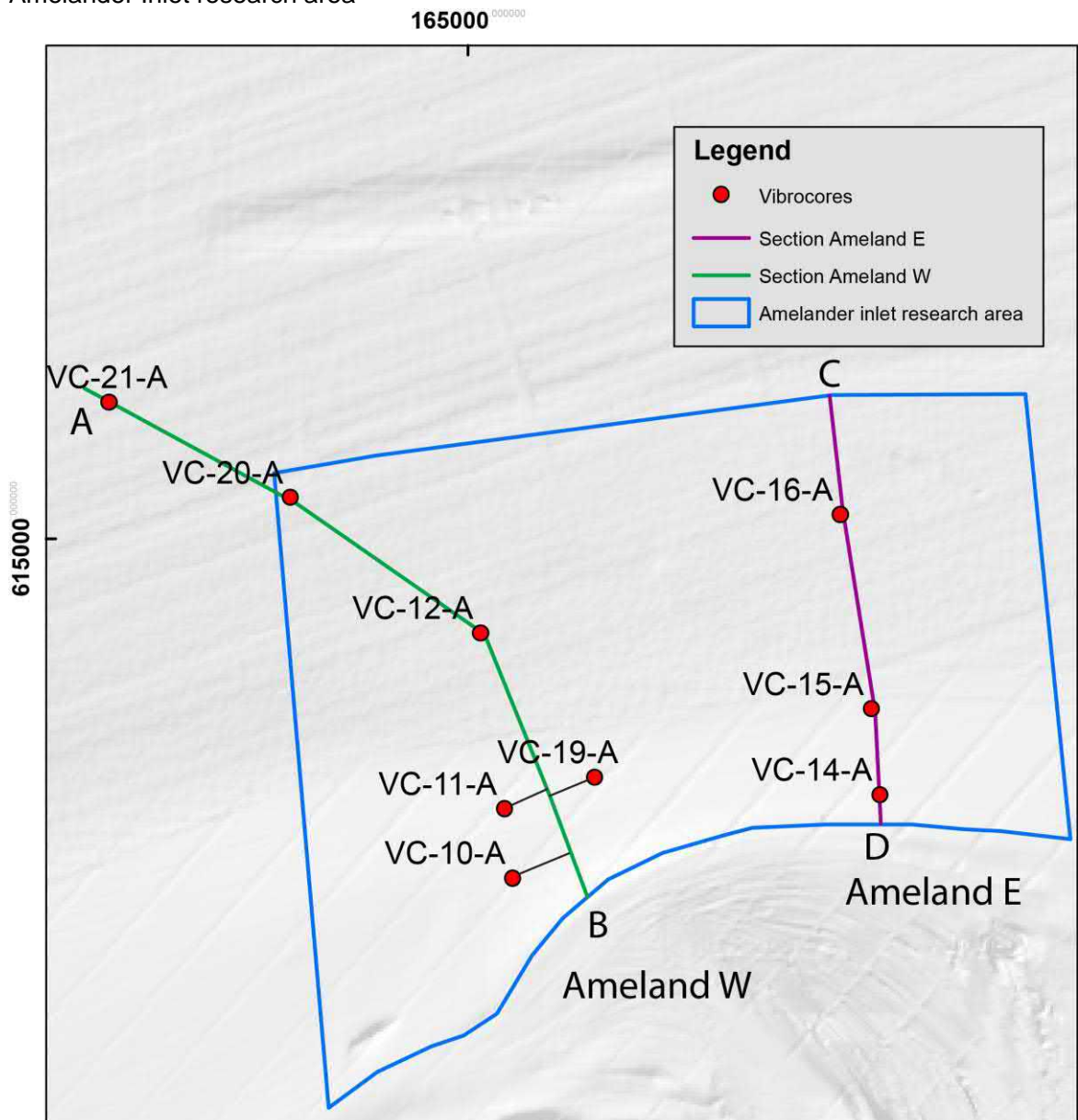


Figure 3.7 Overview map of the boreholes and geological cross-sections in the Amelander Inlet research area

The geological cross-section Ameland E (Figure 3.7 and 3.8) shows a northward dipping seabed, with steeper slopes in the south closer to the inlet. An upper layer with shoreface sands is underlain by at least 2 to 4 meters of tidal channel deposits. This general pattern is shown also by the Ameland W section, with exception of two local differences. First, in the Ameland

W section the active layer increases in thickness to the north. This might be related to the presence of a relict seabed feature in the NW part of the study area. The second difference is the occurrence of unstructured sandy and clay deposits at the edge of the ebb-tidal delta. These were interpreted as ebb-shield deposits formed by rapid sedimentation in the ebb-shield of the Akkepollegat channel.

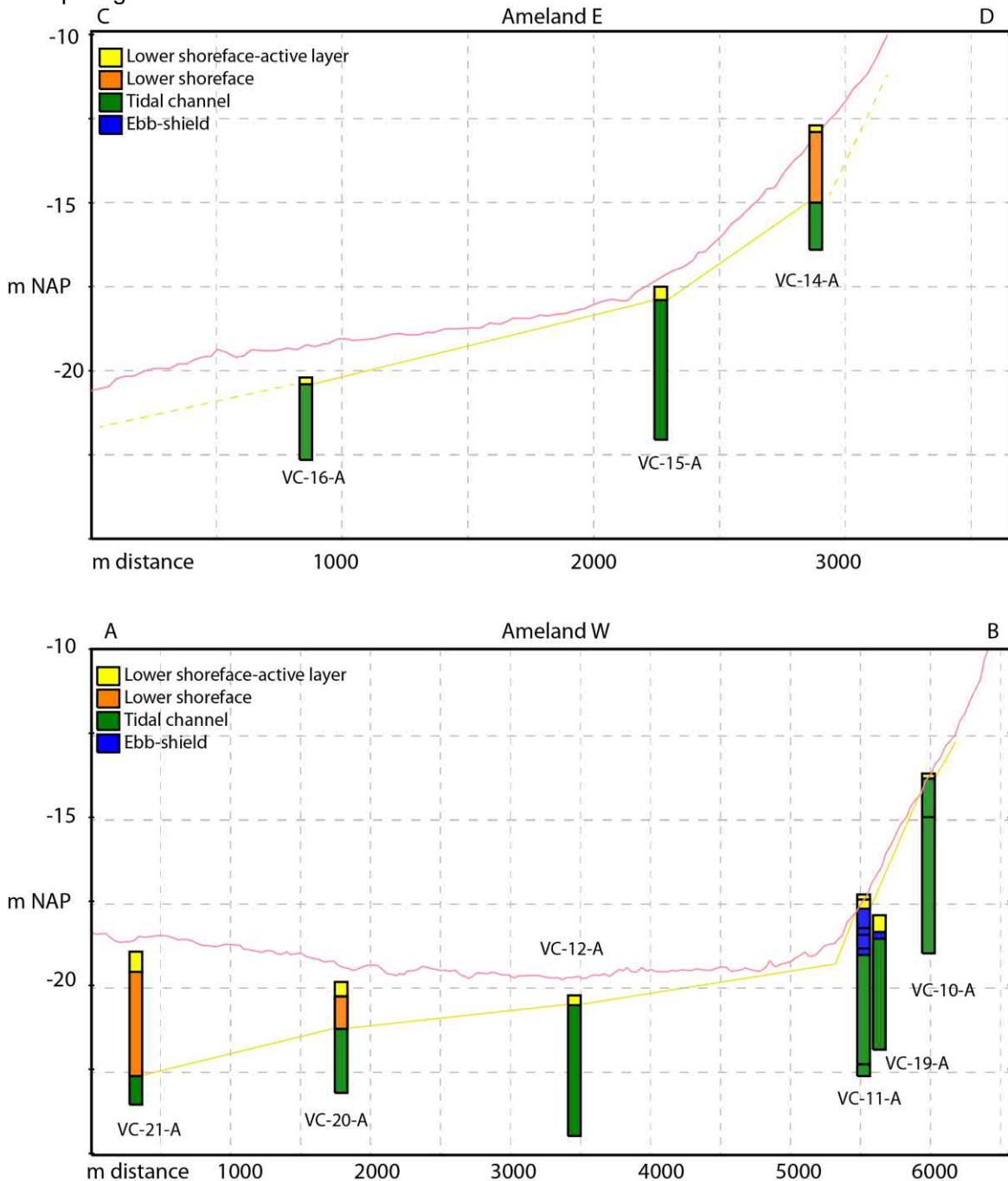


Figure 3.8 Geological cross-sections in the Ameland Inlet research area, showing older tidal channel and ebb-shield deposits, overlain by lower shoreface deposits (which are connected via the yellow line). The red line indicates the bathymetry compilation of depth soundings in the period 2009- 2014.

## 3.3.2 Terschelling research area

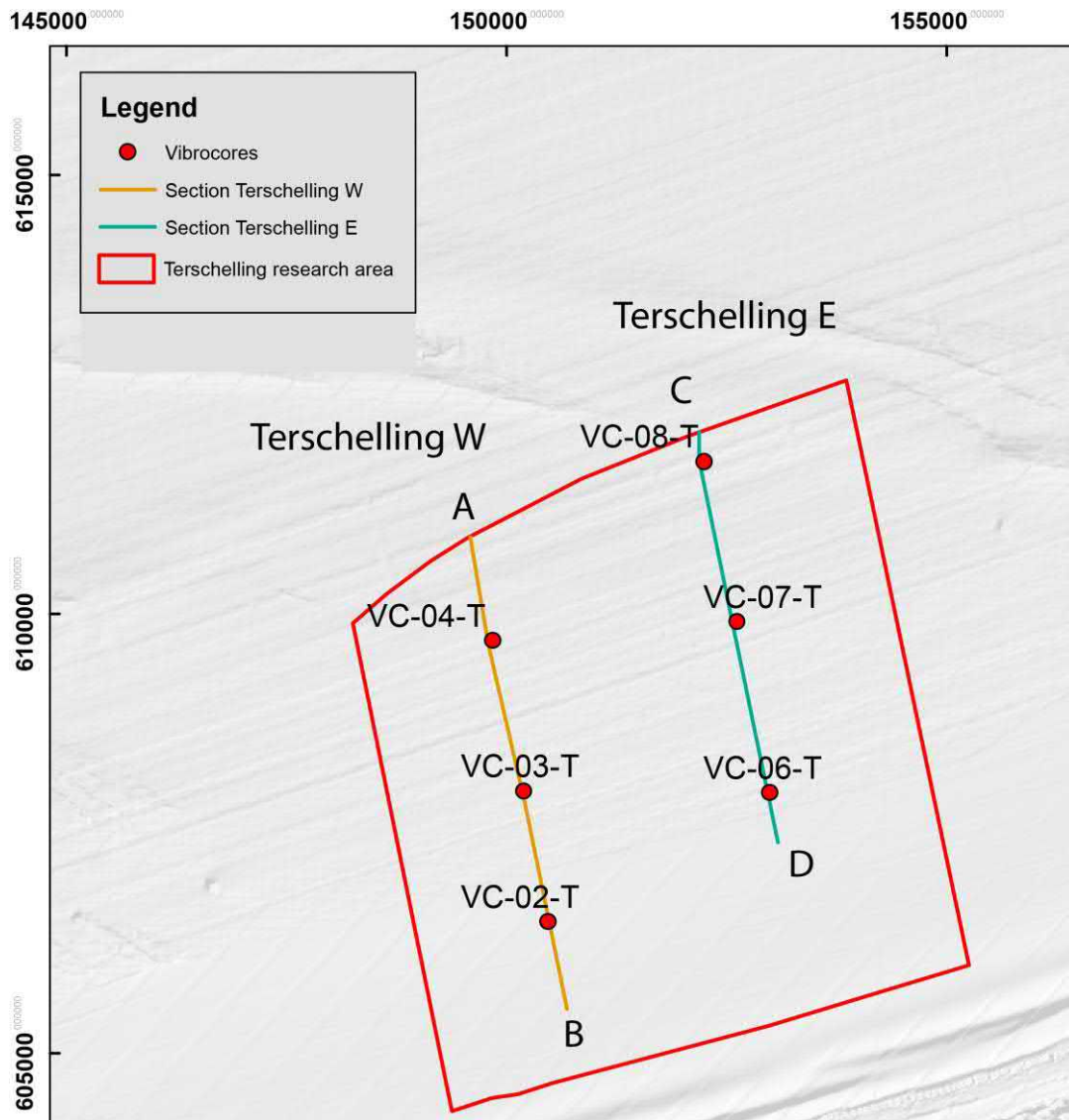


Figure 3.9 Overview map of the boreholes and geological cross-sections in the Terschelling research area

The geological cross sections Terschelling E and Terschelling W (Figure 3.9 and 3.10) show a northward dipping seabed, with relatively constant slopes. The upper layer consists of sandy shoreface deposits. This layer is at best a few decimetres thick and the thickness is higher in the eastern part of the study area. These were all interpreted as being part of the active layer. The shoreface deposits are underlain by at least 3 to 5 meters tidal channel deposits.

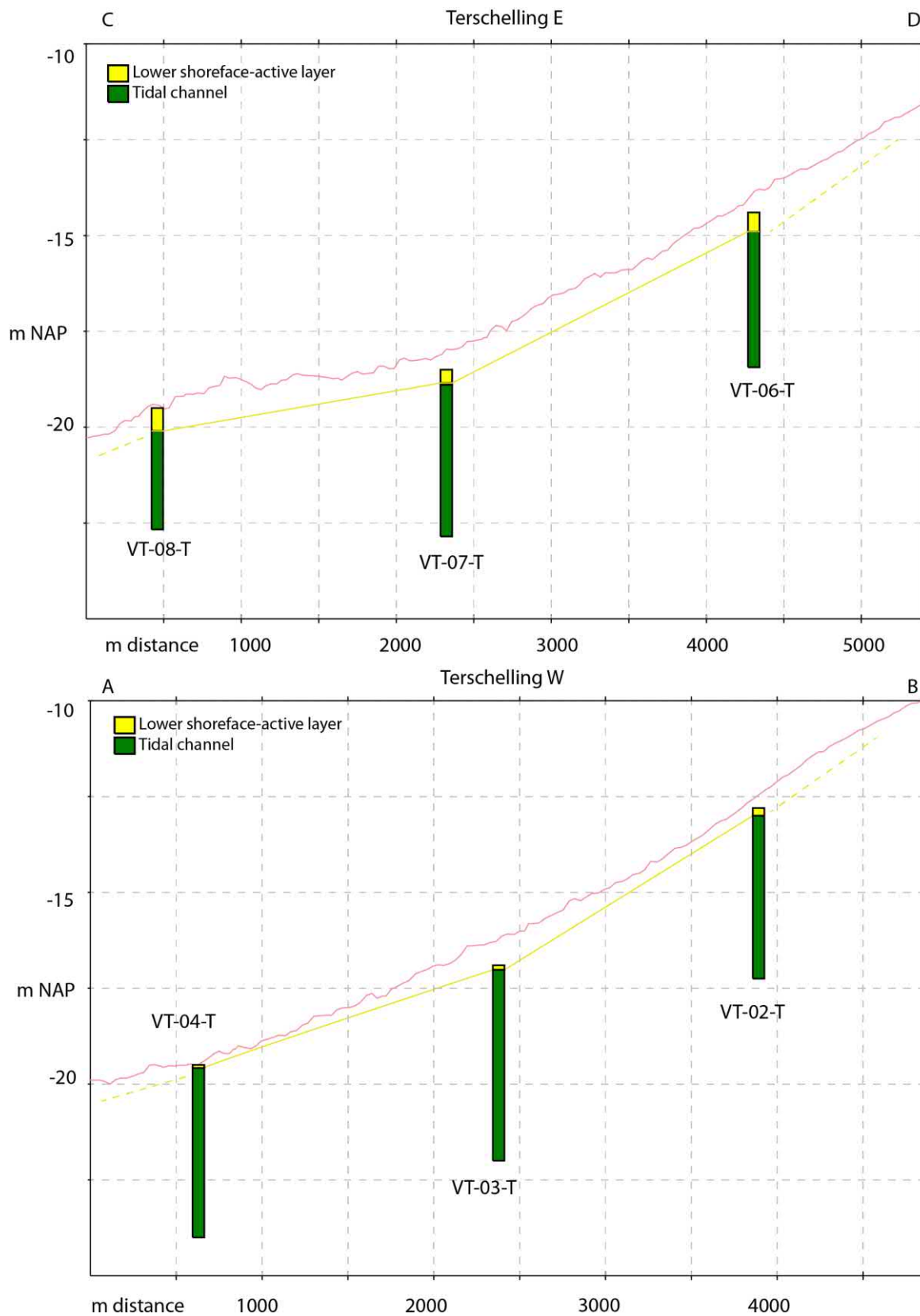


Figure 3.10 Geological cross-sections in the Terschelling research area, showing older tidal channel deposits, overlain by lower shoreface deposits (which are connected via the yellow line). The red indicates the bathymetry compilation of depth soundings in the period 2009- 2014.

## 3.3.3 Noordwijk research area

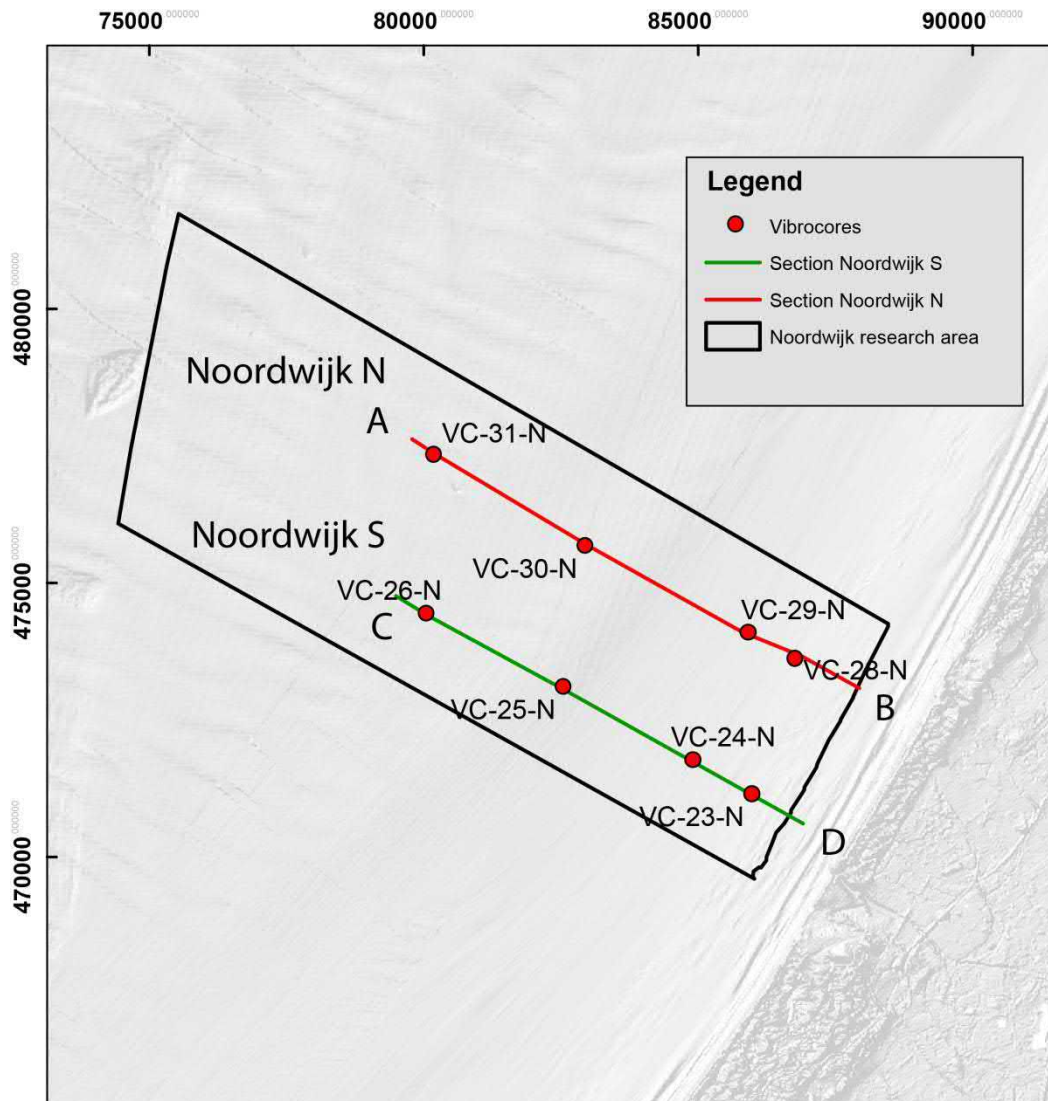


Figure 3.11 Overview map of the boreholes and geological cross-sections in the Noordwijk research area.

The two cross-sections in the Noordwijk study area (Figure 3.11 and 3.12) display an upper layer of shoreface sediments with variable thickness. This locally is underlain by tidal channel deposits. The maximum thickness of seabed deposits is below the sand ridge in the central part of the Noordwijk N profile. The thickness of the active layer increases with depth in offshore direction (see Chapter 5). Fluvial deposits underlie the above described deposits in both profiles.

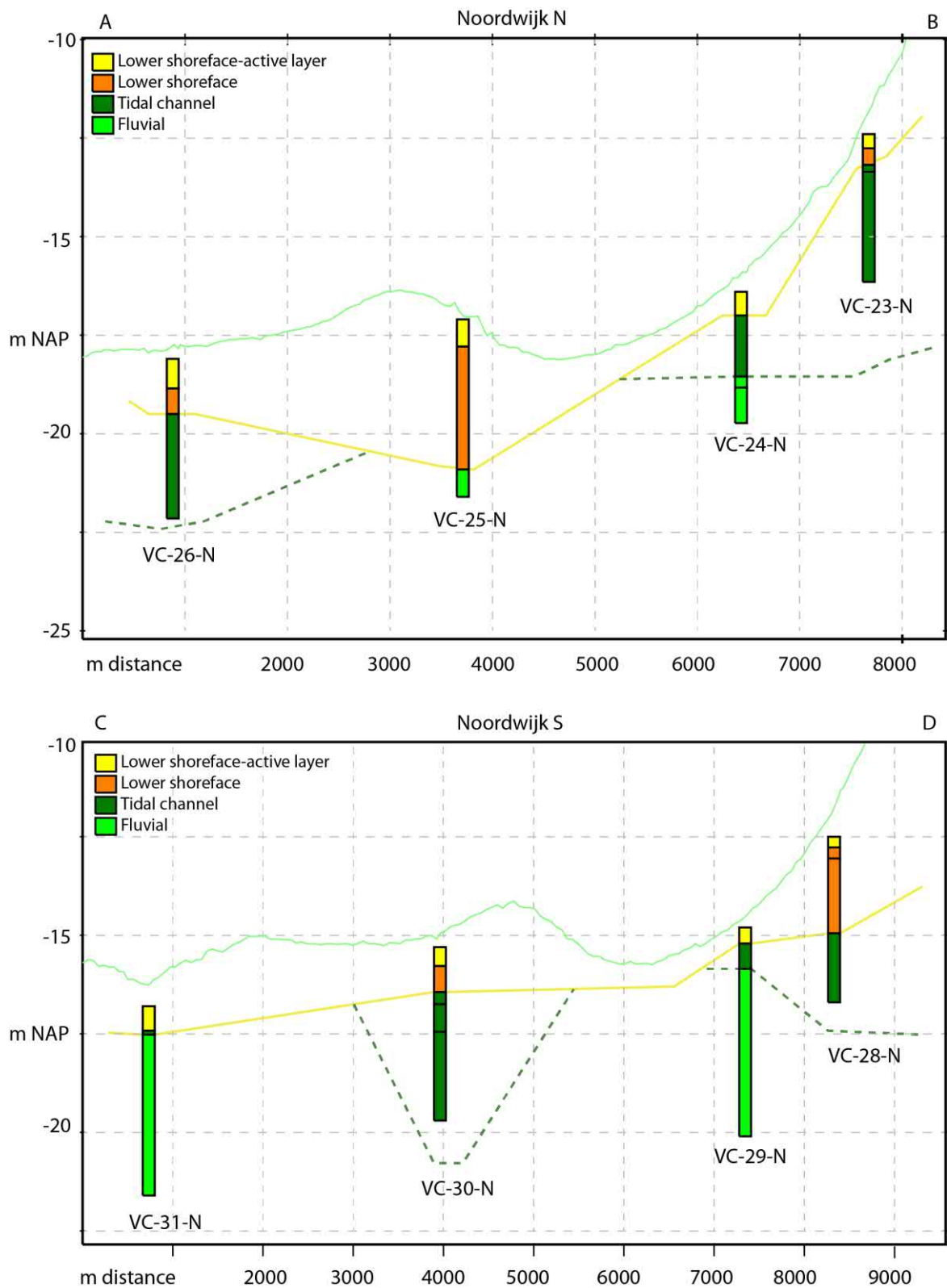


Figure 3.12 Geological cross-sections in the Noordwijk research area, showing older tidal channel deposits overlain by lower shoreface deposits (which are connected via the yellow line) and overlying fluvial deposits. The green line indicates the bathymetry of 2016. The green dotted line gives possible extent of the channel deposits bathymetry compilation of depth soundings in the period 2009- 2014.

### 3.4 Thickness analysis of the shoreface deposits active layer

Figure 3.13 shows the average thickness of the active layer between the three areas. The area of Noordwijk has the thickest active layer, followed by Ameland Inlet and Terschelling. There is a relatively large variation in the thickness, expressed by the high standard deviation of 15 cm (Ameland) to 21 cm (Terschelling). The thickness of the active layer is determined by the height of migrating bedforms and reworking of the sea bed by storm waves.

Figure 3.14 shows the thickness of the active layer against water depth. In the area of Noordwijk and, less clearly, in the Ameland Inlet area, the active layer thickness increases from -12m to -20m. For Terschelling there seems to be no correlation.

The increase of active layer thickness with depth is also visualized on a map for the area of Noordwijk and Ameland Inlet (Figure 3.15 and Figure 3.16, respectively). These maps give the indication that the increase of active layer thickness might be correlated to the morphology. Around -12m the samples are from the steeper part of the shoreface, with few bedforms present, while further offshore at the larger water depths, sand waves and sand banks are clearly visible and megaripples are known to be present. The relation with morphology will become clearer when comparing the data with the newly acquired multibeam data from these research areas.

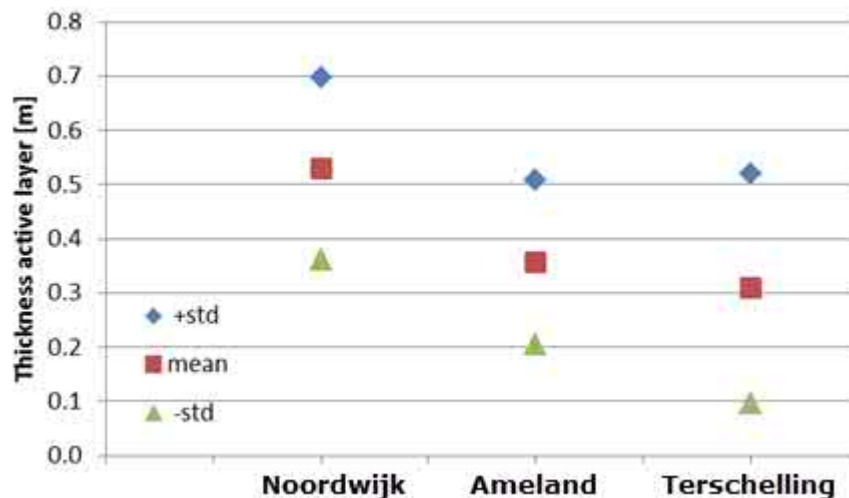


Figure 3.13 Mean value and standard deviation of the active layer thickness in the three study areas.

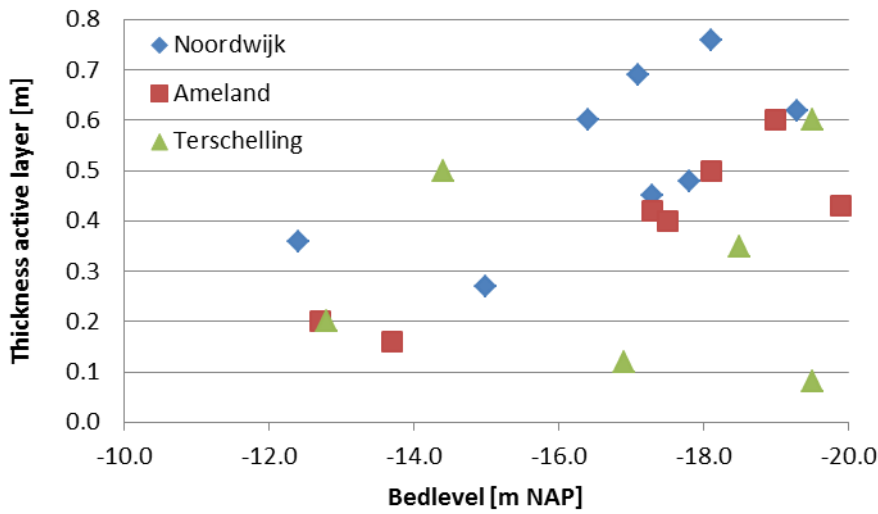


Figure 3.14 Active layer thickness to water depth plot

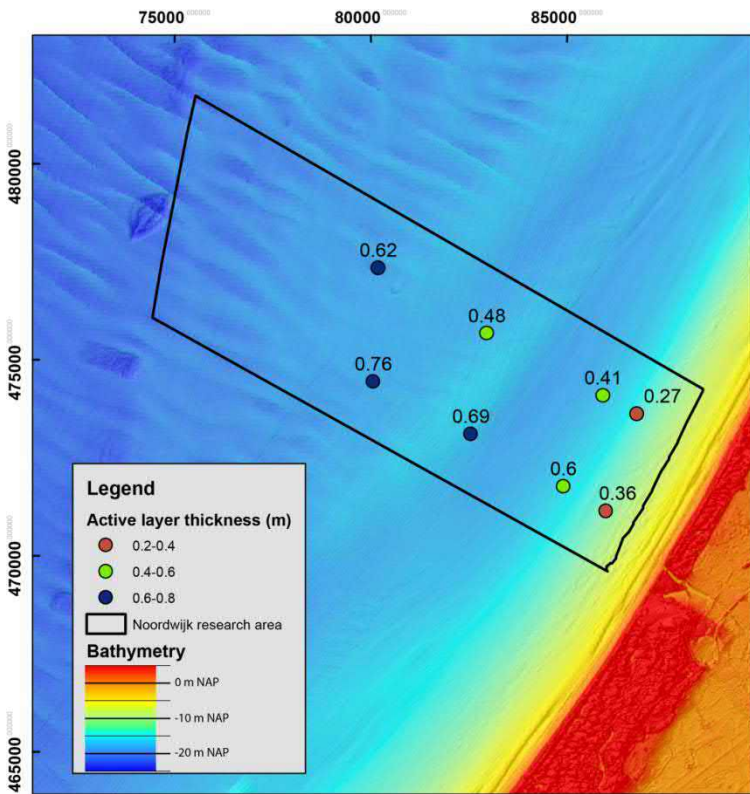


Figure 3.15 Measured active layer thicknesses in the boreholes in the Noordwijk research area (bathymetry compilation of depth soundings in the period 2009- 2014)..

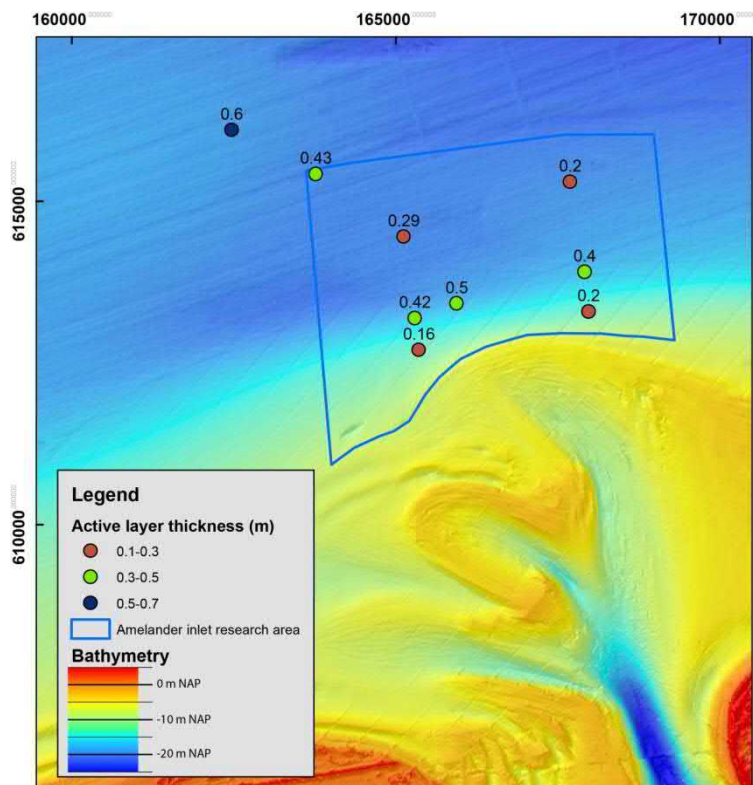


Figure 3.16 Measured active layer thicknesses in the boreholes in the Amelander Inlet research area (bathymetry compilation of depth soundings in the period 2009- 2014).



## 4 Box core descriptions

### 4.1 Introduction

In 2017 42 round box cores were taken covering the research area evenly. In 2018 48 rectangular box cores were taken along one profile (Terschelling, Noordwijk) and two profiles (Ameland) in the area. As the quality of the rectangular box cores was much better than that of the round cores, observations are more extensive. Here, the observations per area are discussed for the 2017 and 2018 box cores.

### 4.2 Box cores Ameland area

#### 4.2.1 Introduction

In 2017 14 round box cores have been collected along four profiles perpendicular to the coast, namely (ordered in increasing depth): BC17-BC21; BC24-BC22; BC25-BC27 & BC30-28. Water depths vary between -10m and -20.6m.

In 2018 16 rectangular box cores were collected along two profiles perpendicular to the coast (Figure 2.2) between -8 and -20m water depth, namely AM01 to AM09 and AM10 to AM16.

#### 4.2.2 Description of the observations on round box cores 2017

*Table 4.1 Detailed analysis of the lower shoreface deposits in the Amelander Inlet research area based on round box cores of 2017 description. BN=Borehole number. SA=shell abundance: 0: absent, 1=traces, 2=few, 3=many. Shell species: Spi=Spisula, Car=Cardium, Don=Donax, Ens=Ensis, Myt=Mytilus, Mac=Macoma, Ang=Angulus. WD=Water Depth. d50 = 50% percentile (by volume) grain diameter as determined with laser particle sizer of the sand fraction (Malvern).*

<b>BN</b>	<b>SA</b>	<b>Spi</b>	<b>Car</b>	<b>Don</b>	<b>Ens</b>	<b>Myt</b>	<b>Mac</b>	<b>Ang</b>	<b>WD (m NAP)</b>	<b>d50 (microns)</b>
<b>Box core</b>										
<b>17</b>	1	1	0	0	0	0	0	0	-10.0	223
<b>18</b>	1	0	0	1	1	0	0	1	-13.1	211
<b>19</b>	1	0	1	0	1	0	0	0	-16.8	209
<b>20</b>	1	1	0	0	0	0	1	0	-20.6	223
<b>21</b>	0	0	0	0	0	0	0	0	-20.0	232
<b>22</b>	1	0	0	1	0	0	0	0	-20.1	228
<b>23</b>	1	0	0	2	0	0	0	0	-20.2	224
<b>24</b>	1	0	0	0	0	0	0	0	-12.0	192
<b>25</b>	1	0	0	0	0	0	1	0	-15.0	186
<b>26</b>	2	1	0	3	2	0	0	1	-19.4	226
<b>27</b>	1	0	0	3	0	0	0	1	-19.8	227
<b>28</b>	1	0	0	1	0	0	0	0	-20.4	217
<b>29</b>	1	1	0	1	0	0	0	1	-19.2	218
<b>30</b>	2	0	0	3	1	0	1	2	-15.6	207

## Grain-size distributions

The grain-size distributions as measured with Malvern for the surface samples of the round box cores of 2017 are given in Table 4.1 and Figure 4.1 & Figure 4.2. The samples of 2017 show the following characteristics:

- 1) They consist of sediments smaller than 500 microns and with a d50 <250 microns (Table 4.1).
- 2) Roughly speaking there are two zones: one with d50's around 200 micron and a coarser zone in deeper water. These two groups are separated by a zone where no samples are taken between -15.6 and -19.2m. In general, an increase of d50 with increasing depth can be observed starting -13 to -15m and ending around -20m.
- 3) Above -15m a fraction < 63 micron is sometimes present at the east side of the ebb-delta lobe (Figure 4.3). The increase in grain size pattern with increasing depth is more evident for 2018 than for 2017, which might be due to the four separate profiles taken in 2017.

## Fauna

Shell abundance is higher closer to the inlet and very low further offshore (see Figure 3.2). Donax and Ensis are the most abundant species found within the lower shoreface deposits.

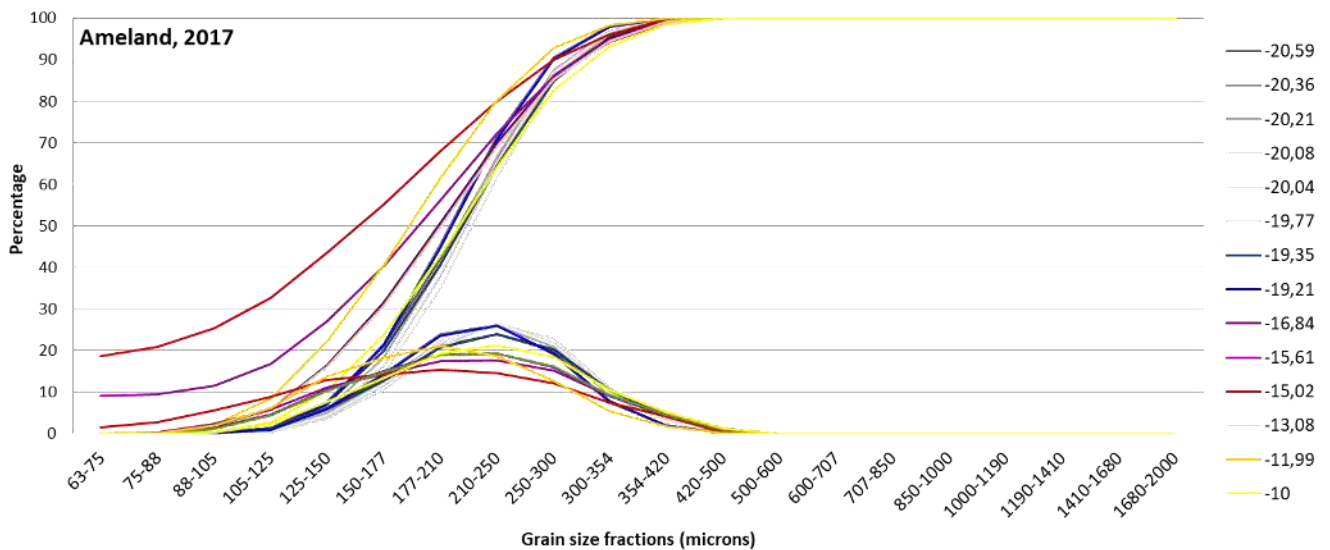


Figure 4.1 Grain size per size fraction and cumulative distribution for the sand fraction of the round box core samples of the Ameland site, taken in 2017. Colours and figures right indicate depth with reference to NAP.

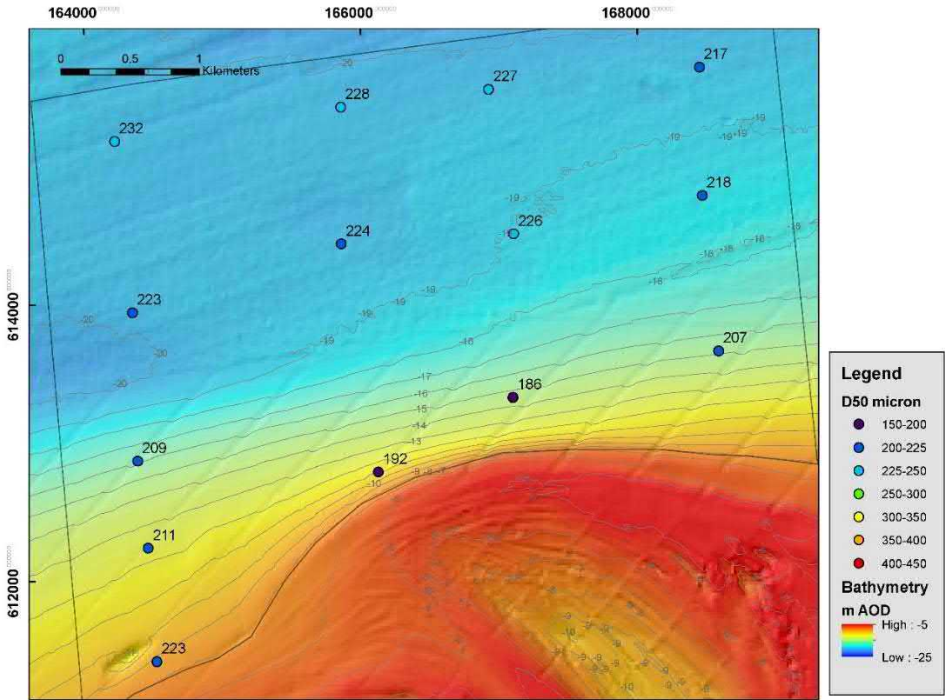


Figure 4.2 Overview of the d50 grain sizes in the upper layer of the samples taken in 2017. Note the pattern of increase in grain size in a seaward direction (bathymetry compilation of depth soundings in the period 2009-2014).

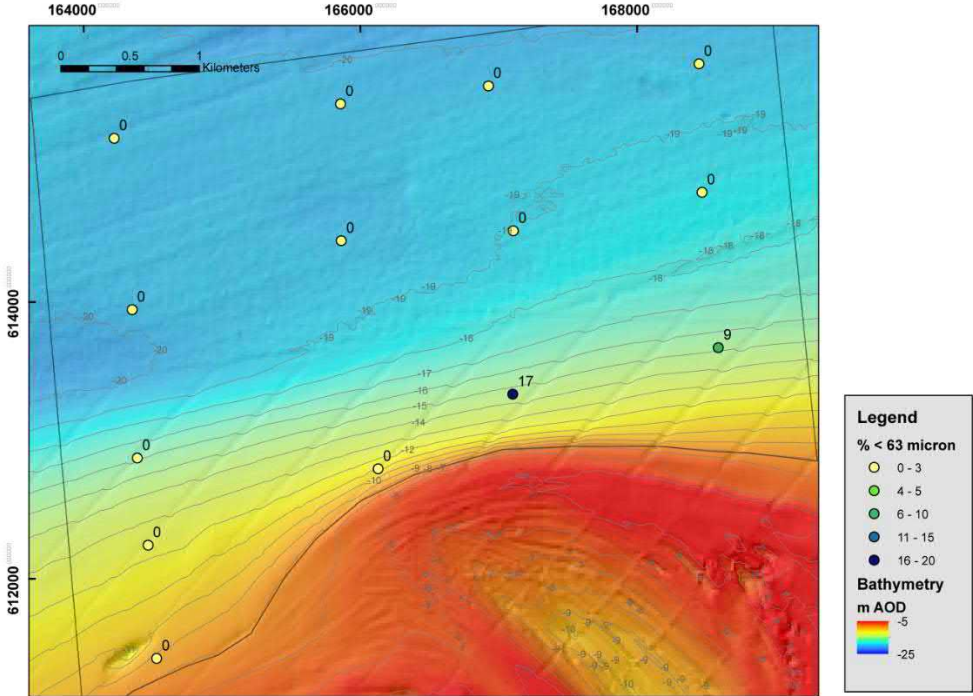


Figure 4.3 Overview of the mud percentage in the upper layer of the samples taken in 2017 (bathymetry compilation of depth soundings in the period 2009-2014)..

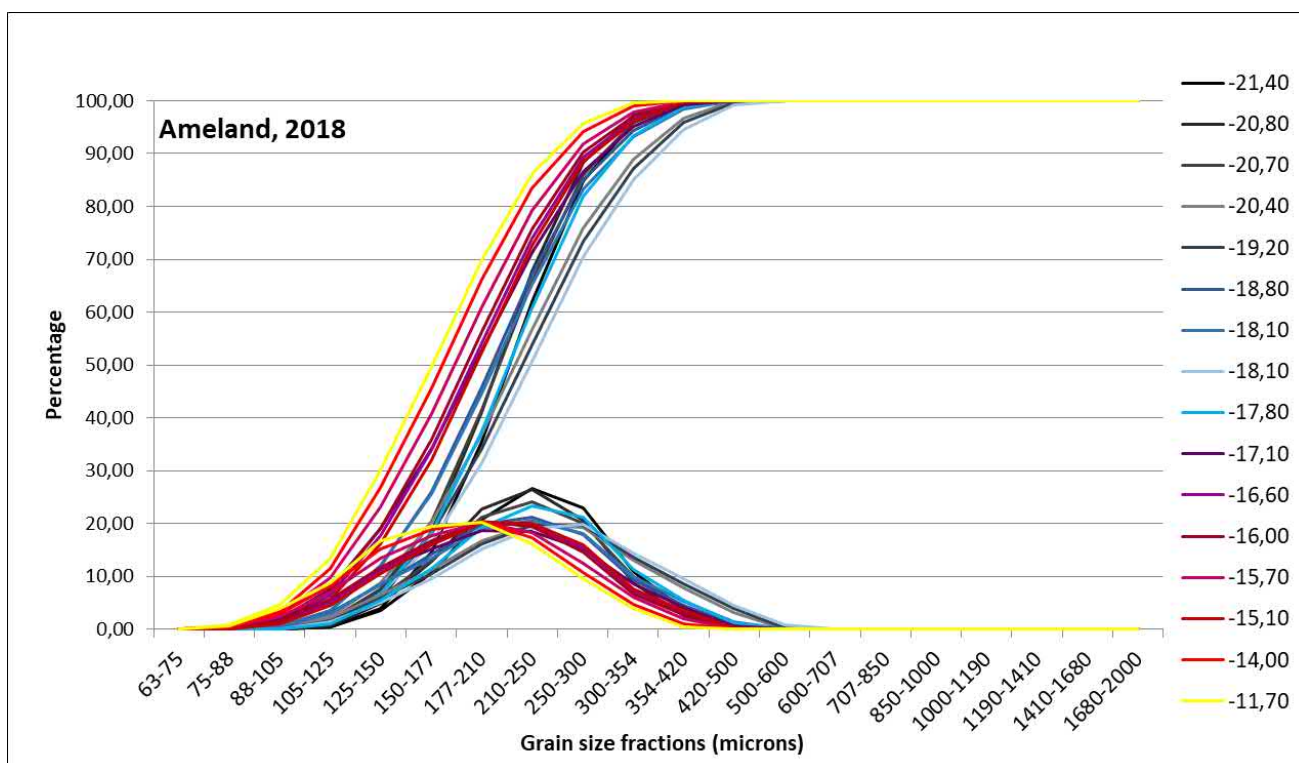
#### 4.2.3 Description of the observations box cores 2018

Table 4.2 gives an overview of the samples taken with rectangular box cores in the Amelander Inlet research area. The grain-size distributions for the rectangular box cores of 2018 are given in Figure 4.4 and 4.5. The samples of 2018 show the following characteristics:

- 1) They consist of sediments smaller than 500 microns and with a d50 <250 microns (Table 4.2).
- 2) As in the 2017 observations also in these observations there is a zone with a d50 up to ca. 200 microns and a deeper zone with coarser d50 values. These are here separated by the -15/-16m line (Figure 4.4). Below -18.1m d50 grain sizes are large, but variable. Using all samples an increase of d50 with increasing depth can be observed starting at -15.1 to -15.7m and ending around -18m.
- 3) Above -19m a fraction < 63 micron is sometimes present at either side of the ebb-delta lobe, but with higher percentages at the eastern side (Figure 4.6).
- 4) Many of the samples show a built up of 2 or more layers (Table 4.2 and Figure 4.7 to 4.12). Of these, the top layer is often more bioturbated than the lower layer(s); see below. The top layer is probably the result of the long and quiet period between February and September 2018.
- 5) Many box cores show that the physical structures of the lower layer are capped by an irregular upper surface (Figure 4.7) Some of these might be due to bioturbation during the more quiet part of the year (for example: AM2, AM10, AM11, AM13). However, in other box cores the layer above the irregular surface consists of physical structures, sometimes with a shell concentration at the base, pointing to reworking during a higher-energy event (for example: AM3, AM5, AM7, AM10 & AM15). The higher-energy event might be a storm with strong wave action influencing the seabed, the erosion caused by the passage of a ripple through, or beam trawling or scraping off the upper layer for fishery. The occurrence of an escape burrow from the irregular surface downward with at the end a death young sea urchin; AM10; Figure 4.10) suggests severe damage to the organism somewhere after spring. Similarly, dead doublets of the fast digging American jack-knife clam (AM1) suggest strong and sudden sediment removal. The observations might well point to fishery action.

**Table 4.2 Schematic description of the 2018 box cores in the Ameland Inlet research area. Volumetric percentage of sediment < 63 micron is given, as well the mean grain size (by volume) of the sediment d50. Presence of clay layers, physical structures, American jack-knife and sea potatoes given as: 0 = not present; 1 = present. Physical structures given as: ang = angular; par = parallel. Erosional surfaces are given at the depth they occur; bioturbation is given as: 0 = not present; 1 = traces; 2 = medium; 3 = abundant. Red = data from observations on board only. Layers indicated from 0 (top layer) downwards (first layer below = -1, etcetera).**

No	Coordinates		Water depth (m - NAP)	Lower boundary			Grain sizes		Physical structures	Biogene structures			Sea potato					
	x (m)	y (m)		0 (cm)	-1 (cm)	-2 (cm)	<63 in %	d (0.5) (microns)		Erosional boundary depth (cm)	0	-1		-2	0	-1	total	American Jackknife adults
AM01	668960	5931123	15.1	9	16.5		4	206	0	0	0	3	3	0	0	0	1	
AM02	668941	5931235	16	9	15.5		5	200	1	9	1 ang	1 par	3	1	1	0	1	1
AM03	668919	5931360	17.1	4	11		0	205	0	4	1 ang&par	1 ang	1	0	1	0	1	0
AM04	668901	5931468	18.1	4	6		4	220	0	4	1 par	1 par	2	2	1	0	1	0
AM05	668887	5931551	18.1	6	5		0	249	0	11	1 ang/par	1 ang	0	0	1	0	1	0
AM06	670872	5933116	19.2	0	0		0	242	0		1 ang/par		2	1	1	0	1	0
AM07	668848	5931781	20.4	7	4		0	236	0	5	1 ang	1 par	2	0	1	1	0	0
AM08	668685	5932737	21.4	3	11		0	232	0	11	1 ang	1 ang	3	1	0	0	0	1
AM09	668511	5933759	20.8	14.5			0	223		0			3	3	0	0	0	1
AM10	671147	5931502	11.7	5	9		5	178	0	5	0	1 ang	3	2	1	0	1	1
AM11	671128	5931613	14	4.5	15.5		4	184	0	4.5	0	1 angp	3	1	1	1	1	1?
AM12	671106	5931739	15.7				6	192		0	0		3	3	1	0	0	1?
AM13	671088	5931846	16.6	5	10		5	203	0	6	1 ang	1 par	3	2	1	1	1	0
AM14	671063	5931994	17.8	7	8	17	4	231	1		1 ang/par	1 ang/wav	0	0	1	0	1	1
AM15	671035	5932159	18.8	6	14		7	218	0	6	1 ang	1 ang	0	0	0	0	0	0
AM16	670872	5933116	20.7	4	9,5		0	224	0	?	0?	1 ang	1	0	1	0	1	0



**Figure 4.4 Grain size per size fraction and cumulative distribution for the sand fraction of the rectangular box core samples of the Ameland site, taken in 2018. Colours and figures right indicate depth with reference to NAP.**

- 6) Physical sedimentary structures are visible in most box cores in the lower layer(s), and often as well as the upper layer. They consist of large- to small-scale cross-bedding in 1 or 2 directions and parallel bedding. The latter is difficult to interpret, because it may be a parallel cut of cross-bedding or plane bedding due to very high (upper stage plane beds) or quite low (lower stage plane beds) current velocities. Sometimes irregular erosive surfaces (see below) are filled up by cross-bedding. The bi-directionality might be explained by tidal currents, but storm-driven currents might also be the cause. As for the example in Figure 4.7 (AM05) the different orientations of the cross-bedding infill directly on top of the erosional surface irregularity might be explained by currents generated by tides, storm-driven currents, or both. In AM14 (Figure 4.12) a small wave ripple might be present, suggesting the influence of wave action at greater depths (-17.8m).
- 7) Mud drapes are visible in AM14 (Figure 4.12) and point to very quiet hydrodynamic conditions. This might be the quiet phase after a storm when large amounts of fines can settle or the period around neap tide when current velocities are low.
- 8) Sedimentary structures in the upper layer of the box cores vary with water depth. In box cores collected down to ca. -15.6 (western profile: AM01) & -16.6m (eastern profile: AM10 to AM12) bioturbation is the only visible structure in the upper layer. In the zone below that physical structures and bioturbation are both present to water depths of -18.1m (western profile) and -17.8m (eastern profile). In the zone below that the upper layer only shows physical structures to water depths of -18.2m (western profile) and -18.8m (eastern profile). Still deeper and further out of the coast bioturbation in the upper layer becomes more important, resulting in dominant bioturbation in the locations far from the coast (AM09 and AM06). In most cases the burrowing action of the sea urchin is responsible for bioturbation. The changes might be explained by the presence of food which enhances biotic action. In most cases abundant bioturbation coincides with the occurrence of mud in upper layer (see table 4.2), which is normally food rich.

Especially for the deeper water zone the lack of storms during the long and quiet period from February to September of 2018 might be an explanation for the lack of physical structures in the upper layer: physical structures were probably originally present, but have been reworked by bioturbation. The fact that upper layers consist only or partially of physical structures in the zones between -14.5m to -17.2m shows that current activity is relatively important when compared to bioturbation. As these deposits in the upper layer are most likely formed relatively recently and internal erosional structures are not strongly developed (which might be expected during winter) it seems likely that the sedimentary processes are governed by tidal currents. In the layer below the upper layer physical structures are more dominant (table 4.2). These may partially have been formed by tides and partially by higher energy events, which is also illustrated by the erosional surface which often separates the upper from the lower layer.

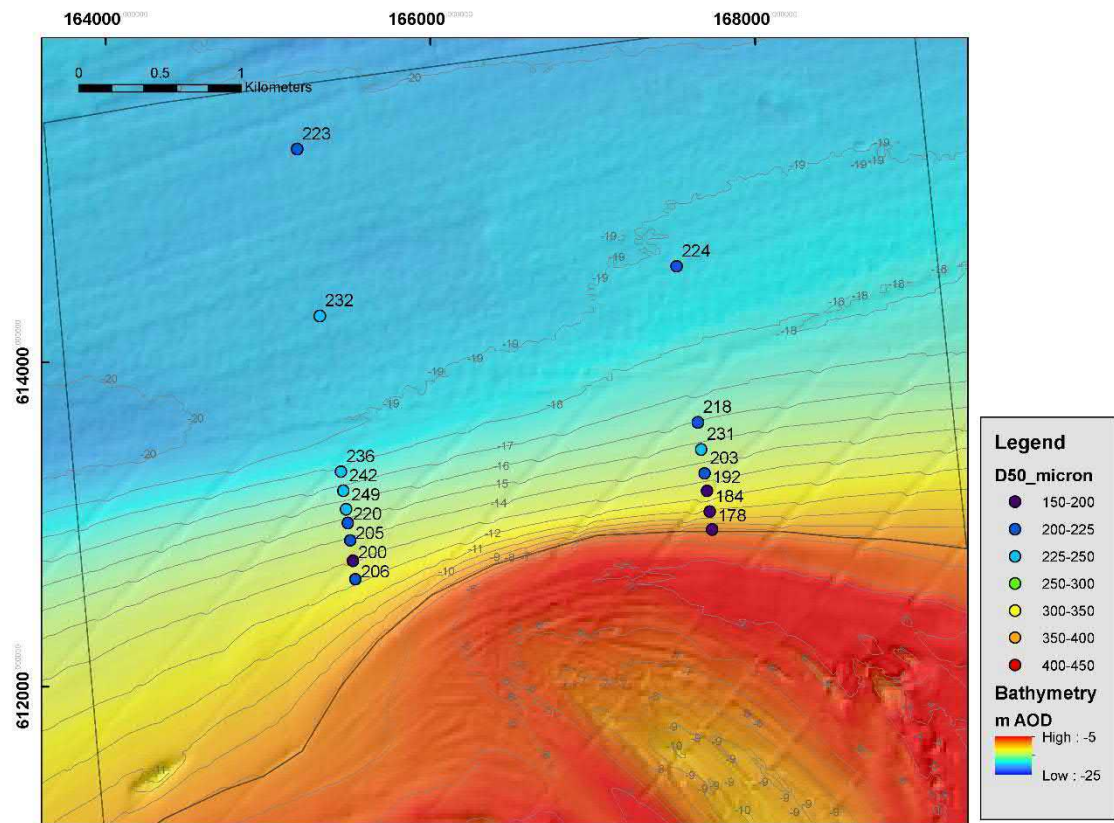


Figure 4.5 Overview of the grain sizes in the upper layer in 2018(bathymetry compilation of depth soundings in the period 2009- 2014).

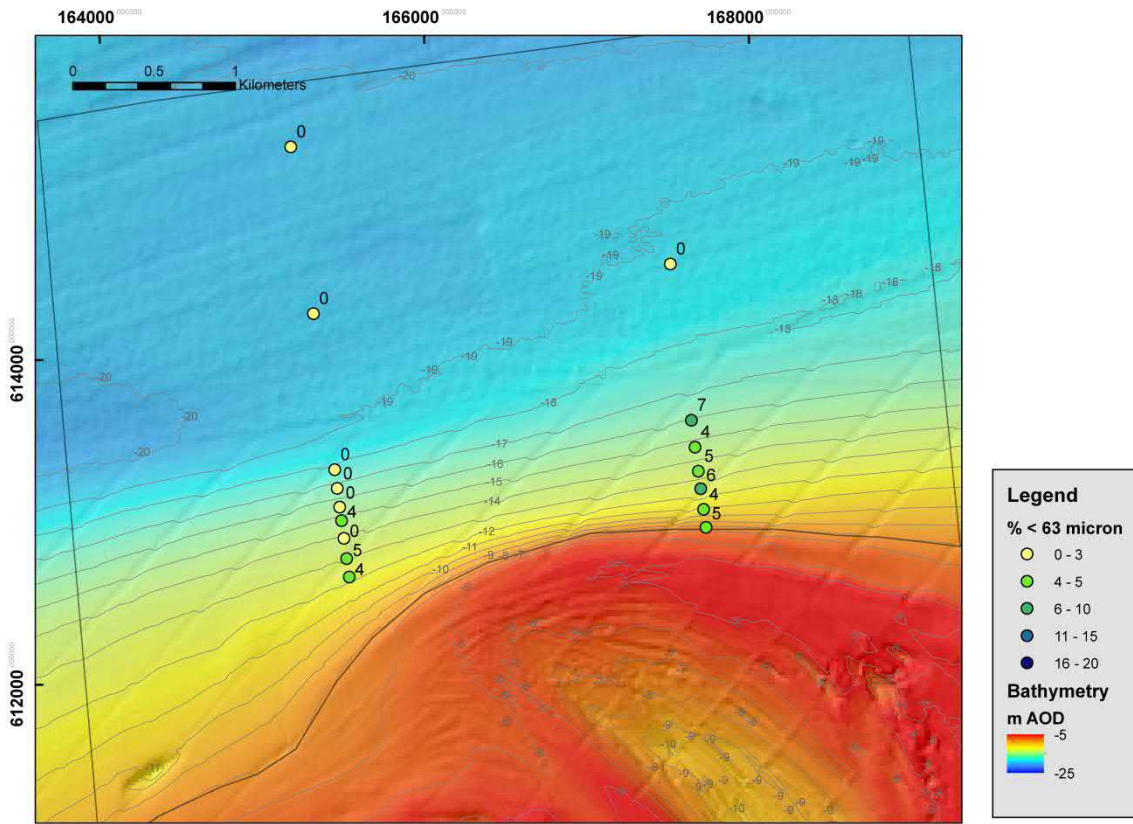


Figure 4.6 Overview of the mud percentage in the upper layer of the samples taken in 2018 (bathymetry compilation of depth soundings in the period 2009- 2014).



Figure 4.7 AM05: foresets in two directions caused by bidirectional currents in the lower and the upper part of the core. A doublet of a horizontally lying American jack-knife is present just below the erosion surface in the shell lag, pointing to sudden sediment removal and the formation of a shell lag which was washed out. The somewhat swaly (wavelike) upper deposits directly above it fill up the erosional surface.

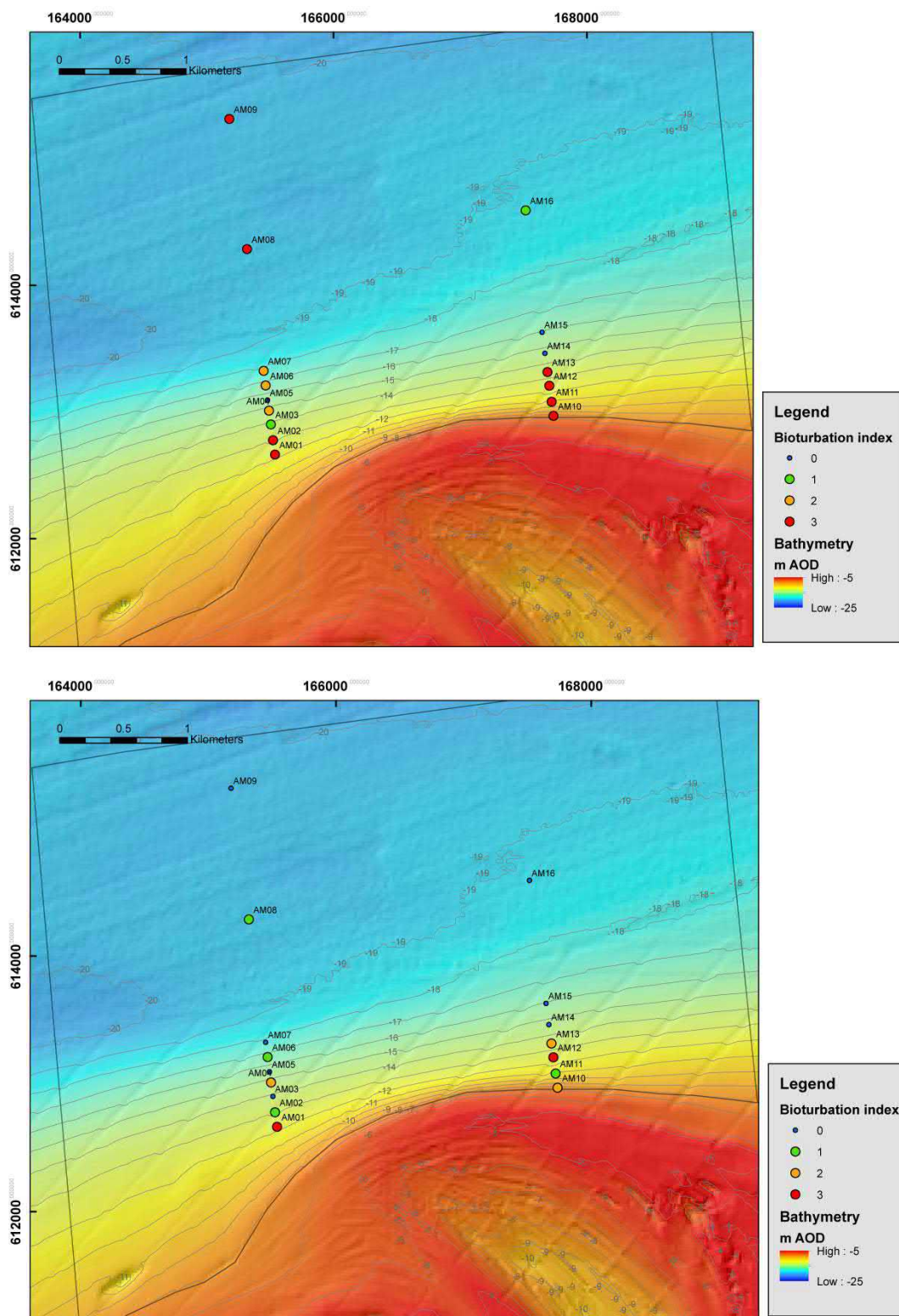
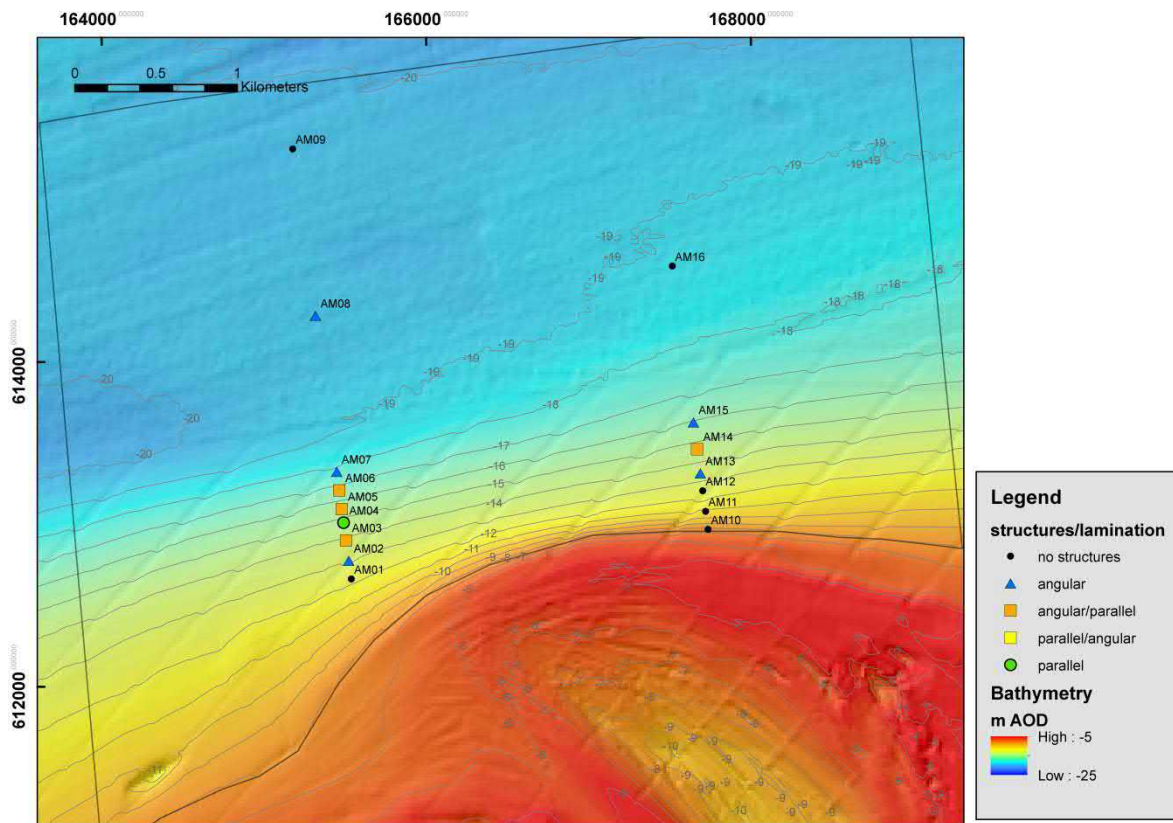


Figure 4.8 Bioturbation upper layer (above) and lower layer (below) of the box cores of 2018. Intensity comparable to table 4.4 (bathymetry compilation of depth soundings in the period 2009- 2014).



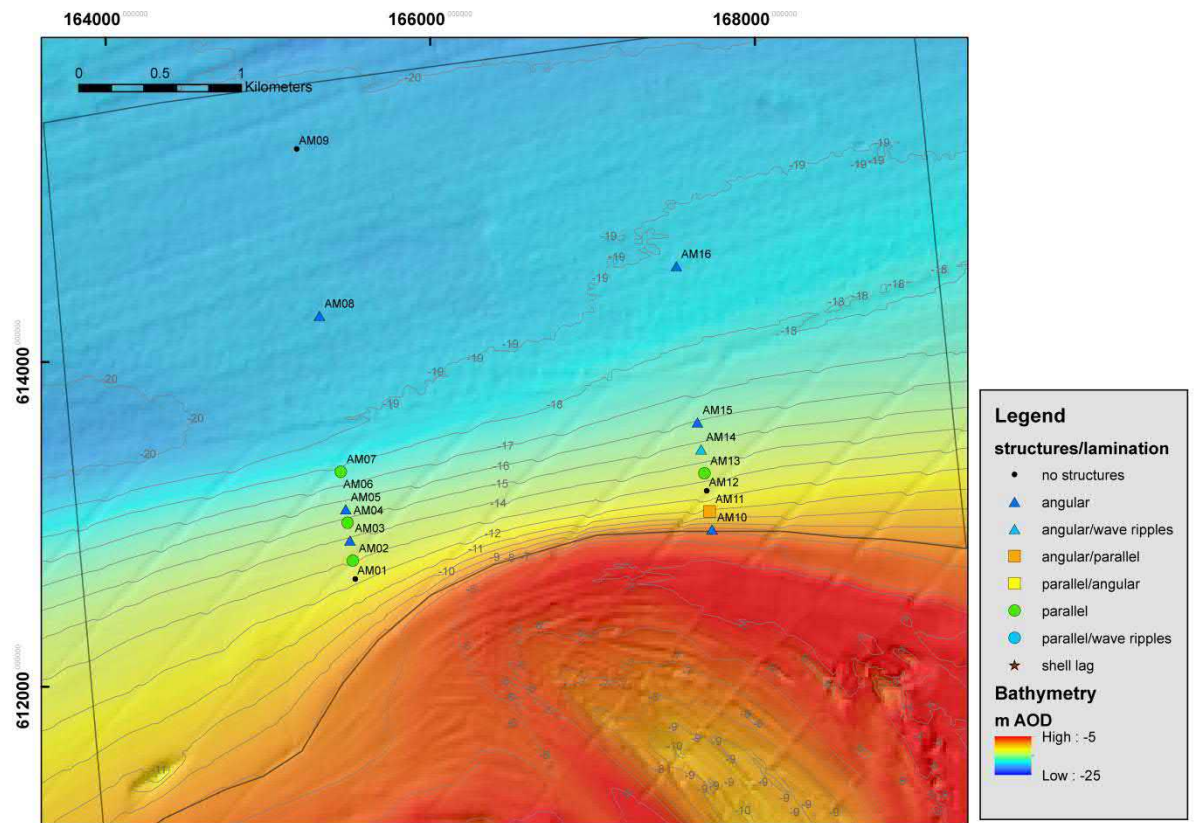


Figure 4.9 Structure upper layer (above) and lower layer (below) of the box cores of 2018. First structure mentioned dominates (bathymetry compilation of depth soundings in the period 2009- 2014).

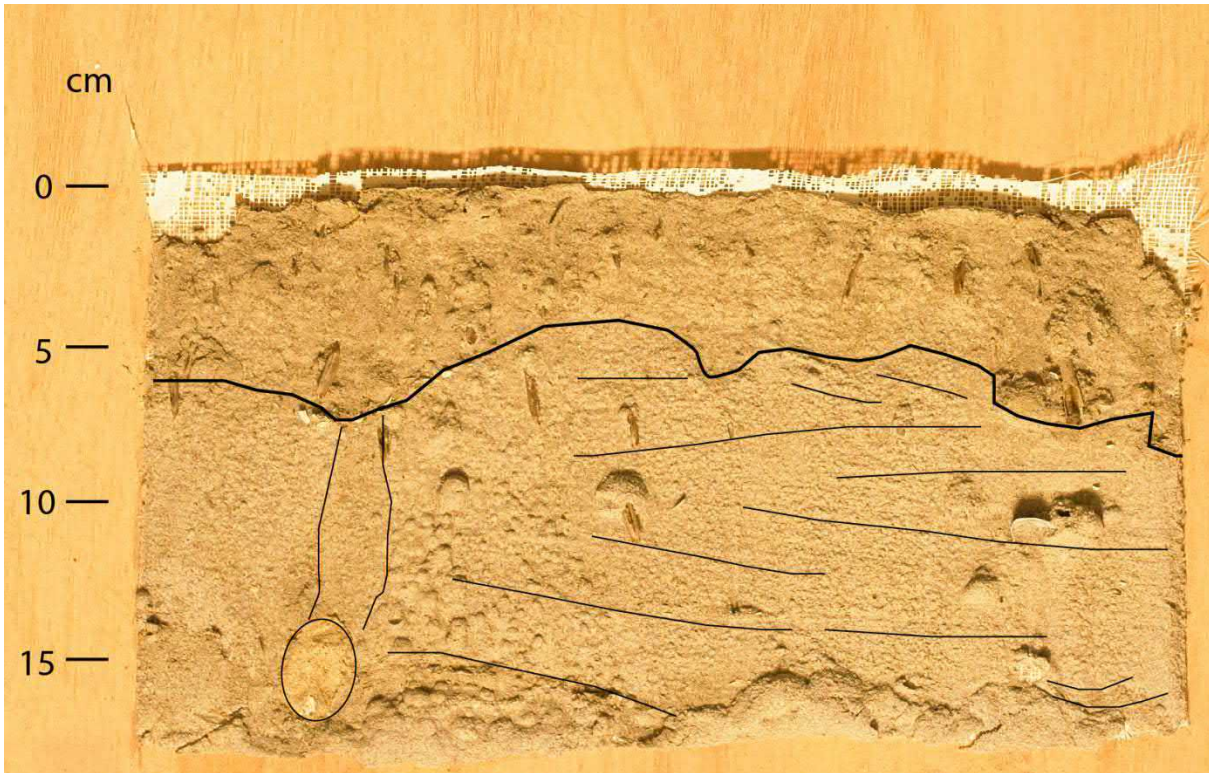


Figure 4.10 AM10: erosional surface (top black line) with downward escape burrow of the sea potato (left side of the panel) with the dead animal (oval) at the end. More to the top abundant juvenile American jack-knife clams can be observed.

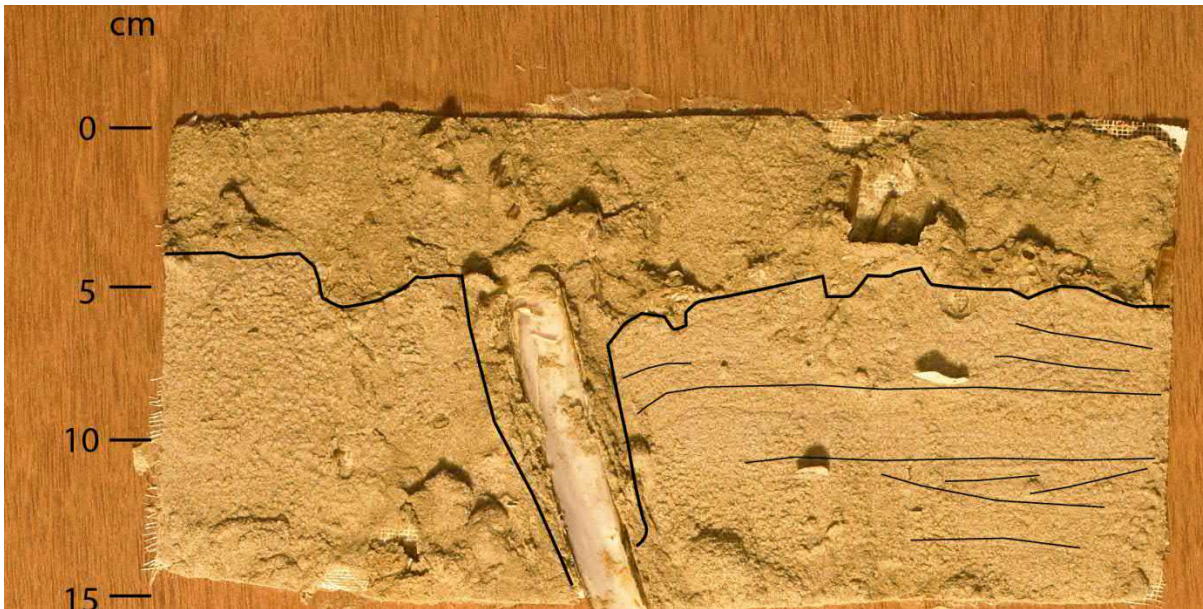


Figure 4.11 AM11: parallel bedding possibly due to high currents at the lower part and bioturbated sediment in the upper part. An irregular surface is separating the two. The American jack-knife tried to escape from sampling and retreated to deeper levels. Cm scale to the left.

- 9) Living American jack-knife clams were present in most box cores, see e.g. Figure 4.11; with exception of AM01, AM08, AM09 and AM15. Adult specimen have been observed

in AM07, AM11, AM13 and AM14, thus at the slope of the ebb-tidal delta lobe. Shell layers are especially well developed from halfway the front of the ebb-tidal delta lobe (at least from -16.6m onwards; AM03, AM05 & AM13), but may occur in water depths up to -18.9m (AM07).



Figure 4.12 AM14; physical structures are the dominant structures in this core. Bi-directional foresets indicate two current directions. Clay drapes (in yellow) indicate very low current velocities enabling settling of fines. Erosion is filled in by small ripple foresets (below upper mud layer). Above the upper clay drape large-scale foresets are present with some smaller ripples intercalated. The latter might be due to wave action or result from backflow at the base of a larger ripple.

#### 4.2.4 Interpretation

The increase in grain size towards deeper water may have several explanations. The deposits are largely underlain by older channel deposits. As a result of erosion, the coarser grains will form a lag deposit which will be found especially in deeper waters. At shallower depths (part of the) finer sediments can still be present resulting in smaller grain sizes. Another explanation is that tidal forces are larger in deeper water than in shallower depths allowing only coarser grain sizes to remain in deeper parts of the deeper shoreface. On top of that hydrodynamic modelling indicates that a relatively weak landward directed bottom current may lead to winnowing of the sediments in that direction. The current is brought about by the combination outflow near the surface of the less saline currents from the backbarrier, balanced by a coastward directed density driven bottom current (Grasmeijer et al., 2019). As for the shallower reaches of the deep shoreface another factor is likely that the Ameland inlet brings out finer sediments from the Wadden Sea. The latter might explain the marked grain size differences with much finer deposits in the shallower part of especially the more sheltered eastern profile as compared to the western profile.

Many cores show a top layer that was probably formed during the long quiet period between February and September 2018. In several cases it is separated from the underlying sediment layer by an irregular surface which is sometimes characterized by a high shell content. This points to a higher-energy event. In some cases, it is likely that this was due to bottom-trawling fishery; in other cases, it can be due to storms with waves reaching deeper water levels and relatively large currents or due to passage of ripple troughs. The physical structures present in the upper and deeper layer(s) are formed by tidal currents in two directions and perhaps to occasional higher energy events. In the top layer, bioturbation is important in the shallower reaches and in the deeper reaches. In between bioturbation did not rework the original structures completely, pointing to a relative smaller role for bioturbation there. This pattern is not yet fully understood.

### 4.3 Box cores Terschelling research area

#### 4.3.1 Introduction

In 2017 16 round box cores have been collected along four profiles perpendicular to the coast, namely (ordered in increasing depth): BC13-BC16; BC09, BC08, BC02 & BC01; BC11, BC03, BC12 & BC04. Water depths vary between -9.6 and -20.4m.

In 2018 10 rectangular box cores were collected along one transect between -12.4 and -19.4m (TS01-TS10). The remaining 6 cores have been taken in deep water (around -20m) and is concentrated in a zone where sediment-starved ripples seem to occur according to multibeam observations.

#### 4.3.2 Description of the observations round box cores 2017

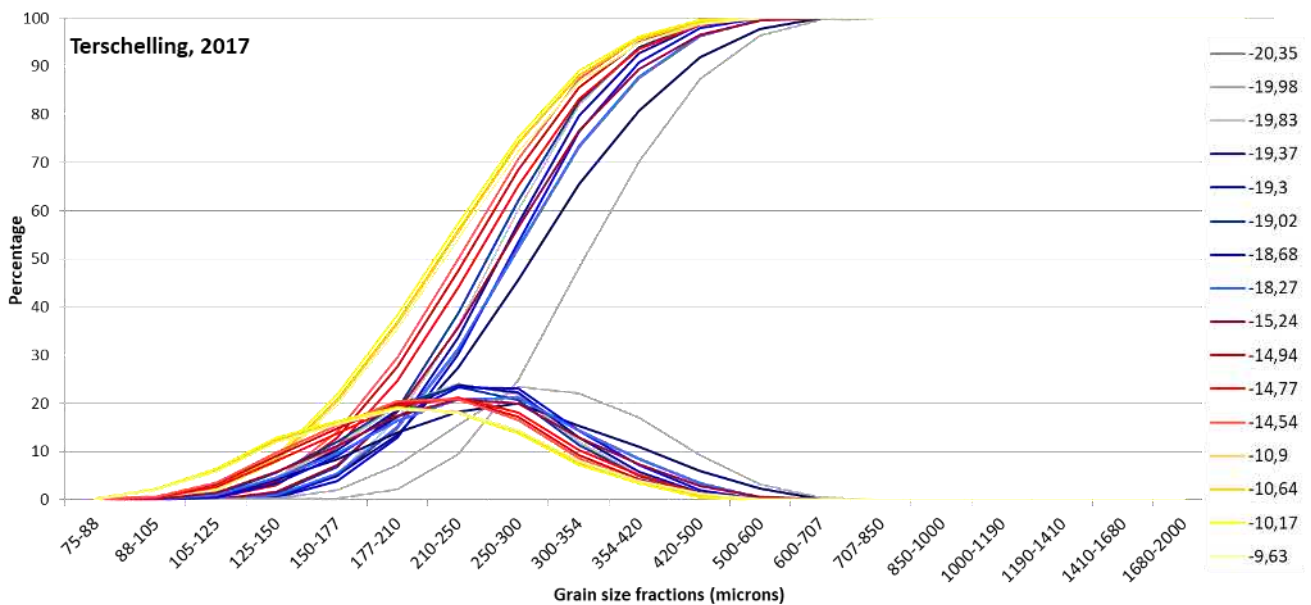


Figure 4.13 Grain size per size fraction and cumulative distribution for the sand fraction of the round box core samples of the Terschelling site, taken in 2017. Colours and figures right indicate depth with reference to NAP.

Table 4.3 Detailed analysis of the lower shoreface deposits in the Terschelling research area based on round box cores of 2017 description. BN=Borehole number. SA=shell abundance: 0=absent, 1=traces, 2=few, 3=many. Shell species: Spi=Spisula, Car=Cardium, Don=Donax, Ens=Ensis, Myt=Mytilus, Mac=Macoma, Ang=Angulus. WD=Water Depth. d50 = 50% percentile (by volume) grain diameter as determined with (Malvern).

Box core number	SA	Spi	Car	Don	Ens	Myt	Mac	Ang	WD (m NAP)	d50 (microns)
1	1	0	0	0	0	0	0	0	-20.0	304
2	3	1	0	3	0	1	0	0	-19.4	260
3	3	0	1	3	0	0	1	0	-14.5	210
4	1	1	0	1	0	0	0	1	-19.3	237
5	1	0	0	0	0	0	0	0	-19.8	232
6	2	2	0	2	0	0	0	0	-18.7	244
7	1	0	0	1	0	2	0	0	-14.9	214
8	1	1	0	2	0	0	0	0	-15.2	237
9	1	1	0	0	1	0	0	0	-10.6	199
10	2	2	1	0	0	0	0	1	-10.9	200
11	3	3	0	0	0	0	0	0	-10.2	197
12	1	1	0	0	0	1	0	0	-18.3	245
13	1	1	1	0	1	0	0	1	-9.6	202
14	3	1	0	2	0	0	0	2	-14.8	220
15	2	3	1	0	0	0	0	2	-19.0	229
16	3	3	3	1	0	0	1	0	-20.4	246

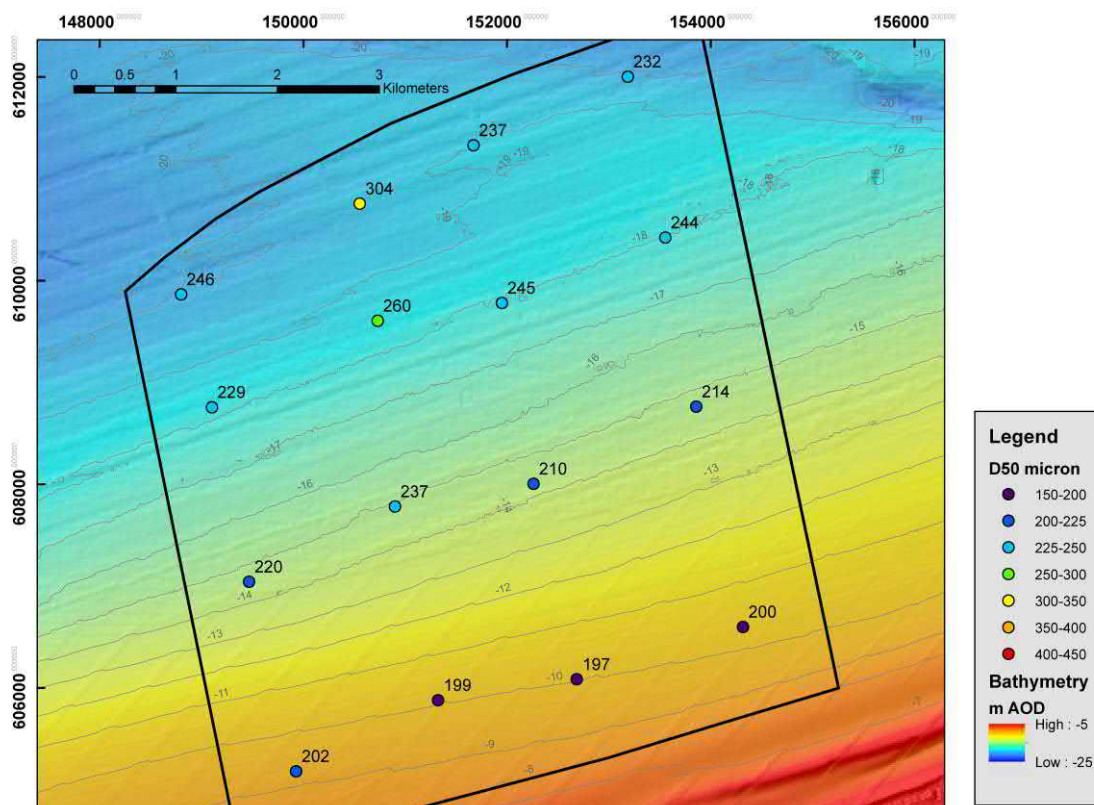


Figure 4.14 Overview of the d50 grain sizes in the upper layer of the samples taken in 2017. Note the pattern of increase in grain size in a seaward direction (bathymetry compilation of depth soundings in the period 2009-2014).

## Grain-size distributions

The grain-size distributions for the samples taken from the round box cores of 2017 are given in Table 4.3 and Figure 4.13. The samples consist mainly of sand of less than 600 microns and a d50 larger than 200 microns (Table 4.3). As was the case for the Ameland area, the sediments are mainly around 200 microns in the upper zone whereas below -15m the grain sizes are large (Figure 4.14). Below -18.7m d50 grain sizes are large, but variable. An increase of d50 with increasing depth can be observed to start somewhere between -9.6 and -10.2m and (leaving one point out at -14.8m out) ending between -18.3 to -18.7m. A mud-fraction is absent in the samples.

## Fauna

Table 4.3 and Figure 3.4 present the faunal assemblage and grain size of the lower shoreface deposits. Shell abundance is low to very high across the area with no clear spatial pattern. *Donax*, *Spisula*, *Angulus*, and *Macoma* are the most abundant species.

### 4.3.3 Description of the observations rectangular box cores 2018

The box cores in the Terschelling research area are mainly taken along one transect between -12.4m and -19.4m (TS01-TS10). The remaining 6 cores have been taken in water around -20m in a zone where sediment-starved ripples seem to occur according to multibeam observations of 2017. Table 4.4 gives an overview of the samples taken in 2018 in the Terschelling research area. The grain-size distributions for these box cores are given in Figure 4.15 and 4.16.

*Table 4.4 Schematic description of the box cores in the Terschelling research area. Volumetric percentage of sediment < 63 micron is given, as well the median size of the sediment d50. Presence of clay layers, physical structures, American jack-knife and sea potatoes given as: 0 = not present; 1 = present. Physical structures given as: ang = angular; par = parallel. Erosional surfaces are given at the depth they occur; bioturbation is given as: 0 = not present; 1 = traces; 2 = medium; 3 = abundant. Red = data derived on board to be considered as tentative data. Layers indicated from 0 (top layer) downwards (layer below = -1, etcetera).*

No	Coordinates		Water depth m -NAP (cm)	Lower boundaries			Percentag Grain sizes			Physical structures			Biogene structures			Sea potato				
	x (m)	y (m)		0	-1	-2	-3	< 63	d (0.5)	clay layers present	Erosional boundary (cm)	0	-1	-2	0		-1	-2	total	adults
TS01	655454	5924791	12.4	9	12		0	218	0	9	1 ang	0	1 ang	1	2	0	1	0	1	0
TS02	655415	5924937	12.8	8	12		0	220	0	8	1 ang/1par	1 ang	0	2	1?	0	1	0	1	0
TS03	655391	5925074	13.2	15			0	208	0		1 par	0	1 par	2	3	0	1	0	1	1
TS04	655351	5925228	13.6	9			0	211	0		0			3			1	1	1	1
TS05	655290	5925508	14.3	10	11		0	213	0	10	0	shell lag		3	0		1			1
TS06	655226	5925793	14.9	14			0	217	0		0			3	1		1	1	1	1
TS07	655135	5926202	16	2	11	14		216	0		1 par	0	1 par/1 ang	3	3	0	1	0	1	1
TS08	655019	5926739	17.1	11	12		0	229	0	11	1	shell lag		3	0		0	0	0	1
TS09	654926	5927162	17.9	4	12	14		250	0	9	1 ang/1par	1 par/wav	1 ang	2	0	0	1	0	1	1
TS10	654591	5928676	19.4	4	14.5		0	250	0	4	0			2			1	1	0	0
TS11	652603	5927829	20.2	4	10	16		230	0	6	1 ang	1 par		0	0		1	0	1	0
TS12	652633	5927838	20.5	6	9	15	16	234	0	5	1 ang	1 ang	1 ang	2	0	0	1	0	1	0
TS13	652658	5927850	20.3	5	7.5	11.6	16	242	1	4	0	1 ang	1 par/ang	3	0	0	1	0	1	0
TS14	652673	5927859	20.2	1	15		0	256	0		1 par	1 ang		1	0		1	0	1	0
TS15	652668	5927808	20.8	7	15		0	244	0	9	1 par/ang	1 ang		2	0		1	0	1	1
TS16	652647	5927718	20.6	1	14		0	248	0	1	0			2			0	0	0	0

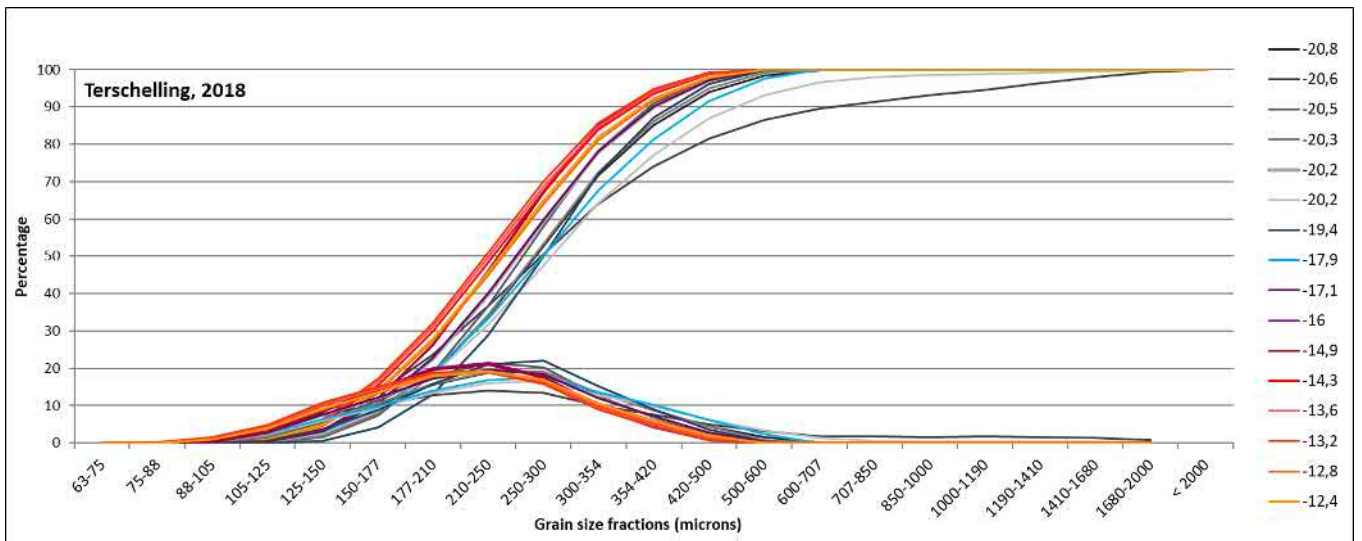


Figure 4.15 Grain size per size fraction and cumulative distribution for the sand fraction of the rectangular box core samples of the Terschelling site, taken in 2018. Colours and figures right indicate depth with reference to NAP.

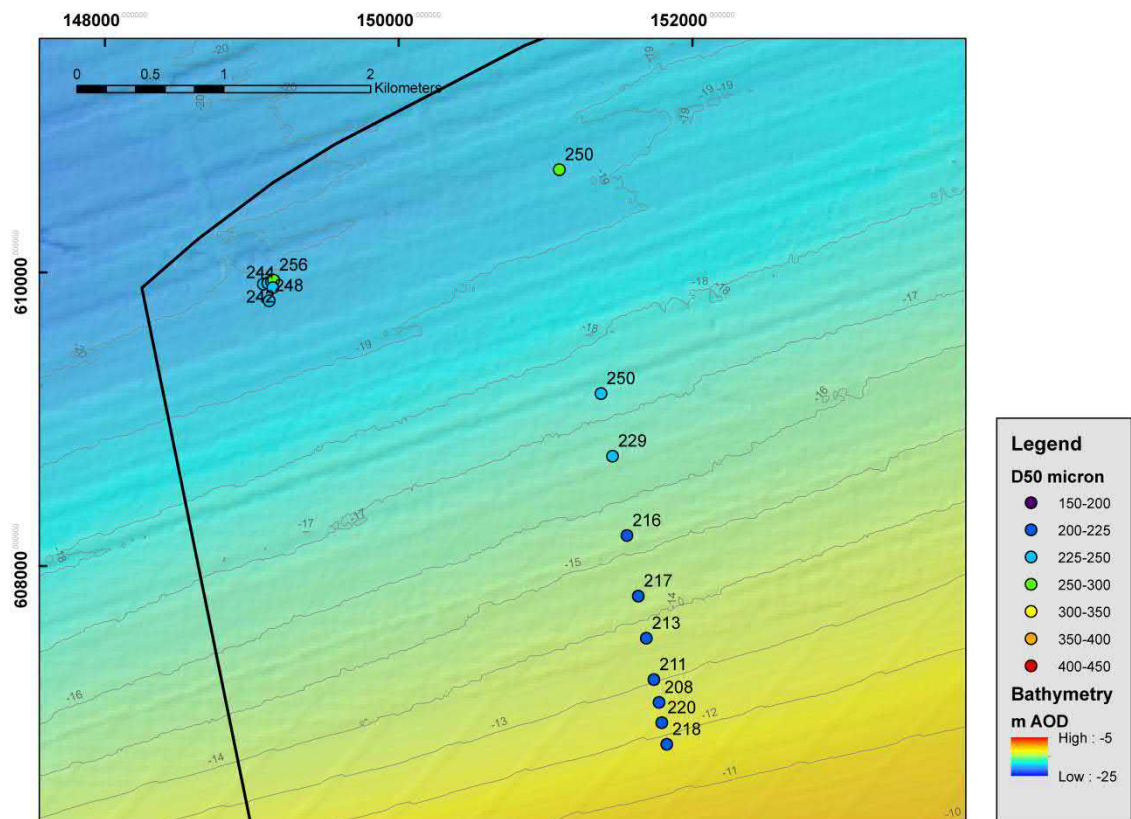


Figure 4.16 Overview of the grain sizes in the upper layer at the Terschelling area (bathymetry compilation of depth soundings in the period 2009- 2014).

The box cores along the profile (TS01-TS10) show the following characteristics:

- 1) They consist mainly of sand of less than 600 microns and a d50 larger than 200 microns (Figure 4.16; Table 4.4). A mud-fraction is absent in the 2018 samples, which is

comparable to the 2017 samples. The larger grain sizes occur mainly in deeper reaches. Below -17.8m d50 grain sizes are large and variable. An increase of d50 with increasing depth starts between -12.8 and -13.2m and (leaving one point out at -16m out) ends between -17.9 to -19.4m. Guillén & Hoekstra (1996) observed a similar trend for the Terschelling area.

- 2) Many of the profiles show a built up of 2 or more layers (Figure 4.17 and Figure 4.18). Of these the top layer is often more bioturbated than the lower layer(s); see below. The structure of the top layer is considered to be the result of the long and quiet period between February and September 2018.
- 3) Many box cores show a disruption of the physical structures of the lower layer with an irregular upper surface. Some of these might be due to bioturbation during the summer half year of 2018 (for example: TS02). However, in other box cores the layer above the irregular surface comprises physical structures, sometimes with a shell concentration at the base, pointing to a high-energy event (for example: TS09). Shell layers are encountered as the upper part of the lower disturbed layer at -14.3m (TS05) and -17.1m (TS07). As in Ameland, high energy events due to storms and large waves or due to fishery can be the cause of the formation of the disturbed layer. In three cases TS09 (-17.9m), TS13 (-20.3m) and TS12 (-20.6m) there are relatively strong indications of storm and related wave influences (see text Figure 4.19 & Figure 4.18).
- 4) Foresets of larger ripples (sometimes bi-directional, indicating to 2 current directions; Figure 4.17; Figure 4.18) are visible in many box cores in the lower layer(s), as well as in the upper layer, except in water depths between -13.6 and -14.9m (TS04-TS06) and at -19.4m, where bioturbation has obliterated all physical structures. Also, parallel bedding is present in several cases. As discussed for the Ameland case attribution to a process is uncertain.
- 5) Bioturbation occurs on all water depths along the profile, especially in the upper layer. However, it is especially strong from -13.2 to -17.1m (Table 4.4). In that zone bioturbation is mainly caused by the sea potato (TS03; Figure 4.20 & Figure 4.21) and the American jack-knife clam, the latter being less abundant than in the Ameland area. Mark that the main bioturbation zone -13.2 to -17.1m differs in depth from Ameland area (above -14.5m and below -17.2m).

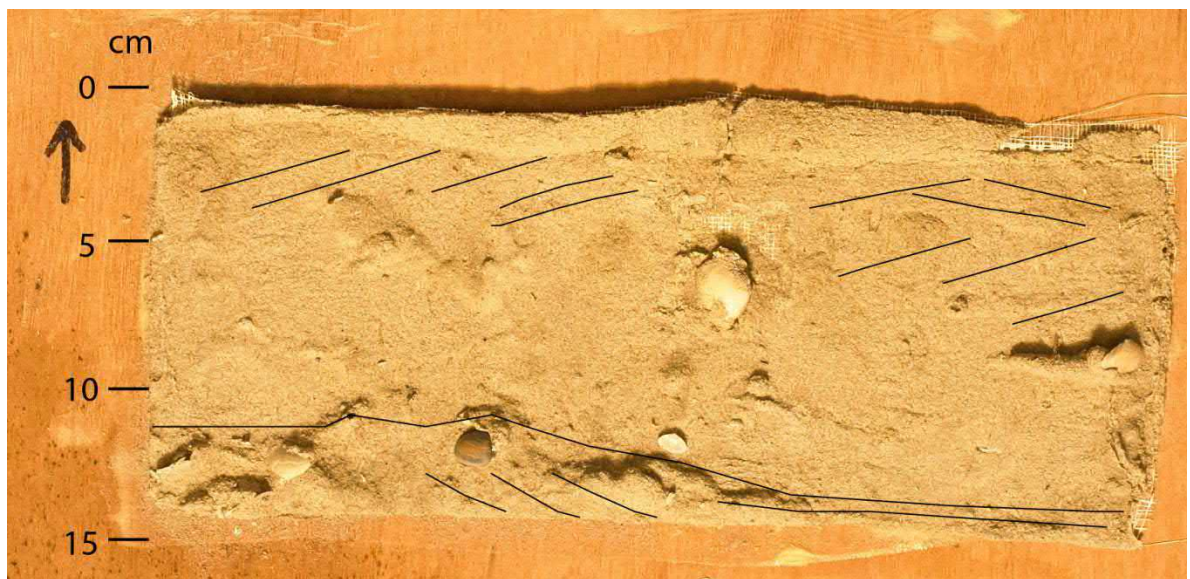


Figure 4.17 TS01 two layers separated by an erosional boundary (black continuous line at -12 cm). Bi-directional foreset orientation indicates two current directions. In the upper layer the physical sedimentary structures are partly obliterated by bioturbation. *Spisula elliptica* shell burrow is visible in the centre.

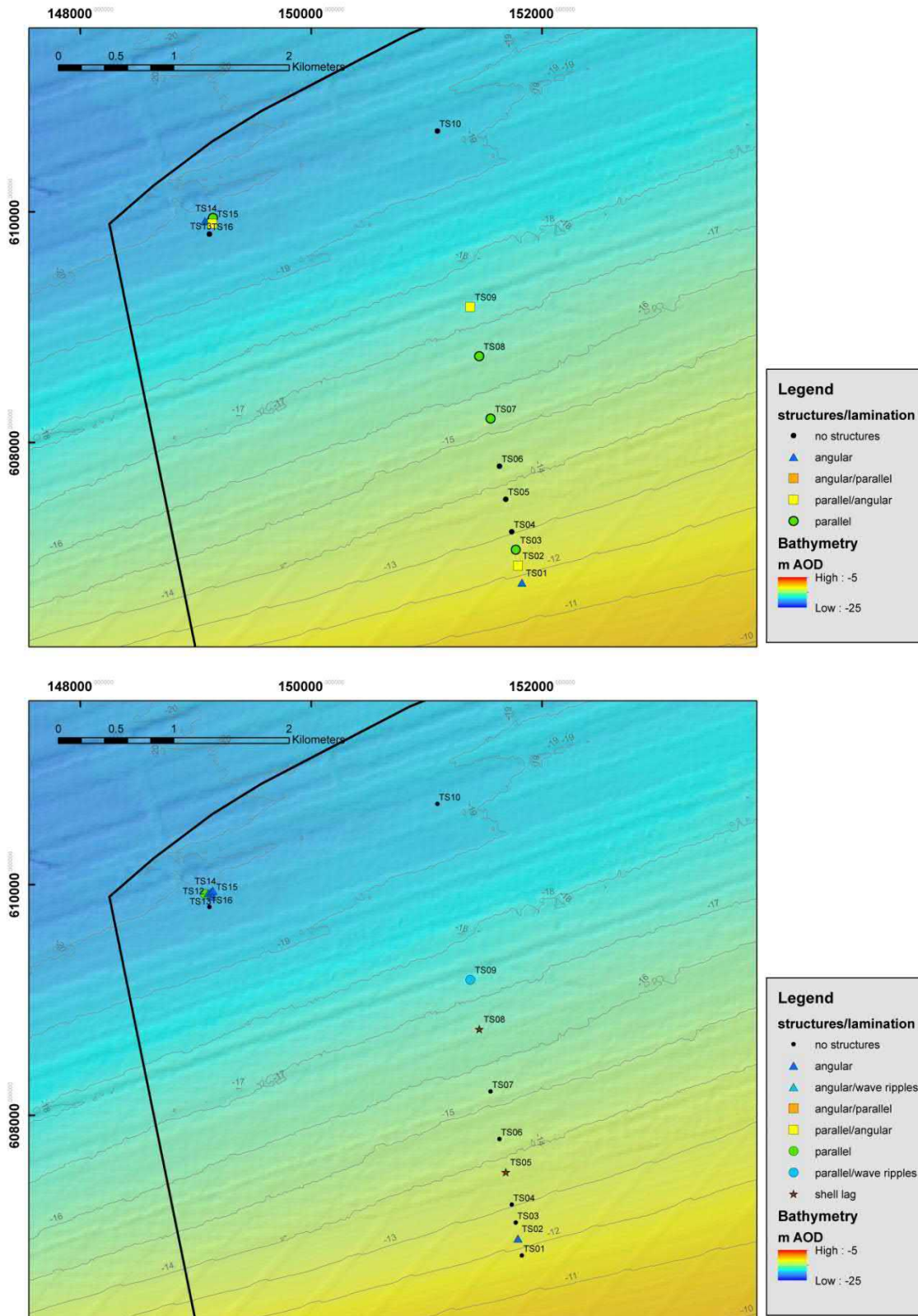


Figure 4.18 Structure upper layer (above) and lower layer (below) of the box cores of 2018. First structure mentioned dominates (bathymetry compilation of depth soundings in the period 2009-2014).



Figure 4.19 TS13 foresets at the base of the lacquer profile, truncated by parallel to swaly bedding (possibly indicating storm wave influence on the seabed and relative high bed shear stresses) truncated by a distorted shell layer (indicating wash out and even higher energy conditions) which is overlain by foresets followed by a clay drape, indicating a marked decrease in bed shear stresses. This is followed by bioturbation at the top. The whole sequence might be explained by deposition by tidal currents (foresets in the deepest part), followed by sedimentation under wave influence during a storm (swaly parallel bedding), followed by even stronger currents which washed out a part of the sediment and left a shell bed behind. Thereafter storm influence on the sea bed disappeared and clay was deposited. Later, bioturbation obliterated sedimentary structures are in the top layer.

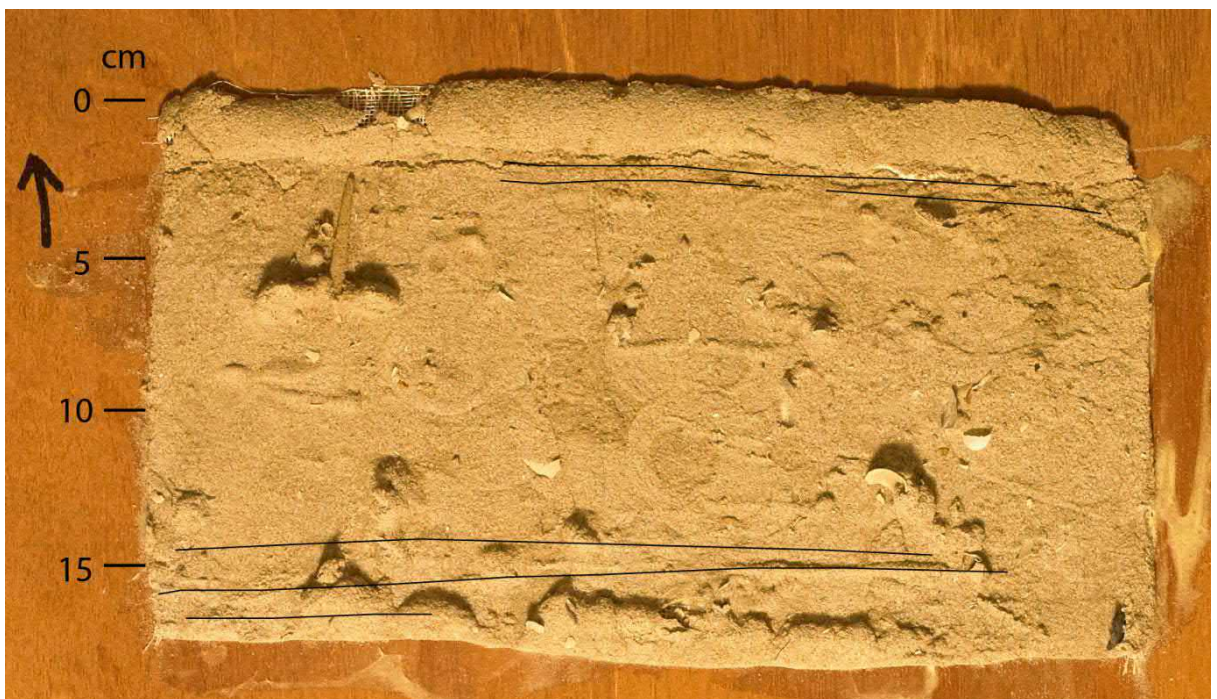
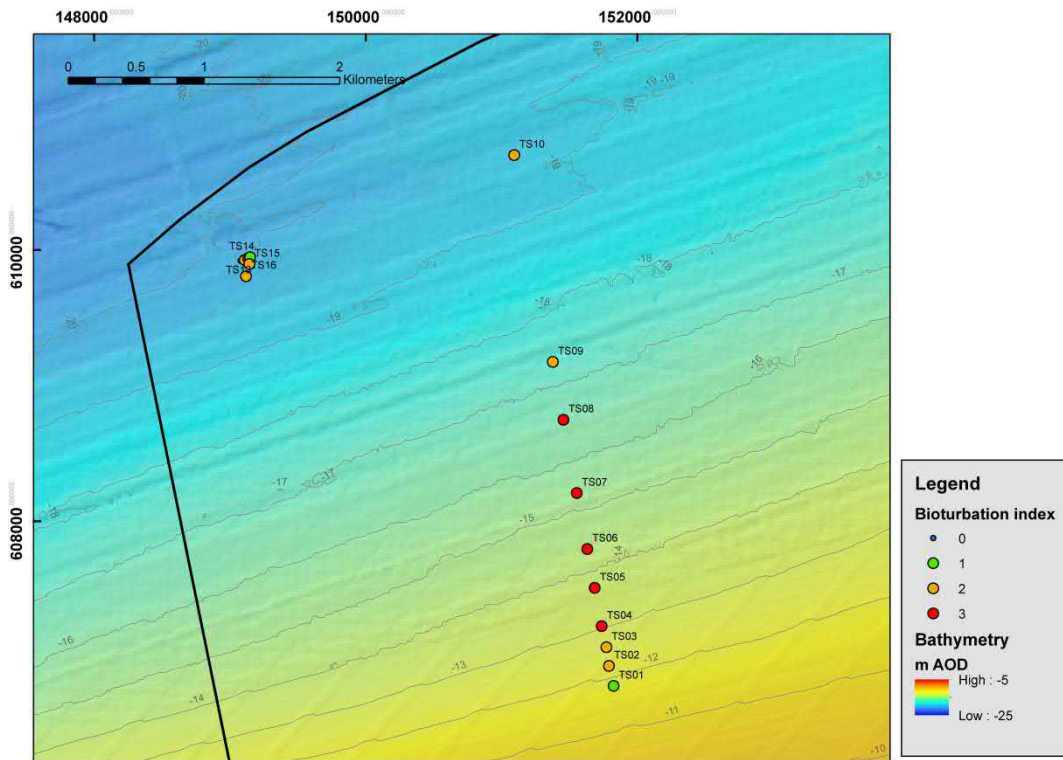


Figure 4.20 TS03 the circular features are bioturbation traces of the sea urchin ('sea potato'). Compare figure 2.4 when it was still fresh.



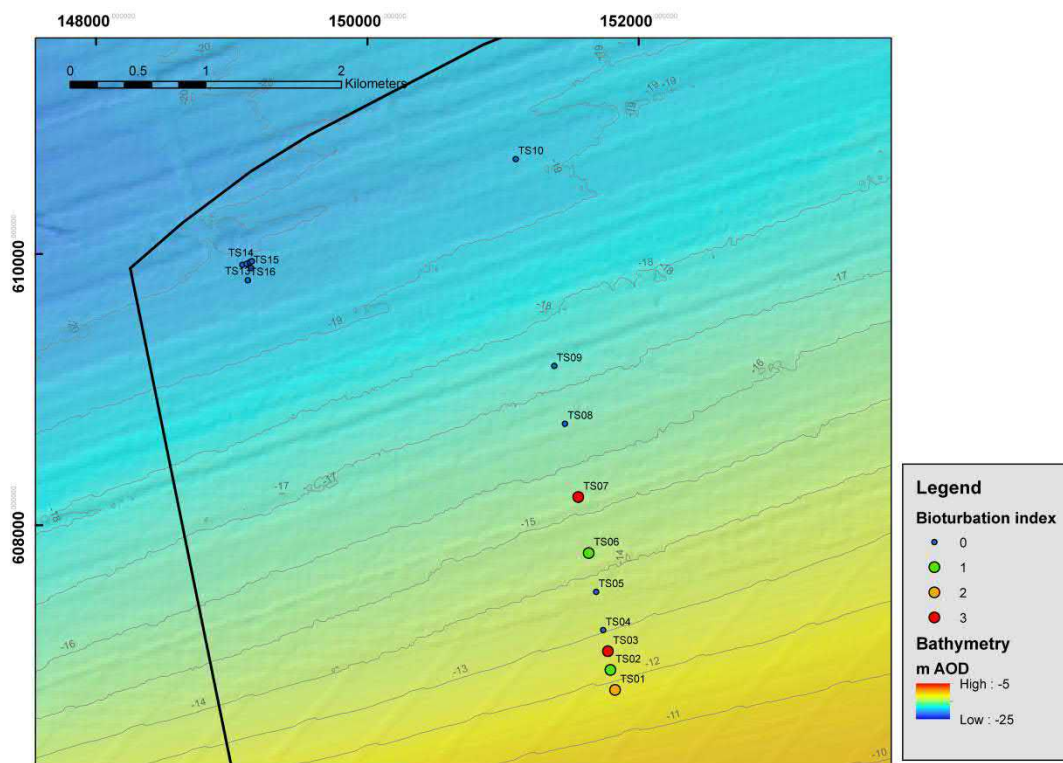


Figure 4.21 Bioturbation upper layer (above) and lower layer (below) of the box cores of 2018. Intensity comparable to table 4.5 (bathymetry compilation of depth soundings in the period 2009- 2014).



Figure 4.22 TS14 cross-bedded shell lag which has been truncated at the upper level: area of the starved sediment ripples.

- 6) For the samples that were collected at the NW side of the Terschelling area (TS11-TS16) at water depths of approximately -20m, it occurs that in general the grain sizes and bioturbation level of these sediments do not strongly differ from the sediments from shallower water depths. This with exception of cores TS14 (Figure 4.22) and TS16, which both to a large extent consist of a massive sandy shell layer. They show angular bedding and are reminiscent of channel lag shell deposits. Large ripples are most likely insufficient to explain these thick shell layers.

#### 4.3.4 Interpretation

The increase in grain size towards deeper water may have several causes. One cause might be that the large part of the subsurface exists of subfossil channel deposits (Chapter 3.3.3) which are near or on the surface (see figure 4.22), due to erosion of these deposits during Holocene coastal retreat. With increasing depth tidal current strength increases resulting in a washing out of the finer fractions. Furthermore hydrodynamic modelling indicates that a relatively weak landward directed bottom current is present which may lead to winnowing of the sediments in that direction. The current is brought about by the combination outflow near the surface of the less saline currents from the backbarrier, balanced by a coastward directed density driven bottom current (Grasmeijer et al., 2019). Another cause might be transport during storm conditions of finer grain sizes from the higher shoreface towards deeper water where energy is low enough to allow deposition, as proposed by Cleveringa (2000). However, the importance of such processes is still an open question.

Many box cores show several layers of which the top layer was in most cases probably formed during the quiet long period between February and September 2018. In several cases the layers are separated by an irregular layer, sometimes characterized by a shell layer. This points to a high energy event. In some cases, it is likely that this was due to bottom-trawling fishery; in other cases, a storm with wave reaching greater water depths and relatively large currents, or the passage of a ripple trough. In the top layer bioturbation is important in the zone from -13.2 to -17.1m. Foresets point to ripple migration in two directions (tidal currents) (ST09, ST12 and ST13). Storm (waves) may have caused changes down to water depths of -20.3 m.

## 4.4 Box cores Noordwijk research area

### 4.4.1 Introduction

In 2017 12 round box cores have been collected along three profiles perpendicular to the coast, namely (ordered in increasing depth): BC31-BC24; BC38-BC35 & BC39-BC42. Water depths vary between -12 and -21.2m.

In 2018 13 rectangular box cores were collected along a profile in the centre of the area, from -11.9 to -18.1m. The profile is gentle: going down some 6m over 6 km. Three other samples (NW14 to NW16) were collected somewhat to the south at water depths of -11.8 to -13.9m. This is an area of special interest where erosional patterns were observed in the area on the multibeam survey data collected in 2017.

### 4.4.2 Description of the observations on round box cores 2017

#### *Grain-size distributions*

The grain-size distributions as measured with the Malvern laser particle sizer for the surface samples of the round box cores of 2017 are given in Table 4.5 and Figure 4.23. The samples of 2017 show the following characteristics:

- 1) They consist of sediment with grain sizes up to 2000  $\mu\text{m}$ . The  $d_{50}$  varies between 232 and 415 microns (Table 4.5 & Figure 4.24).
- 2) Looking at the three sampling profiles perpendicular to the coast, it shows that the grain size increases with increasing depths starting at or above -12m and ending between -18.1 and -18.7m.
- 3) The sediments are in general somewhat coarser and shows larger variation in  $d_{50}$  values (with exception of some sub-fossil deposits) than in the two Wadden Sea sites Terschelling and Ameland.
- 4) Some mud is present near the coast (Figure 4.25).

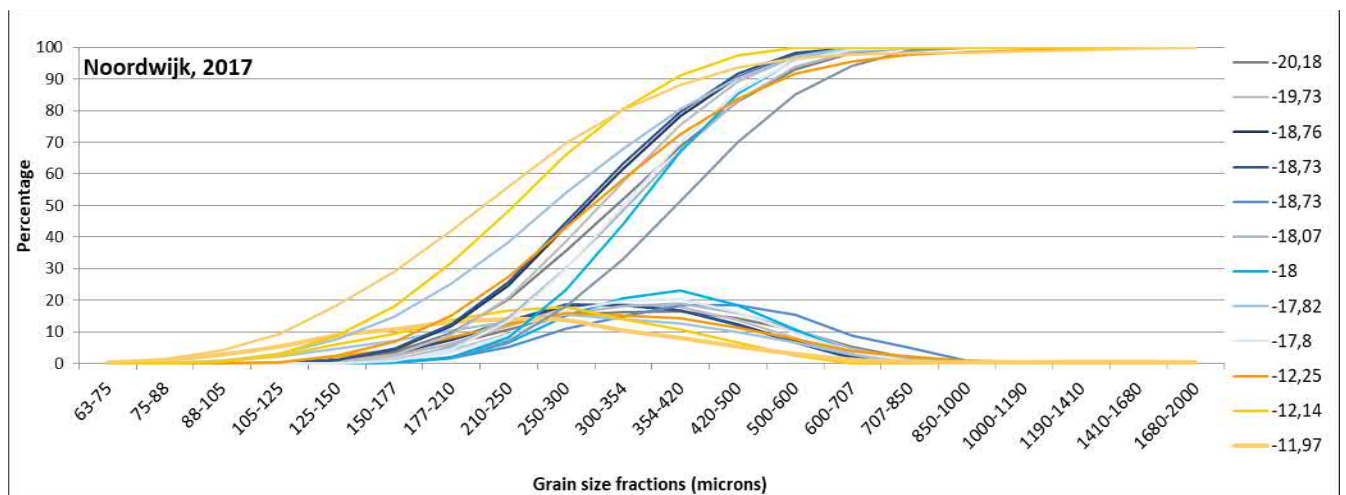


Figure 4.23 Grain size per size fraction and cumulative distribution for the sand fraction of the round box core samples of the Terschelling site, taken in 2017. Colours and figures right indicate depth with reference to NAP.

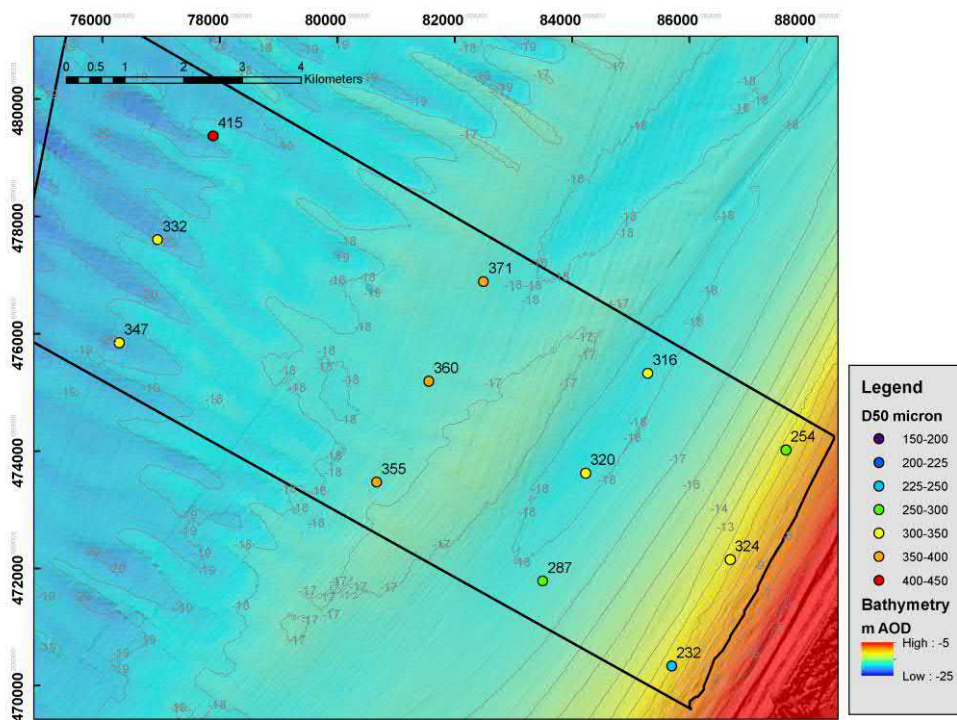


Figure 4.24 Overview of the d50 grain sizes in the upper layer of the samples taken in 2017 (bathymetry compilation of depth soundings in the period 2009- 2014).

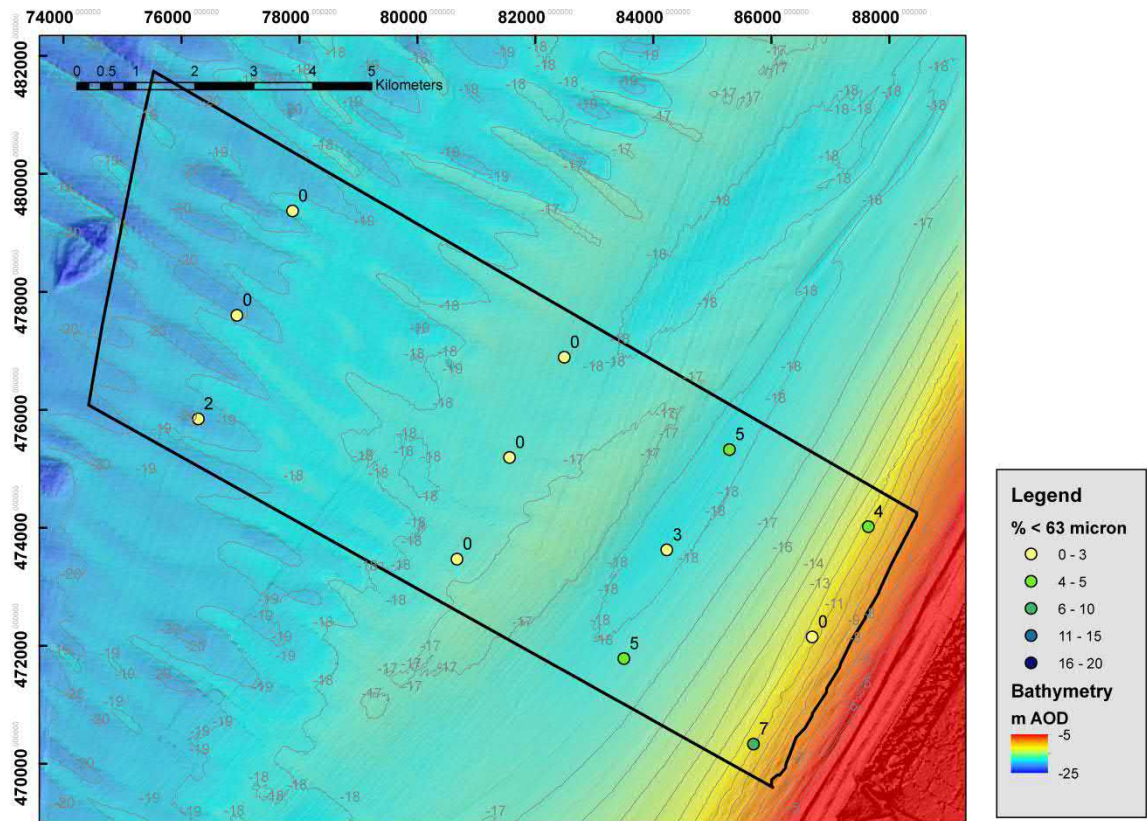


Figure 4.25 Overview of the mud percentage in the upper layer of the samples taken in 2017 (bathymetry compilation of depth soundings in the period 2009- 2014).

Table 4.5 Detailed analysis of the lower shoreface deposits in the Noordwijk research area based on the box cores description. BN=Borehole number. SA=shell abundance: 0=absent, 1=traces, 2=few, 3=many. Shell species: Spi=Spisula, Car=Cardium, Don=Dona 1, Ens=Ensis, Myt=Mytilus, Mac=Macoma, Ang=Angulus. WD=Water Depth

BNN	SA	Spi	Car	Don	Ens	Myt	Mac	Ang	WD (m NAP)	d50 (microns)
31	2	3	1	0	0	0	1	0	-12.0	232
32	3	3	0	0	0	0	0	1	-17.8	287
33	1	1	0	1	0	0	0	0	-17.8	355
34	3	3	0	0	0	0	0	0	-20.2	347
35	1	0	0	0	1	0	0	0	-19.7	332
36	1	3	0	0	0	0	0	0	-18.1	360
37	1	0	0	0	1	0	0	0	-18.8	320
38	2	3	0	0	2	0	0	1	-12.3	324
39	1	0	0	0	1	0	0	0	-12.1	254
40	2	3	0	1	1	0	0	0	-18.7	316
41	1	1	0	0	1	0	0	0	-18.0	371
42	1	0	0	0	1	0	0	0	-18.7	415

## Fauna

Table 4.5 and Figure 3.6 present the faunal assemblage and grain size of the lower shoreface deposits. Shell abundance is very different across the area, varying from none to very high. *Spisula* is the dominant species in the faunal assemblage.

### 4.4.3 Description of the observations of the rectangular box cores of 2018

Table 4.6 gives an overview of the samples taken with rectangular box cores in the Noordwijk research area. The grain-size distributions for the rectangular box cores of 2018 are given in Figure 4.26. The box cores samples taken along the profile (NW01-NW13) show the following characteristics (Figure 4.26 to Figure 4.29):

- 1) They consist of sediment with grain sizes up to 2000 mm. The d50 varies between 228 and 367 microns. In general, the d50 grain size of the sediments of the samples taken in 2018 increases with increasing depth. This starts between -13.8 and -14.9m and (leaving point at -17m out) ends between -17.5 and -17.9m. Also, the sand becomes brown in colour and angular from NW09 onwards, especially in the box cores NW11-NW13. The grain size patterns of the samples collected in 2018 are comparable to those of 2017. Also, in both the samples of 2017 and 2018 there seem to be two separate groups which differ some 50 microns (Figure 4.28).
- 2) Mud is absent in station NW10 to NW13 (Table 4.6; Figure 4.29).
- 3) In general, the sediments are somewhat coarser (with exception of some older deposits) than on the two Wadden Sea sites Terschelling and Ameland.
- 4) Several of the lacquer profiles show 2 or more layers (Figure 4.30 & Figure 4.31). Of these the top layer is often more bioturbated than the lower layer(s). The top layer is probably the result of the long and quiet period between February and September 2018.

Table 4.6. Schematic description of the box cores in the Noordwijk research area. Volumetric percentage of sediment < 63 micron is given, as well the median size of the sediment d50. Presence of clay layers, physical structures, American jack-knife and sea potatoes given as: 0 = not present; 1 = present. Physical structures given as: ang = angular; par = parallel. Erosional surfaces are given at the depth they occur; bioturbation is given as: 0 = not present; 1 = traces; 2 = medium; 3 = abundant. Red = data derived on board to be considered as tentative data. Layers indicated from 0 (top layer) downwards (layer below = -1, etcetera).

Coordinates	Waterdepth		Lower boundaries				Volume %		Grain sizes		Physical structures			Biogene structures				American Jackknife	Sea potato				
	(m)	(m -NAP)	(cm)				%	(microns)	(cm)			Bioturbation											
No	x	y	0	-1	-2	-3	< 63	d (0.5)	clay layers present			Erosional boundary			Bioturbation				total	adults	juveniles		
NW01	594795	5788017	11.9	2.5	9		2,445	318	0		1 par	1 ang		0	0	0	0	0	0	0	0	0	
NW02	594661	5788086	12.3	6	10	17	3,047	319	0	10	1 ang	shell	1 ang	0	0	0	0	0	0	0	0	0	
NW03	594523	5788156	13.1	7	16		5,592	266	0		1 par	1 ang		1	1		0	0	0	0	1		
NW04	594388	5788225	13.8	8	9	16	10,24	259	0		0	1 ang	0	1	0	1	1	1	0	0	0		
NW05	594125	5788360	14.9	6	17		4,212	256	1?	6	1 par	1 ang		3	1		0	0	0	0	1		
NW06	593852	5788499	15.8	7	16		12,202	260	1	7	0	1 ang		3	0		0	0	0	0	1		
NW07	593351	5788756	17	17			9,752	276	0		0			3			1	1	0	1	1		
NW08	592776	5789050	17.9	7	13.5		6,781	299	0		0			3			1	0	1	1	1		
NW09	592098	5789397	18.4	4	6	10	16	6,347	309	1	16	0	0	0	3	0	1	0	0	0	1	1	
NW10	591346	5789782	16.9	6	13		0	337	0	6	1 par/ang	1 ang		1	0		0	0	0	0	0		
NW11	590737	5790093	16.4	9	13		0	336	0		1 ang	1 par/1 ang		1	0		0	0	0	0	0		
NW12	589900	5790521	17.5	7	14		0	360	0		0			3	3		0	0	0	0	1		
NW13	588057	5791464	18.1	4	16		0	367	0	9	1 ang/a par	1 ang		1	0		0	0	0	0	1		
NW14	593818	5787070	13.8	6	19.5		3,283	304	0 old		1 ang	1 ang		3	0		0	0	0	0	1?		
NW15	594226	5787044	12.8	2	9		6,434	228	1 old		1 par	1 par		1	0		0	0	0	0	0		
NW16	594238	5787010	11.8	6	13	19	5,291	265	0	13	0	0	0	1	0	0	1	0	1	1	0		

- 5) Some box cores show a disruption of the physical structures of the lower layer with an irregular upper surface. Some of these might be due to bioturbation during the summer half year (for example: NW06; Figure 4.32). However, in other box cores the layer

above the irregular surface comprises physical structures, sometimes with a shell concentration at the base, pointing to a higher-energy event (for example: NW02; Figure 4.33). In one example (NW13, -13.1m) a possible storm-deposit is present (Figure 4.34) consisting of truncated large-scale foresets, on top of which parallel layered sediments are present, followed by (likely) wave ripples topped by a parallel horizon. If this is a storm deposit resulting mainly from density driven currents (Aigner, 1985) the interpretation is as follows: truncation during high velocity current conditions; parallel layered sediments = upper stage plane bed deposits; wave ripples formed under extreme wave conditions; parallel upper horizon might be lower stage plane bed. An alternative explanation might be that the deposits were formed by the combination of high current velocities and extreme wave conditions. At the base current velocities dominate and during the waning of the high current velocities the wave influence becomes relatively more dominant, finally giving way to the draping by parallel sands (parallel upper horizon) in the final stages of the storm. To differentiate between both possibilities shallow seismics or multibeam observations are needed.

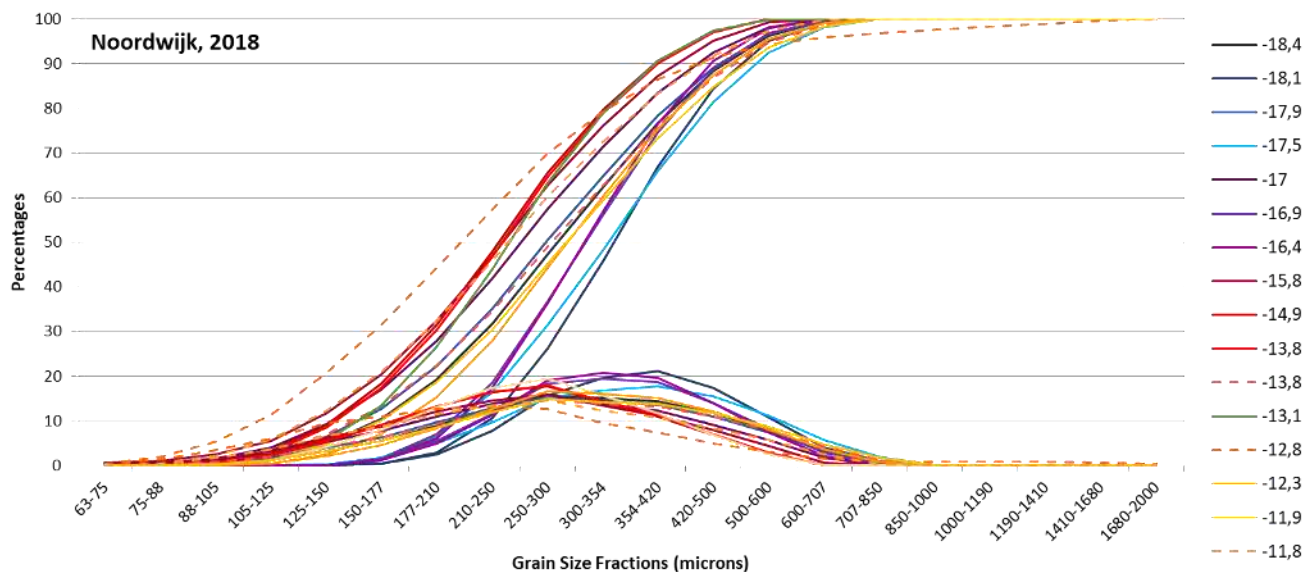


Figure 4.26 Grain size per size fraction and cumulative distribution for the sand fraction of the rectangular box core samples of the Noordwijk site, taken in 2018. Colours and figures right indicate depth with reference to NAP.

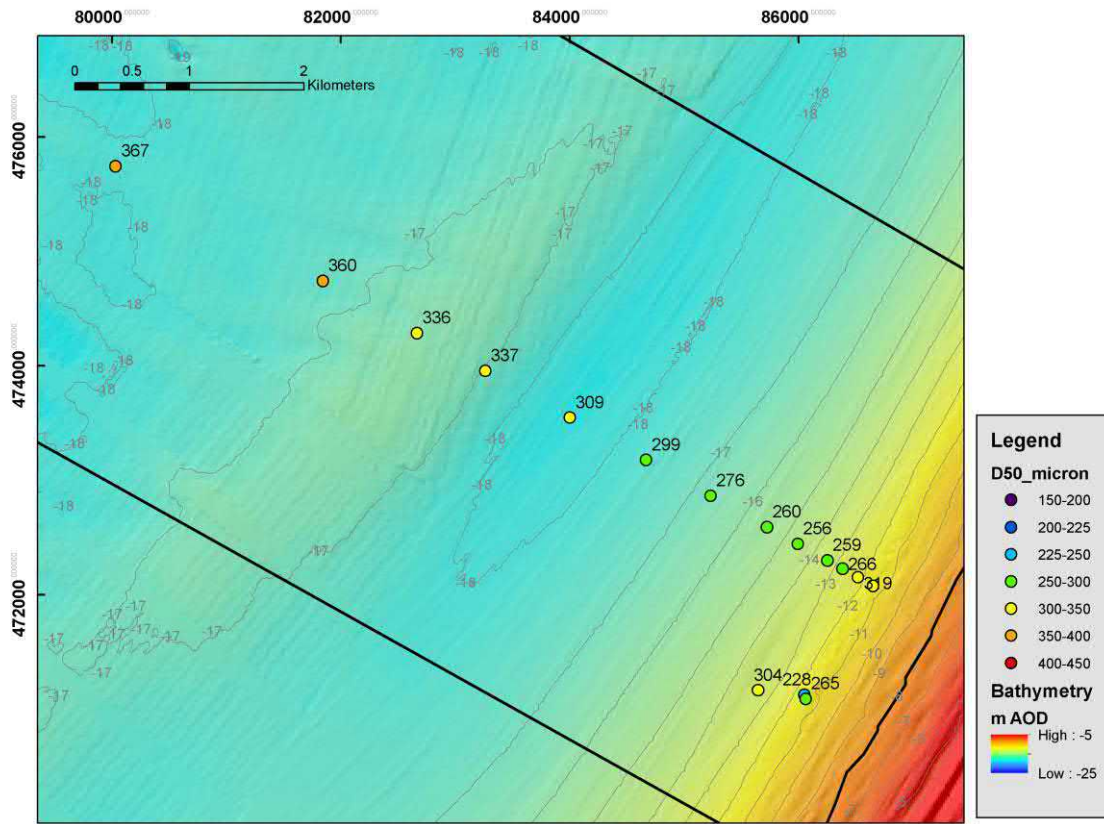


Figure 4.27 Overview of the d50 grain sizes in the upper layer of the samples taken in 2018.

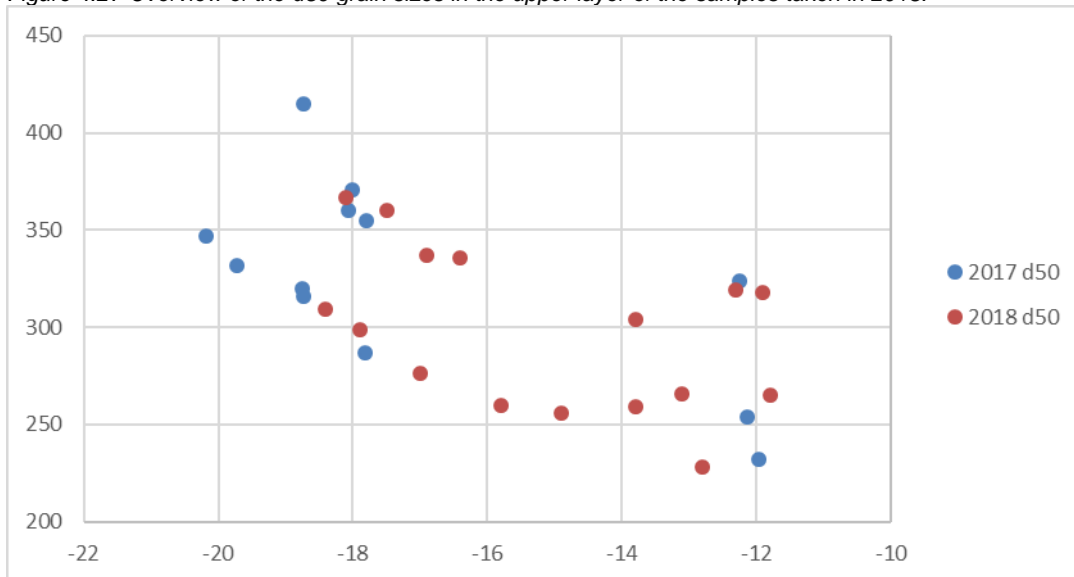


Figure 4.28 Overview of the d50 to water depth for all observations of 2017 and 2018

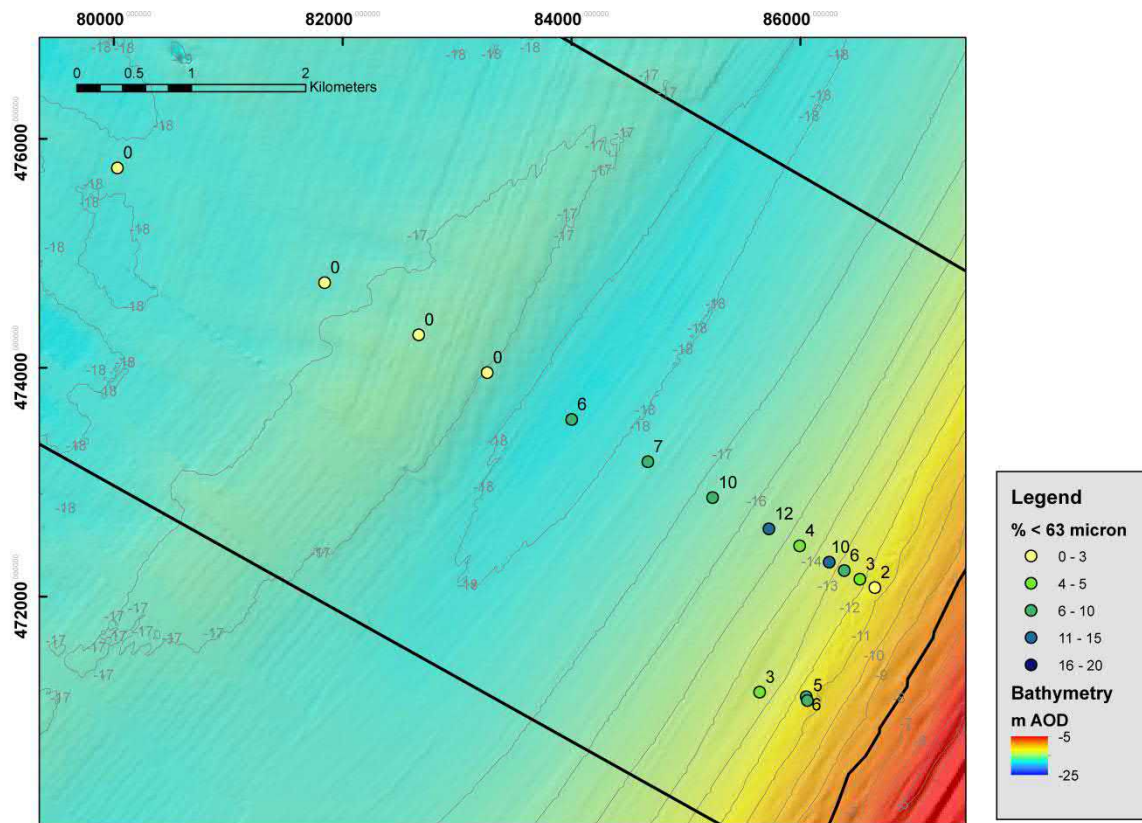


Figure 4.29 Overview of the mud percentage in the upper layer of the samples taken in 2018.

- 6) Foresets of larger ripples (sometimes bi-directional, indicating to 2 current directions) are visible in several box cores especially in the lower layer(s).
- 7) In the upper layer bioturbation occurs on most water depths along the profile. Between -13.8 to -18.4m (NW 14 & NW05 to NW09 and NW12 to NW13) bioturbation has obliterated much or all the physical structures. Exceptions can be found at the landward slope (NW09) and on top (NW10) of the shoreface connected ridge. On those locations the sediment dynamics are apparently too strong to be obliterated by bioturbation.
- 8) Shell layers are encountered in the cores at -12.3m (NW02) and -18.4m (NW09).

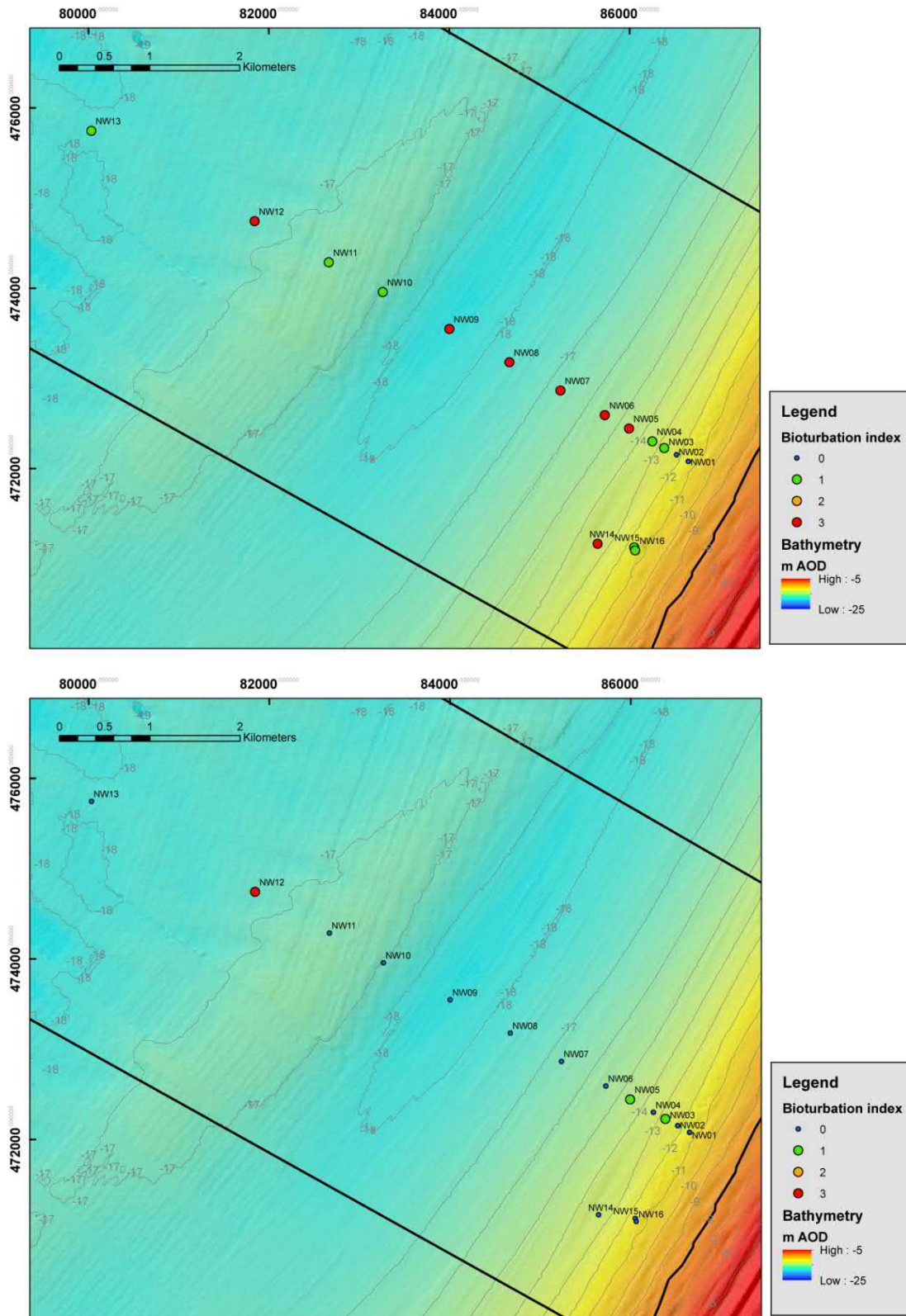
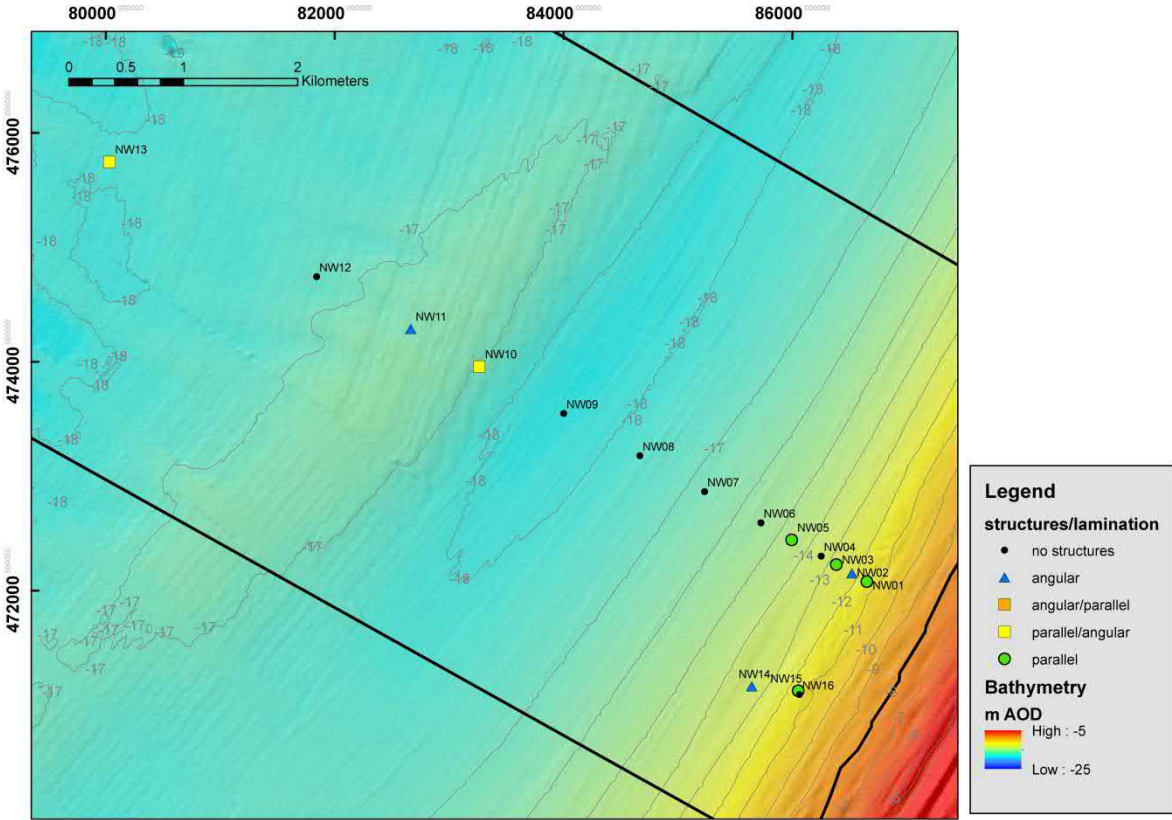


Figure 4.30 Bioturbation upper layer (above) and lower layer (below) of the box cores of 2018. Intensity comparable to table 4.6.



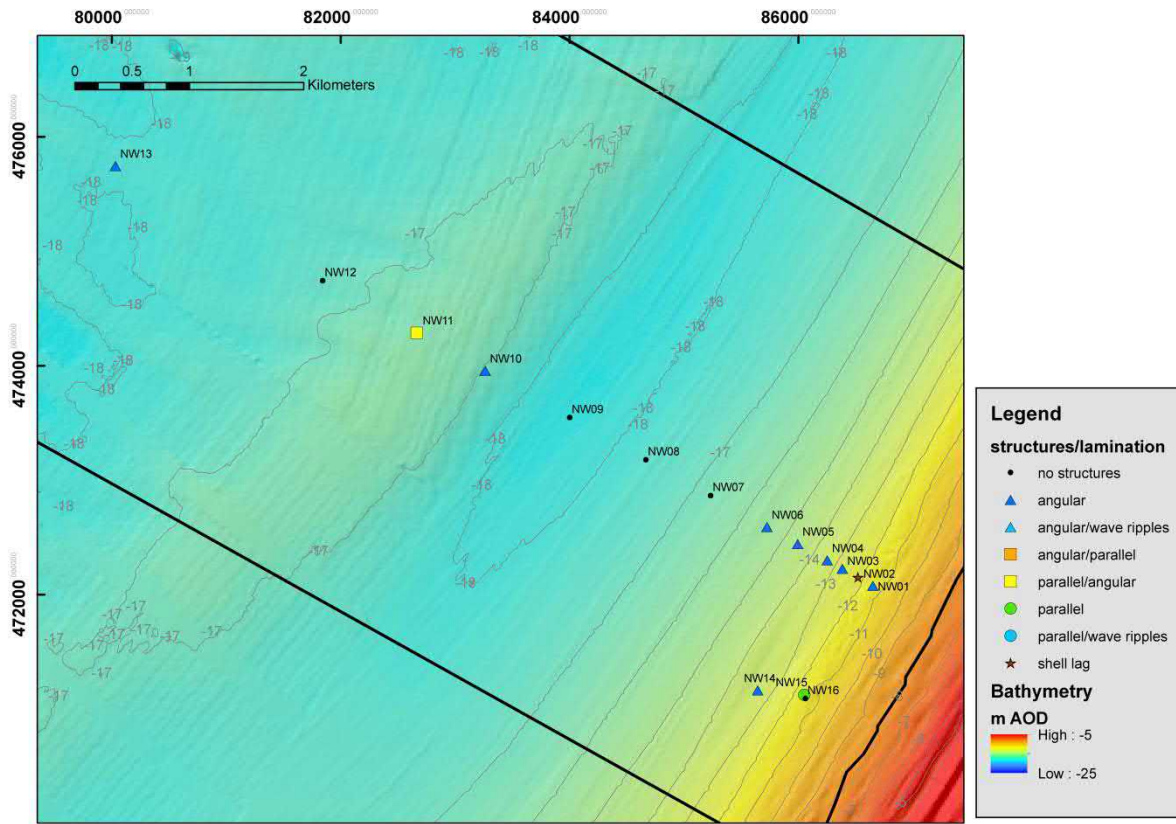


Figure 4.31 Structure upper layer (above) and lower layer (below) of the box cores of 2018. First structure mentioned dominates.

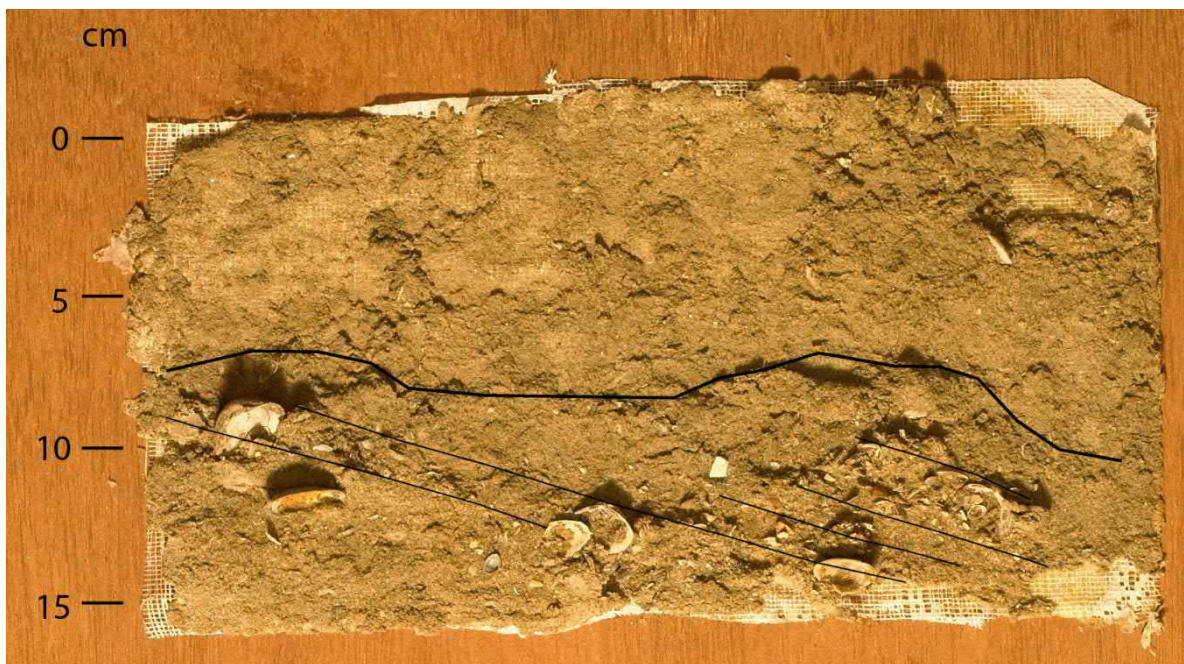


Figure 4.32 Lacquer peel from Box core NW06 (-15.8m): foresets formed by one-directional flow truncated by muddy strongly bioturbated deposits.



Figure 4.33 Lacquer peel from Box core NW02 (-12.3m): foresets formed by one-directional flow truncated by shell rich layer with foresets in opposite direction (pointing to a high energy event), followed by foresets and on top parallel laminae.

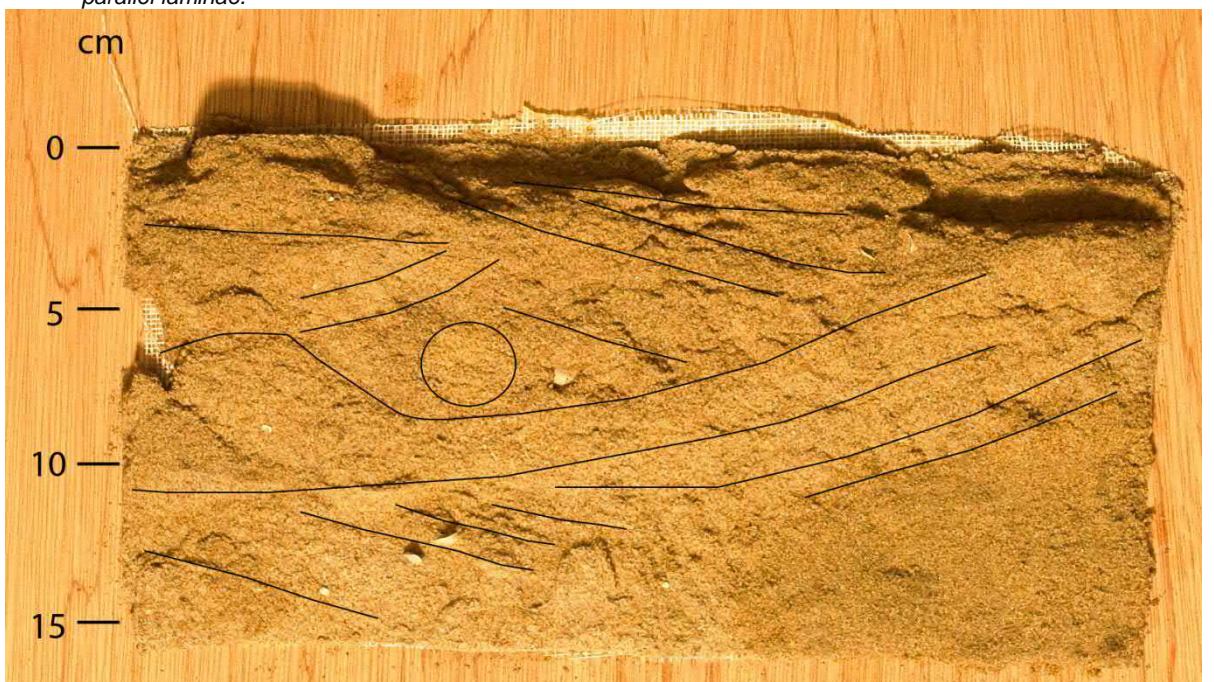


Figure 4.34 NW13 with coarse sediments and very clear bidirectional physical structures pointing to 2 different current directions. In between (lower number '5') parallel laminae are present which truncate the lower foresets, pointing to a relative high energy event. The small foresets near the number '40' are indicative of wave ripples.



Figure 4.35 NW14, compact clay covered by relatively coarse sand.

- 9) For the samples that were collected at the south side of the Noordwijk area (NW14-NW16; Figure 4.35) at water depths between -11.8 and -13.8m, a compact clay occurs in the lower parts of NW14 and NW15. In both cases the clay is covered with a thin layer of sand. The clays are without recent shells and have thin streaks of sand in them. From the structure they seem to be lagoonal, lacustrine or fluvial in origin. NW16 contains a 5 cm thick shell layer.

#### 4.4.4 Interpretation

The presence of recent muds can be explained by suspension transport which may be attributed to supply via the so-called 'Kustrivier' (Coastal River). In this estuarine spiralling circulation pattern brought about by fresh water supply of the rivers, muds are concentrated and may be deposited on those places where the local energy conditions allow this. The increase in grain size towards deeper water might be due to erosion of the older deposits and/or selective sediment transport due to differences in tidal velocity, comparable to the situation in the Terschelling and Ameland sites. Geological inheritance may also explain the much more angular and coarse sands which can be found seaward of NW09, which point to deposits which were originally fluvial. Furthermore, hydrodynamic modelling indicates that landward directed bottom current is present which may lead to winnowing of the sediments in that direction. The current is brought about by the combination the lower density of fresh fluvial waters near the surface, balanced by a coastward directed bottom current (Grasmeijer et al., 2019).

A part of the cores shows several layers of which the top layer was in most cases probably formed during the quiet long period between February and September 2018. In several cases the layers are separated by an irregular layer sometimes characterized by a shell layer. This

points to a higher energy event. In at least one case it is likely that a storm with waves reaching deeper water levels and relatively high energy hydraulic conditions are the cause (NW13 at -18.1m). In the top layer bioturbation is important almost everywhere, except on the top of the shore-face connected ridge and its landward flank, where the deposits show current dominance. Foresets point to tidal currents in two directions.



## 5 Discussion: integration of observations

### 5.1 Introduction

In this chapter we try to discuss and integrate the observations per study area and for all the three sites together.

### 5.2 Ameland area

An increase in grain size was observed with increasing depth. The d50 of the samples taken at the east side in 2017 increased (from -15 to -19.8/-20.4m) and those taken in 2018 (all samples: from -15.1/-15.7 to -18m; samples at the east side: from  $\geq$ -11.7 to -17.8/-18.8m). A part of the explanation might be the development during the Holocene. During the past 5000 years the coast at the Ameland site has retreated landward (retrogradation) over several km's (Sha, 1990). Hence, older channel deposits (which normally comprise up to 80% of the tidal deposits), formed in a former backbarrier or tidal inlet setting, can be expected to underlie the recent shoreface deposits. Indeed, a large part of the sediments present, often less than 0.5m below the surface, are interpreted as tidal channel deposits (Chapter 3). As is pointed out in Chapter 3, ebb-shield deposits and thick lower shoreface deposits are locally present on top of these sediments (Figure 3.8). The deeper the seafloor, the longer the duration of erosion and the larger the chance that only the coarsest fractions remain. Thus, during this long-term erosion selective transport occurred. The agents are likely (tidal) currents and the occasional higher-energy event of which sedimentary structures can be observed on all water depths. That tides are important is also confirmed by the multibeam observations of 2017 (collected in September at the end of a long quiet period) and 2018 (collected in August after a long quiet period). They reveal that large tidal ripples dominate the area below ca. -14m. In general, this is in good accordance with the observation in the box core profiles of large (bi-directional) tilted layers which have been formed by currents (in different directions) in this zone. On top of that modelling indicates that there is a landward directed bottom current which may attribute to winnowing in that direction. To what extent the smaller fractions are gradually transported upward is presently unknown, but the decrease of the whole grain size distribution including the coarsest grains in that direction suggests that this might be the case.

Many box core profiles show several layers of which the top layer of 2018 was in most cases probably (re-)formed during the long quiet period between February and September. In the top layer, bioturbation is important above -15.1 (western profile) and -15.7m (eastern profile) and in the deeper reaches (-17.2m). In between, bioturbation did not rework the original physical structures fully. It indicates that the balance between physical and biogene reworking of the sediments differs with depth even in summer. In several cases the upper layer is separated from the lower layers by an irregular surface, which is sometimes characterized by a high shell content. It indicates a higher-energy event. In some cases, it is likely that this was due to bottom-trawling fishery; in other cases, it can be due to storms with the wave base reaching deeper water levels and relatively large current velocities or the passage of a large ripple trough can be the cause. The layer below the top layer also shows less bioturbation and more physical structures.

### 5.3 Terschelling research area

Holocene coastal retreat has been dominant in the Terschelling area. Like at the Ameland site, channel deposits are present near the surface and covered by a thin veneer of recent sediments (chapter 3; see also: Sha, 1990). The discussion is comparable to the Ameland area. Sediments are eroded and transported by tides and occasional storm surges. The longer the duration of erosion (the deeper the seafloor) the higher the chance that only the coarser fractions remain. Selective transport thus resulted in an increase in d50 and the whole grain size distribution with increasing depth was observed in both the samples of 2017 (between -9.6/-10.2 and -18.3/-18.7m) and 2018 (-12.8/-13.2 and -17.9/-19.4m). Additionally hydrodynamic modelling indicates that there is a coastward directed bottom current present which may lead to overall winnowing in that direction (Grasmeijer et al., 2019)

Presence of older tidal channel deposits might also explain the high and variable grain-size distributions in even more distal waters (<-20m), observed in the samples of 2017 and 2018. It may be due to the variability of the grain sizes often found in channel lags. This is also in line with the local presence of thick shell layers at that depth (see below), which are most likely channel lag deposits (Figure 4.14). Furthermore, it is in accordance with the findings of paragraph 3.3 (Figure 3.10), which indicate that channel deposits are near the surface.

The fact that fines <63 microns are missing in both the samples of 2017 and 2018 suggests that there is no source of fines available. The difference with the Ameland area might be explained if the presence of backbarrier deposits as a source of the fine fraction via the Amelander inlet.

Many cores show several layers of which the top layer was most likely mainly (re-)formed during the quiet long period between February and September 2018. In several samples, layers are separated by higher-energy event surfaces. In some cases, it might be due to bottom-trawling fishery; in other cases, a storm with waves reaching deeper water levels and relatively large currents or the passage of the trough of a large ripple (which dominate large parts of the area) will be the explanation. In the top layer bioturbation is important in the zone from -13.2 to -17.1m. Foresets point to tides in two directions and (ST09, ST12 and ST13), storm (wave) conditions may have caused changes in relatively deep water; down to water depths of -20.3 m.

In the Terschelling area physical structures are present in almost all box cores signifying the importance of the influence of currents and waves. The only exception is core TS04-TS06 where strong bioturbation has almost completely obliterated the physical structures (except for the shell rich layer present in TS05). The coarser-grained samples are found below -17m where large ripples are present.

The samples TS12 to TS16 are collected in an area where bed forms formed by tidal currents are visible on the multibeam with large ripple troughs, which has been attributed to sediment starvation and local scouring. An indication that this indeed might be the case can be found in box cores TS14 & TS16 which show thick shell-rich layers just below a shallow top layer. The shell-rich layers are most likely older channel lag deposits which have resurfaced after erosion of the overlying layers upon coastal barrier retreat.

#### 5.4 Noordwijk research area

The closed barrier coast at the Noordwijk area consist of fluvial deposits of the river Rhine overlain by tidal channel deposits. The coast at Noordwijk has probably been eroding since Medieval times and retreated landward over 200-1000m since 1600 AD (Van der Spek et al., 1999). Due to the erosion the river and tidal channel deposits are just below the surface. Also, in the Noordwijk area an increase in grain size with increasing depth can be observed (see also Van der Meene, 1994 & Van der Meene et al., 1996). All 2017 profiles taken together indicate an increase of grain size with depth between  $\geq -12$  and  $-18.1/-18.7$ m. Below that grain sizes vary but are large. Also, the d50 of the samples taken in 2018 increases with increasing depth (between  $-13.8/-14.9$ m and  $-17.5/-17.9$ m). The picture seems somewhat blurred by the shore-face connected ridges (see chapter 4). The most likely explanation for the observed differences in the upper ranges of 2017 and 2018 is the lack of samples between  $-12$  and  $-17.8$ m in 2017.

Like in Ameland and Terschelling, the older deposits determined the initial grain-size distribution, which was during the long-term erosion gradually reworked during erosion. The much more angular, yellowish to orange, coarse sands which can be found seaward of NW09 are most likely fluvial in origin. The presence of recent muds may be explained by the estuarine spiralling circulation pattern brought about by fresh water supply of the rivers which concentrates muds which subsequently may be deposited in quiet areas. From literature it can be concluded that the grain-size distribution over the shoreface of the Holland coast is quite persistent along the coast. Coarse sands occur below depths of  $-10$  to  $-12$ m, with fine sand and mud layers in a zone parallel to the coast above it. Above  $-8$  to  $-5$ m the sediments become coarser towards the beach (Van Straaten, 1961, 1965; Terwindt, 1962; Van Alphen, 1987; Van der Valk, 1992 & Cleveringa, 2000). Also here hydrodynamic modelling indicates that there is a coastward directed bottom current present which may lead to overall winnowing in that direction (Grasmeijer et al., 2019).

A part of the cores of 2018 shows several layers of which the top layer was in most cases probably formed during the quiet long period between February and September 2018, with bioturbation being important almost everywhere and deeper layer(s) which have been formed under higher energy conditions<sup>3</sup>. An exception are the sediments at the top of the shore-face connected ridge and on its landward flank, where the top deposits show current dominance instead of bioturbation (NW08 & NW09). Foresets point to tides in two current directions. In several cases the layers are separated by an irregular boundary sometimes characterized by a high shell content. It points to a higher-energy event. In at least one case it is most likely a storm (NW13 at  $-18.1$ m).

On the depth sounding map the shore-face connected ridge is clearly visible. The feature seems to be related to the presence of coarser sand (from NW08 seawards). The strong difference suggests limited sediment exchange between both zones. Seaward of it, coast perpendicular sand waves are present (with a wave length of ca. 800-1000m and a height of 1.5-1.7 m). These bed forms are generated by the tidal currents and are thus of comparable origin as the large ripples at deeper water in the Ameland and Terschelling area.

From the multibeam observations of 2017, collected after a period of storms, it is clear that erosion occurred in the zone between  $-9$  and  $-12$ m, exposing the differing sediments below the

<sup>3</sup> A similar conclusion was reached for the Egmond shoreface (Van der Valk, 1992).

sand. In the multibeam observations of 2018 these erosion traces have largely vanished due to covering by sediments. In that same area, compact older clay forms the lower parts of NW14 and NW15, whereas NW16 contains a thick shell layer. This might help explain the strange erosional structures observed in the multibeam observations of 2017 (compare Van der Meene et al., 1996). Apparently, just below the sandy recent sediments the area consists of older deposits which are relatively immobile (see also Beets et al., 1995). During storms the upper sand layer may be removed.

**5.5 Comparing the various study areas**

Although the various areas are different in terms of geological built-up, orientation, genesis and active bedforms (shore-face connected ridges and sand waves only occur in the Noordwijk area) there are strong similarities for all the lower shoreface areas. All are or have been eroding and hence older underlying deposits can be expected to influence the grain-size distribution in the area. In Terschelling deep water sediments are locally interpreted to consist of channel lag deposits. At Noordwijk a different, more fluvial type, of yellow to orange angular sand is present seaward of the shoreface connected ridges, whereas higher up Holocene clay rich deposits are encountered.

For the site Ameland the mud content is thought to be derived from the backbarrier area via the inlet. For the Noordwijk area mud content is probably supplied by the “Kustrivier”.

*Table 5.1 Upper and lower limits of the fining up sequences encountered in the study areas. The terms “high” and “low” are established by looking at the depths between which the fining up trend reverses.*

Area	Upper limit (m NAP)		Lower limit (m NAP)	
	High	Low	High	Low
Ameland 2017 All	-13	-15		-20
Ameland 2018 All	-15.1	-15.7		-18
Ameland 2017 East		-15	-19.8	-20.4
Ameland 2018 East		-11.7	-17.8	-18.8
Terschelling 2017 All	-9.6	-10.2	-18.3	-18.7
Terschelling 2018 All	-12.8	-13.2	-17.9	-19.4
Noordwijk 2017 All		-12	-18.1	-18.7
Noordwijk 2018 All	-13.8	-14.9	-17.5	-17.9

Grain sizes in all areas increase with increasing depths over a depth range between (rounded means between high and low limits) ca. -10 to -15m and ca. -18 to -19m (leaving out the unreliable -20m determinations of 2017; Table 5.1). The determination of the upper limit of the 2017 observations is hampered by the lack of samples taken in the upper part of the lower shoreface. The differences in the upper limit from site to site for the 2018 samples might point to selection processes which differ from site to site. This might be attributed to wave climate, which is known to differ from over the various localities.

The lower limit seems to be rather constant over time. Also, there seems to be little to no variation from site to site; this, with exception of the Ameland 2017 eastern profiles, which can be attributed to the gap in samples between -19.2 and -15.6m. It suggests strongly that, as far as sediment selection processes are concerned, they were formed by very similar processes. Given the different orientation and bedforms at the Noordwijk site it is unlikely that the storm-driven currents are the driving processes determining the lower limit. The selective sediment transport process which can explain the lower limit are tidal forces. Hydrodynamic modelling

indicates that for all locations there is a coastward directed bottom current present which may lead to overall winnowing in that direction (Grasmeijer et al., 2019). Below the lower boundary grain sizes are large and variable. Apparently, the hydrodynamic forces do not suffice to establish a sorting pattern at these water depths.

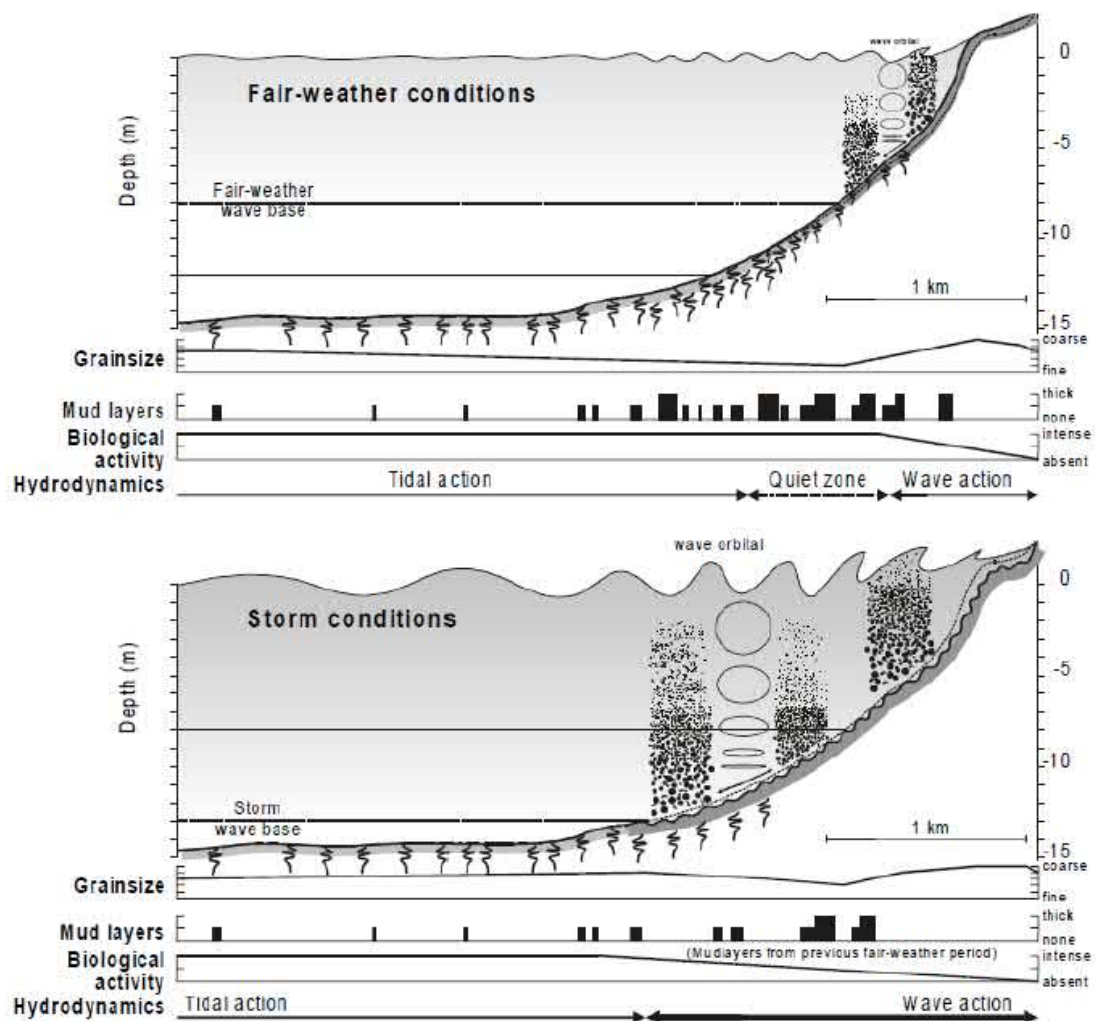


Figure 5.1 Conceptual model by Cleveringa (2000), Upper panel showing fair weather wave conditions where the lower shoreface is dominated by tides which cause a gradual coarsening of the profile. Fines and bioturbation dominate higher in the profile. Lower panel showing storm conditions where part of the bioturbation structures is removed, and physical structures dominate. In the deeper reaches the grain-size distribution becomes less clear than during fair weather conditions (upper panel).

As discussed above and judging from the presence of physical structures at all depths, selective sediment transport may influence the grain-size distribution. The conceptual model proposed by Cleveringa (Figure 5.1; 2000; 2016) based on Holocene coastal deposits of the Holland coast offers a possible explanation. He found that the deposits become coarser with decreasing depth over the middle shoreface (zone from -8 to -6.5m) The coarsening-upward trend in the upper part of the sequence was attributed to the increase in winnowing of fines by wave action within this zone above the fair-weather wave base.

A fining upward trend was observed over the lower shoreface zone of -13 to -8m by Cleveringa (2000). He attributed the basal fining-upward sequence to the decrease of tidal influences from

the North Sea floor up to the shoreface. The lower boundary of the fining up deposits at -18/-19m, as observed in this study, differs significantly from that of Cleveringa (2000). A possible explanation is that the fossil deposits, on which the Cleveringa model was based, mainly show the higher energy conditions, whereas all the box cores have been taken after a calm period, apparently leading to more outspoken grain-size distribution differences. Hydrodynamic modelling and measurements, indicate that, next to tides, also water-density driven, coastward-directed currents, waves and wave-set up related seaward-directed currents play a role. Combined these result in a landward transport of sediments which increases with decreasing depths (Grasmeijer et al., 2019). These currents may contribute to winnowing of sediments, resulting in coarser sediments at larger depths.

On an annual scale quiet periods (fair weather, summer half year) alternate with periods characterized by higher shear stresses (storms, winter half year; Figure 5.1; Cleveringa, 2000). This can also be observed in multibeam observations where after storms local erosion traces (e.g. Noordwijk) and reworking (hummocks), as well as in the box core samples with erosional features and storm deposits. During quiet periods bioturbation is locally dominant over the physical influences. Both erosional structures and the indications of storm erosion indicate that storms also play a role in deeper water, be it less frequently than in shallower reaches.

## 5.6 An answer to research questions

To help answering the knowledge question: *“Which part of the coastal profile actively below MSL contributes to the stability of the coast?”* the following (partial) answers can be given to several underlying research questions:

- a) What is the sedimentary built-up of the coast, in terms of bed forms, sedimentary structures, bottom profiles and grain-size distributions?

The sedimentary built-up of the lower shoreface consists mainly of older Holocene sediments, being: tidal channel deposits (all three sites), lower shoreface deposits (Noordwijk and Ameland) fluvial deposits (Noordwijk), ebb-shield deposits (Ameland). These older deposits are covered with a relatively thin veneer (up to 0.7 m) of more recent active deposits. Indeed coarse, angular, orange/yellowish sands are encountered in deeper water off Noordwijk pointing to a fluvial origin. Furthermore, compacted older clay was encountered less than a dm below the recent sand at Noordwijk in relatively shallow water depths. Also, at Terschelling, thick shell layers are locally present around the -20m depth, which are likely shell lags formed at the bottom of a tidal channel.

The longer the erosion (how larger the water depth), the larger the chance that only the coarsest fractions remain. Indeed, all three research areas are characterized by a decrease of the grain size with decreasing depths in the zone between -18/-19 and -10/-15m. Hydrodynamic modelling indicates that there is an increase of coastward directed between -25 and -15m (Grasmeijer et al., 2019). From the box core samples, it became clear that the recent veneer of sediment (as far as sampled) often consists of 2 to 3 layers, which are often separated by an erosional surface which signifies a higher-energy event. In some cases, there are strong indications that storms may have disturbed the seabed, in at least 1 case disturbance by bottom-trawling fishery seems likely. Furthermore, the passage of the troughs of large tidal ripples might be a cause for the formation of erosional surfaces. As sampling took place after a prolonged period of quiet conditions, the upper layer was often partially or wholly bioturbated, whereas in the layer below it physical structures were often more dominant. However, also in the top layer there were samples where physical structures were dominant. It strongly suggests that even under fair weather conditions physical reworking due to tidal transport may have occurred on the lower shoreface.

Grain sizes vary not only with depth, but also from location to location. At Ameland the d50 varies between 180 and 250 microns, at Terschelling between 200 and 300 microns and at Noordwijk it varies between 230 and 420 microns.

- b) Which processes determine the exchange of sediment between the upper shoreface and the lower shoreface and what is their frequency of occurrence and their contribution?

On the long run (centuries) coastal erosion is the dominant process in the shoreface. Due to this erosion sediment is set free at all water depths and reworked by short-term processes. The longer the erosion lasts the larger the chance that sediments will be sorted and only the coarser grains will remain. This is most likely also determined by the tides which decrease in strength in the direction of the coast leading to a gradient of decreasing energy and may further be helped by coastward directed bottom currents. At the moment it is not fully clear if shoreward transport of finer fractions occurs.

Another short-term process is wave action. During calm weather conditions waves winnow out the sediments of the higher shoreface and the finer sediments are deposited below the wave base. During storms it appears that higher-energy events may be generated to depths of at least -20m and will disturb the sediment distribution pattern which developed during fair weather conditions.

- c) In which subareas (or zones) can the coastal profile be subdivided, which are similar in (stability) of the profile, sedimentary built up and dynamics?

Obviously, there is a lower boundary at ca. -18/-19m below which selective transport could not be inferred from the grain size observations and seafloor sediments seem to be characterized by the older deposits which are at or near the surface. From the Terschelling, Noordwijk and Ameland observations it is clear that the coarser grains are not present in the shallower part of the zone where fining upwards occurs (thus from -18/-19 up to -10/-15m).



## 6 Conclusions

The sedimentary built-up of the lower shoreface consists mainly of older Holocene sediments, with only a thin veneer (<0.7 m) of recent sediments which form the active zone.

Based on the borehole descriptions there were distinguished: tidal channel deposits (all three sites), lower shoreface deposits (Noordwijk and Ameland) fluvial deposits (Noordwijk) and ebb-shield deposits (Ameland). Locally, older sediments are present at or near the surface. Given the erosional history of all sites, the deposits determine the initial grain-size populations. This can also be concluded from the differing grain sizes on the various locations and the different habitus of the grains

These populations are reworked continuously. This will lead to removal of the finer grain sizes which can be transported under less energetic conditions and formation of a relatively coarse rest population. The latter is reworked regularly in migrating bedforms. The observed grain size decreases with decreasing depth (from -18/-19m to -10/-15m) is probably brought about by a combination of a shorter duration of the erosional processes (the deeper, the longer), weaker tidal forces in shallower waters and perhaps coastward directed bottom currents.

From the separate layers observed in the box core samples it becomes clear that the active sediment is formed over the course of one or several years. The irregular surfaces separating the layers are indicative of a higher-energy event: either bottom-trawling fishery, the passage of a large ripple trough and in some cases, most likely a storm. The physical structures also make clear that sediment transport occurs over the whole profile.

All in all, it is concluded that both mechanisms, geological inheritance and selective transport determine the grain size characteristics of the lower shoreface. In order to understand role of the lower shoreface in the (development of the) coastal foundation it is necessary to take all these factors into account.



## 7 Recommendations

In future data collection campaigns, we recommend the use of the rectangular box coring technique, which allows the preservation of sedimentary structures in the active layer, such as cross-bedding and sheet flow laminae. Since these structures appear very sensitive to handling and transportation, the samples should be processed and described directly after acquiring on board of the ship. To preserve the structures in vibrocores, to use of shorter cores (~1m) might give better results. These should also be processed and described directly after acquiring on board of the ship.

Observations clearly show that older sediments dominate the coastal sedimentary built up in the lower shoreface, and to a large extent determine the grain sizes available, and -at least locally- the erodibility of the sea floor. It is recommended to study this in more detail over the entire Dutch coast to obtain a more accurate insight in the sedimentary dynamics of the lower shore face. Given the results of these observations and the multibeam observations a year-round observation campaigns using box cores, hydrodynamic measurements and various non-destructive geophysical methods in combination with dedicated modelling will most likely result in a detailed picture of the morphodynamical developments.

The observations and literature might to imply that there is a net sediment supply from the deeper part of the lower shoreface upwards, but the conclusion needs more validation. It is recommended that earlier research focusing on sediment exchanges along the Dutch coast should be re-evaluated and when necessary new research should be added.



## 8 References

- Aigner, T. (1985) Storm depositional systems, 174 pp
- Cleveringa, J. (2000) Reconstruction and modelling of Holocene coastal evolution of the western Netherlands. Thesis Utrecht University.
- Cleveringa, J. (2016) Kennisvraagspecificatie zeewaartse grens Kustfundament, Kustgenese 2 Ministerie van Infrastructuur en Milieu. Rapport, Arcadis, Nederland.
- Grasmeijer, B., Schrijvershof, R. & J. van der Werf, 2019: Modelling Dutch Lower Shoreface Sand Transport, Report 1220339-005-ZKS-0007.
- Guillén, J., Hoekstra, P. (1996) The “equilibrium” distribution of grain size fractions and its implications for cross-shore sediment transport: a conceptual model. *Marine Geology*, 135, 15-33.
- Hinton, C.L. (2000) Decadal morphodynamic behaviour of the Holland shoreface. PhD thesis, Middlesex University, UK
- Huisman, B.J.A. (2019) On the redistribution and sorting of sand at nourishments. PhD thesis Delft, 149 pp.
- Koomans, R.L. (2000) Sand in motion: effects of density and grain size. PhD thesis, University of Groningen, The Netherlands.
- Marsh, S.W., Nicholls, R.J., Kroon, A., Hoekstra, P. (1998) Assessment of depth of closure on a nourished beach: Terschelling, The Netherlands. In: *International Conference on Coastal Engineering* (Ed. by B. L. Edge), pp. 3110-3124. ASCE, Copenhagen.
- Oost, A. P. (1995) Dynamics and sedimentary development of the Dutch Wadden Sea with emphasis on the Frisian Inlet: a study of the barrier islands, ebb-tidal deltas, inlets and drainage basins. PhD Thesis, Utrecht University, Utrecht, 454 pp.
- Sha, L. P. (1990) Sedimentological studies of the ebb-tidal deltas along the West Frisian Islands, the Netherlands. PhD Thesis, Rijksuniversiteit Utrecht, Utrecht, 159 pp.
- Terwindt, J. H. J. (1962) Studie naar korrelgrootte variaties aan de kust bij Katwijk, Report Rijkswaterstaat, The Hague, The Netherlands.
- Van Alphen, J. (1987) De morfologie en lithologie van de brandingszone tussen Terheijde en Egmond aan Zee., Report Rijkswaterstaat, The Hague.
- Van der Meene, J. W. H. (1994) The Shoreface-connected ridges along the central Dutch coast, PhD thesis. *Nederlands Geografische Studies*, 174, 222.
- Van der Meene, J. W. H., Boersma, J. R. & Terwindt, J. H. J. (1996) Sedimentary structures of combined flow deposits from the shoreface-connected ridges along the central Dutch coast. *Marine Geology*, 131, 151-175.

Van der Molen, J. (2000) Holocene tidal conditions and tide-induced sand transport in the southern North Sea. *Journal of Geophysical Research*.

Van der Spek, A. J. F., Cleveringa, J., Van Heteren, S., Van Dam, R. L. & Schrijver, B. (1999) Reconstructie van de ontwikkeling van de Hollandse Kust in de laatste 2500 jaar, Report NITG-TNO, Utrecht.

Van der Valk, L. (1992) Mid- and Late- Holocene coastal evolution in the beach-barrier area of The Western Netherlands. PhD Thesis, Free University, Amsterdam, 235 pp.

Van Rijn, L.C. (1997). Sediment transport and budget on the central coastal zone of Holland. *Coastal Engineering*, 32, 61–90.

Van Straaten, L. M. J. U. (1961) Directional effects of winds, waves and currents along the Dutch North Sea Coast. *Geologie en Mijnbouw*, 40, 333-346 & 363-391.

Van Straaten, L. M. J. U. (1965) Coastal barrier deposits in South- and North-Holland, in particular in the areas around Scheveningen and IJmuiden. *Mededelingen van de Geologische Stichting*, 17, 41-76.

## A Appendix A

Using available borehole information we provide a general stratigraphic framework where the new boreholes fit. Available boreholes from DINOloket within and around the three research areas were interpreted in terms of facies (Table A1) and consequently plotted in geological cross sections together with the new vibrocores. Notably, the resolution and the accuracy of analysis of the available boreholes is lower than the new boreholes for what regards the shoreface deposits. This hampers their use for the goal of this project. We distinguished the shoreface, tidal channel and fluvial deposits in the available boreholes based on borehole description, specifically the presence or absence of clay layers, on colour, shell abundance and stratigraphic definition.

	<b>Topm NAP</b>	<b>Bottom NAP</b>	<b>facies</b>	<b>Formation</b>
BM110079	-20	-23	Shoreface	
	-23	-31	tidal channel	
	-31	-32	delta	Eem
BM110077	-17.9	-19.9	Shoreface	
	-19.9	-24.9	tidal channel	
	-24.9	-29.9	delta	Eem
BM110074	-9.2	-21.2	tidal channel	
BM080105	-20.8	-23.3	Shoreface	
	-23.3	-29.8	tidal channel	
	-29.8	-32.8	delta	Eem
BQ140008	-11.9	-12	Shoreface	
	-12	-19.2	tidal channel	
	-19.2	-40.19	Fluvial	Kreftenheye
BQ130391	-16.95	-18	Shoreface	
	-18	-21.75	Fluvial	Kreftenheye
BQ130390	-17.6	-19.4	Shoreface	
	-19.4	-22.2	Fluvial	Kreftenheye
BQ130207	-16.5	-17	Shoreface	
	-17	-18.7	tidal channel	
	-18.7	-20.9	Fluvial	Kreftenheye
BQ130168	-18.6	-19.5	Shoreface	
	-19.5	-22.15	tidal channel	
	-22.1	-22.6	Fluvial	Kreftenheye
BQ130124	-16.9	-19.9	Shoreface	
	-19.9	-26.9	Fluvial	Kreftenheye
BQ130118	-20.3	-25.3	Shoreface	
	-25.3	-30.3	Fluvial	Kreftenheye
BQ130113	-19.4	-21.4	Shoreface	
	-21.4	-29.4	Fluvial	Kreftenheye

Table A1 Facies interpretation of the boreholes from DINOloket

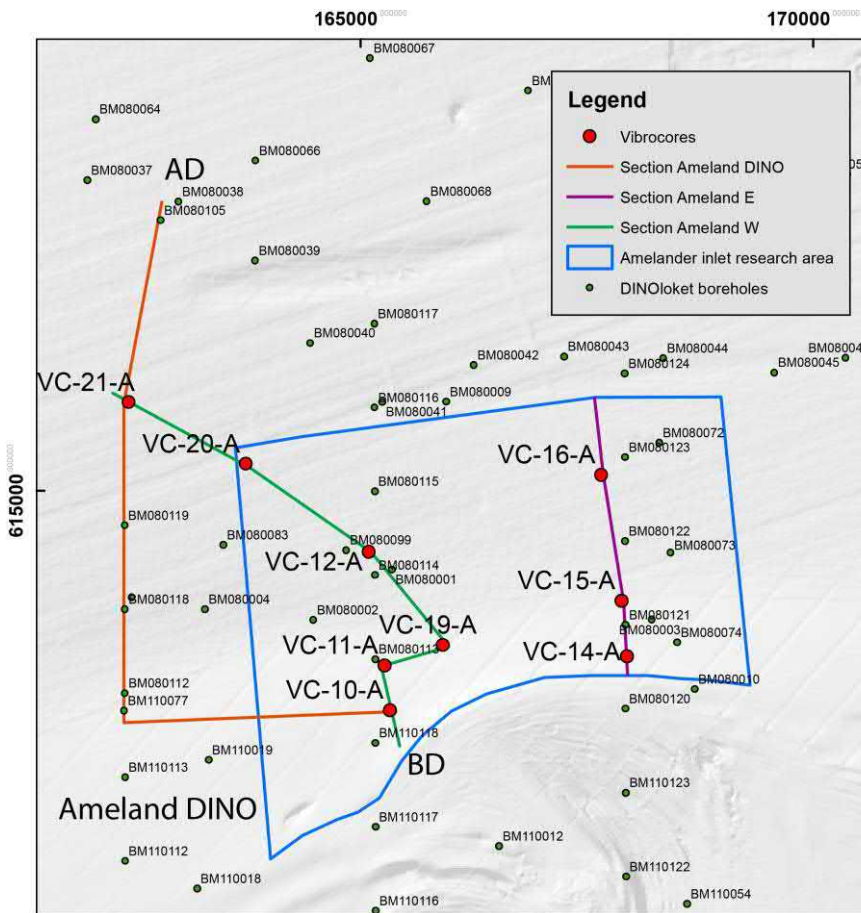


Figure A1 Overview of the geological cross sections in the Amelander Inlet research area.

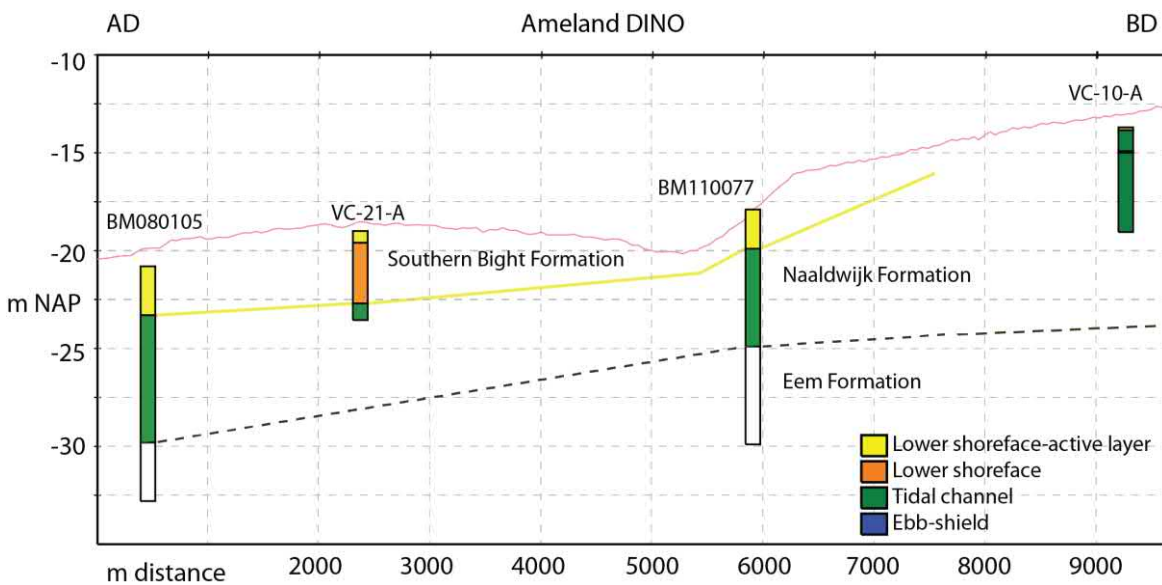


Figure A2 Geological section Ameland DINO, including three boreholes from DINOloket. This section, which includes two boreholes from DINOloket, shows that the Holocene sediment package has a maximum thickness of 7-10 m. The tidal deposits of the Eem Formation lie below the Holocene sediments. The boundary between the two units dips northwards.

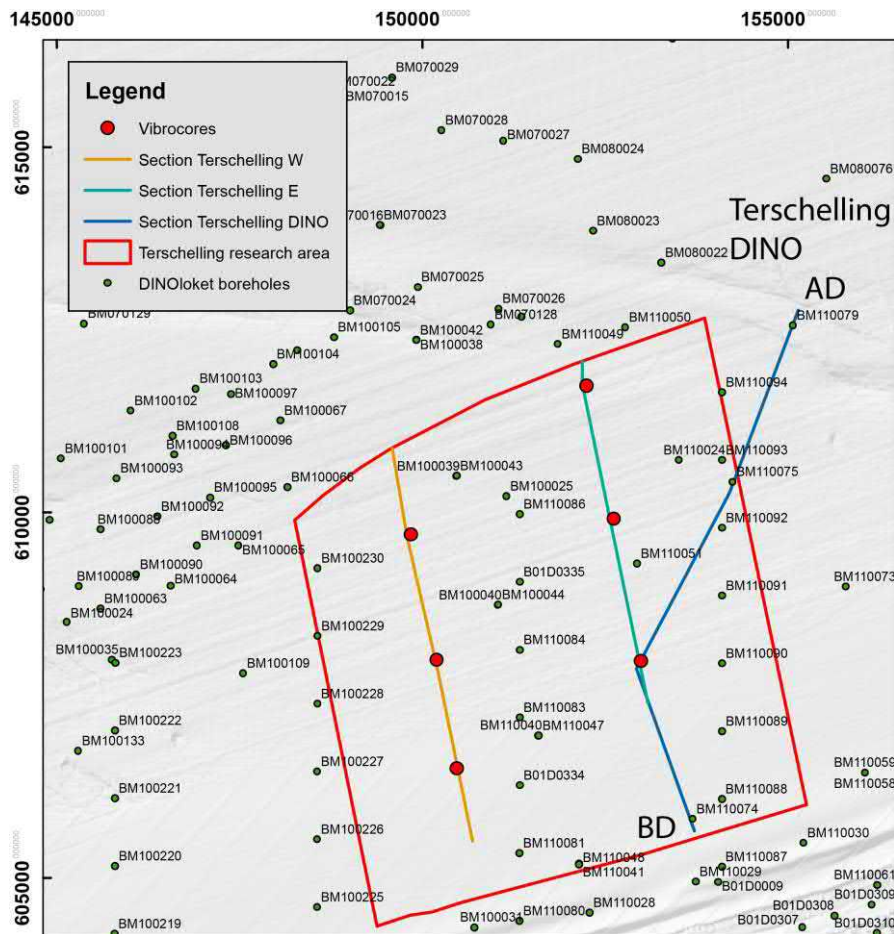


Figure A3 Overview of the geological cross sections in the Terschelling research area.

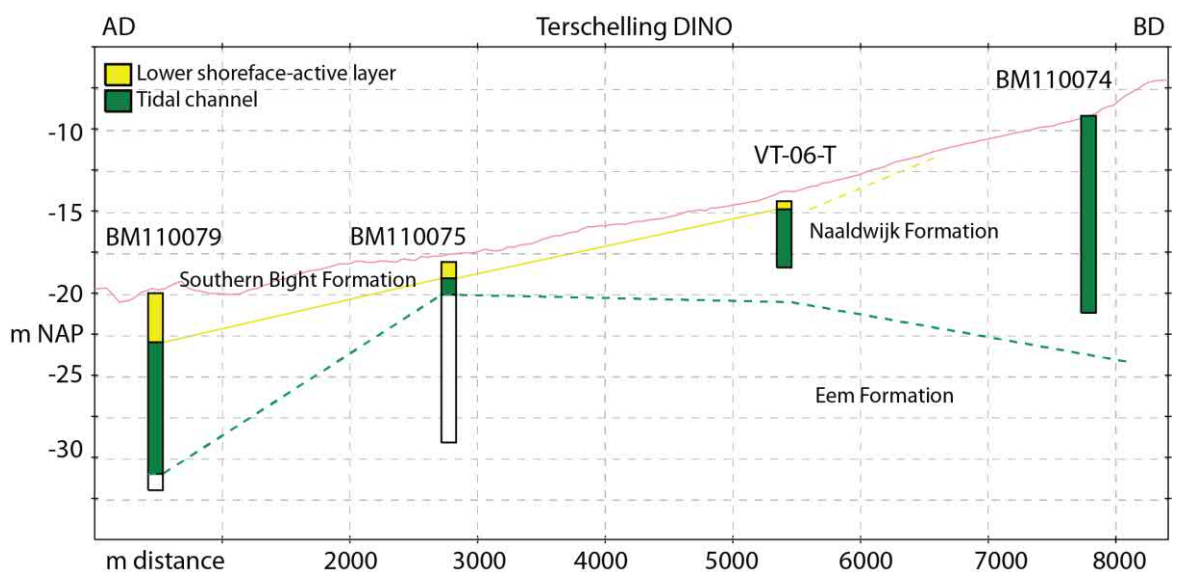


Figure A4 Geological section Terschelling DINO, including three boreholes from DINOloket. This section, which includes three boreholes from DINOloket, shows that the tidal channel deposits thickness varies in the study area from 1 to 15m and that it is underlain by older tidal deposits (Eem formation).



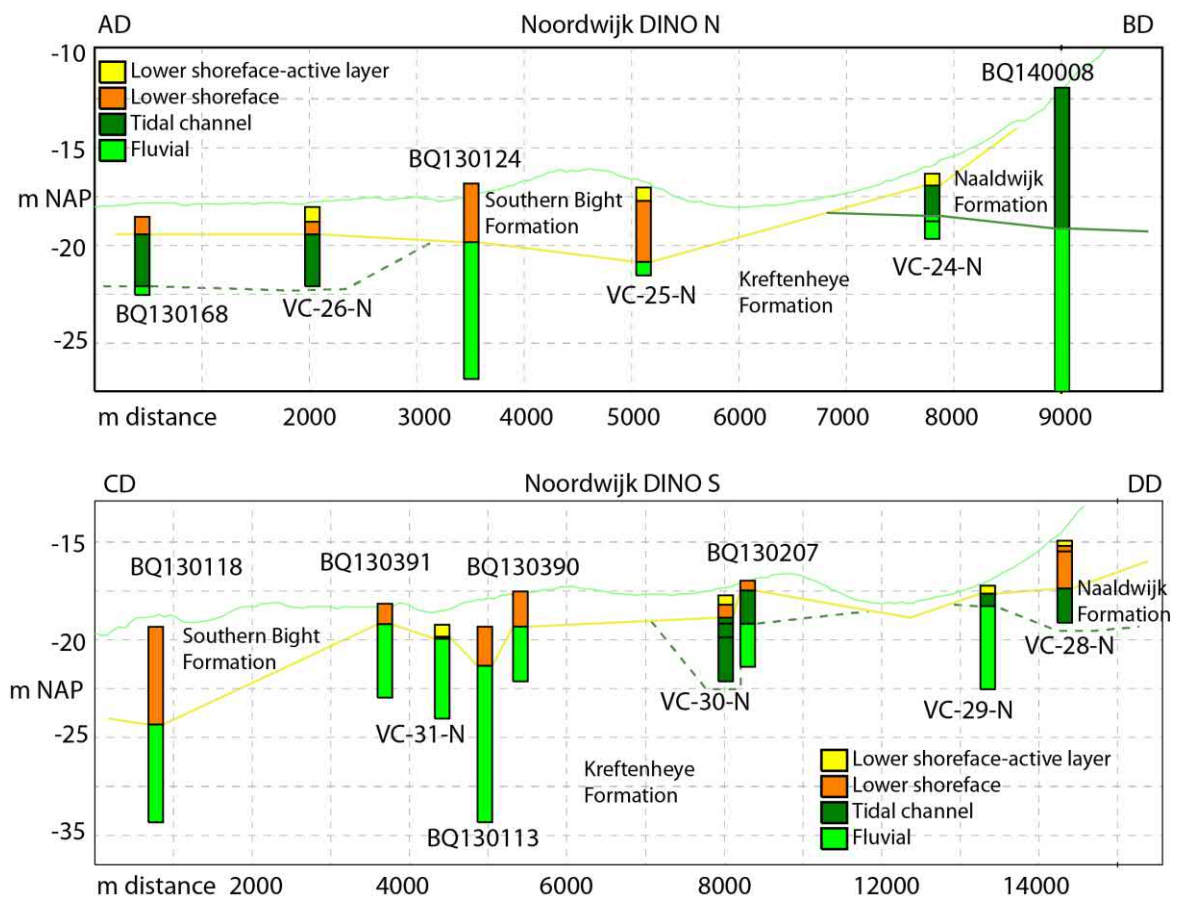


Figure A6 Geological profiles in the Noordwijk research area including boreholes from DINOloket. These two sections highlight the local presence of tidal channel deposits and the large thickness variation of shoreface deposits.

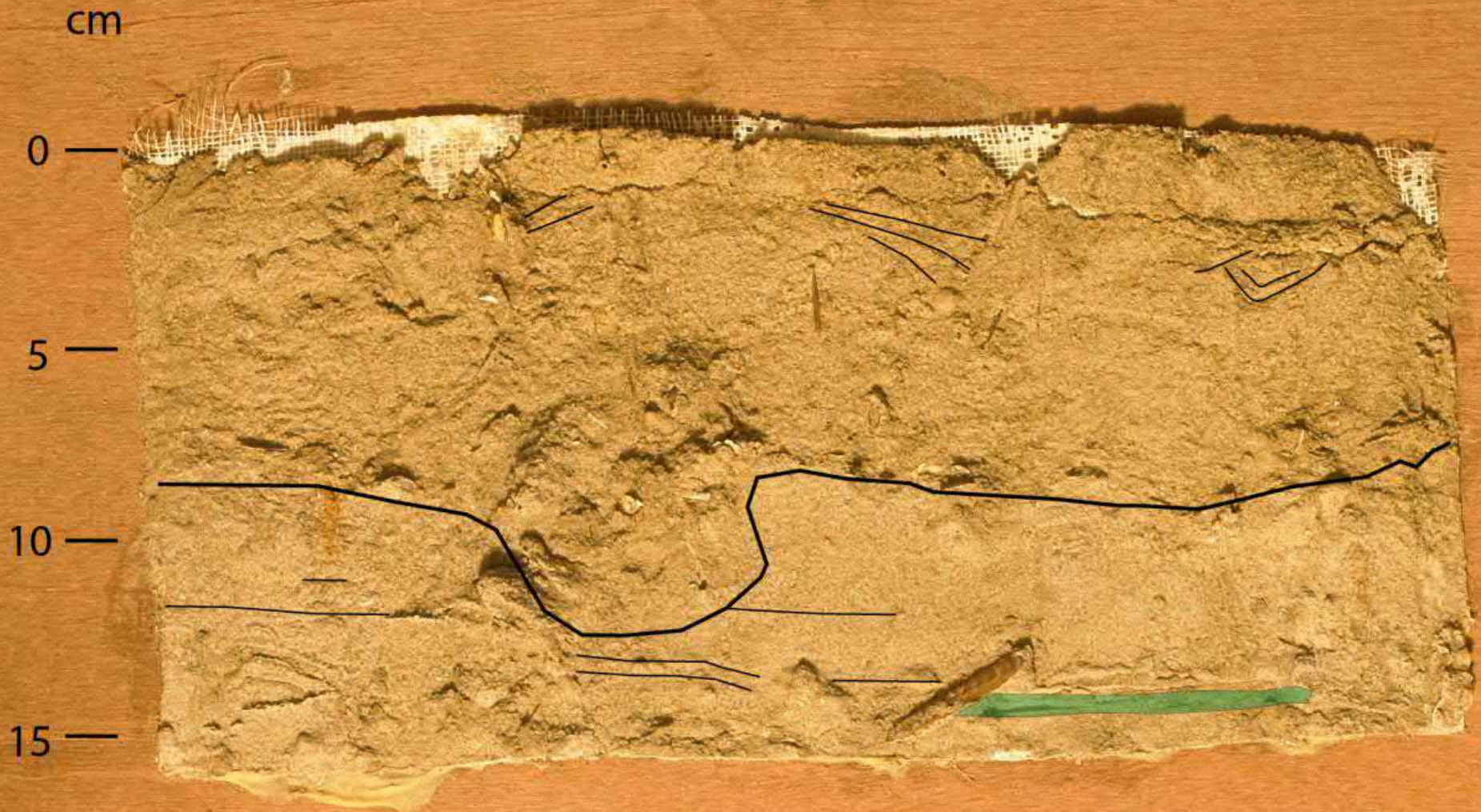


## **B Appendix B**

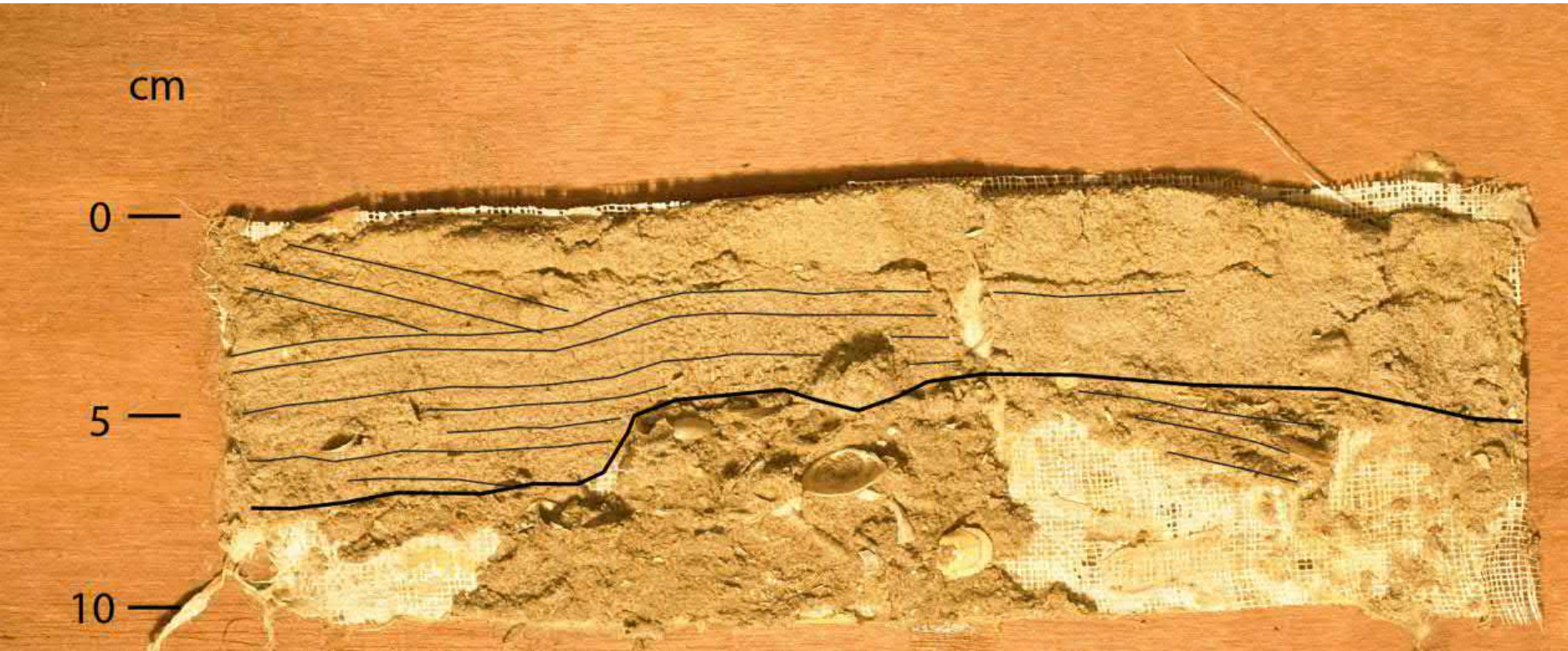
# Appendix B

Lacquer profiles from the rectangular  
boxcores taken on the deeper  
shoreface in 2018

# Boxcore AM02



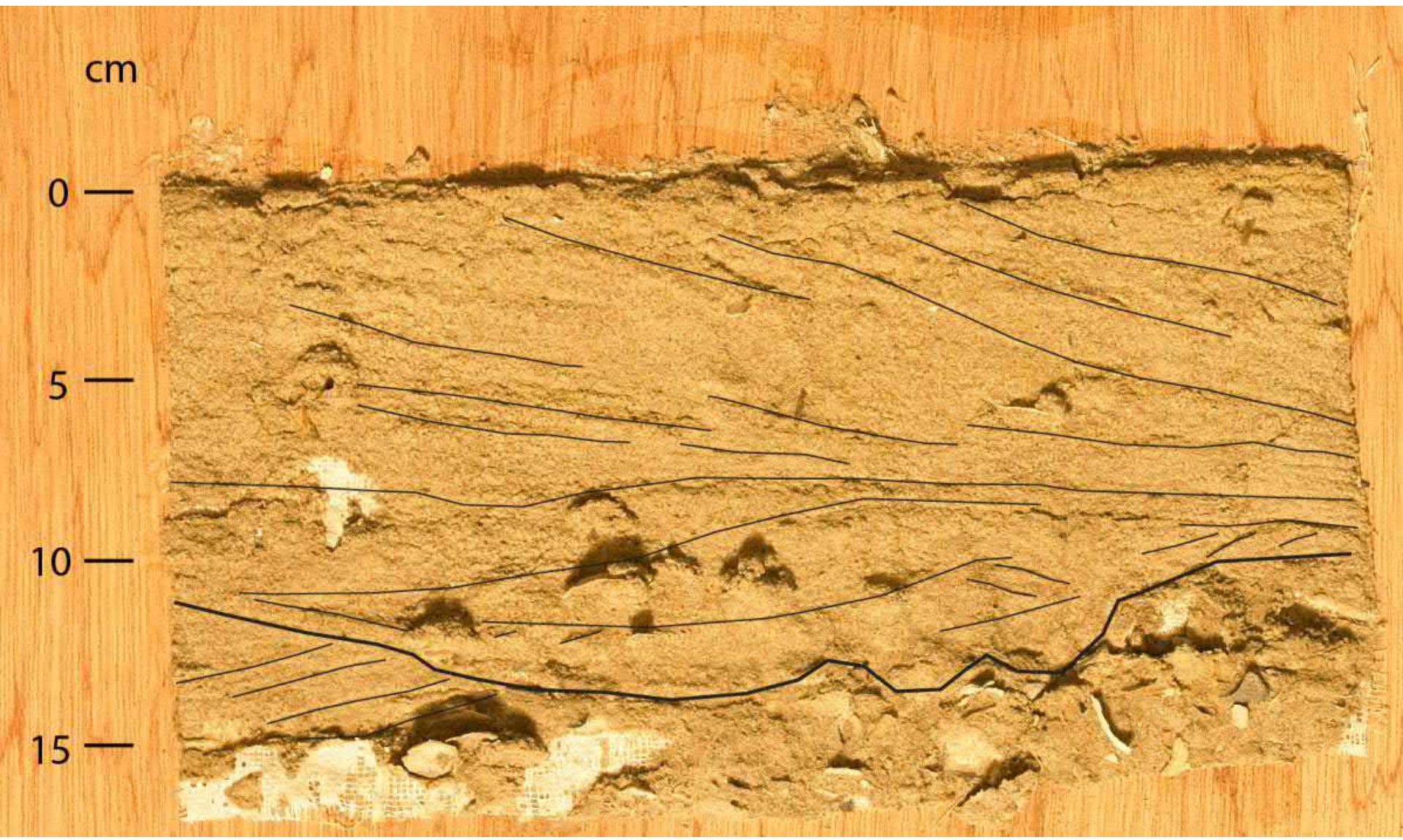
# Boxcore AM03



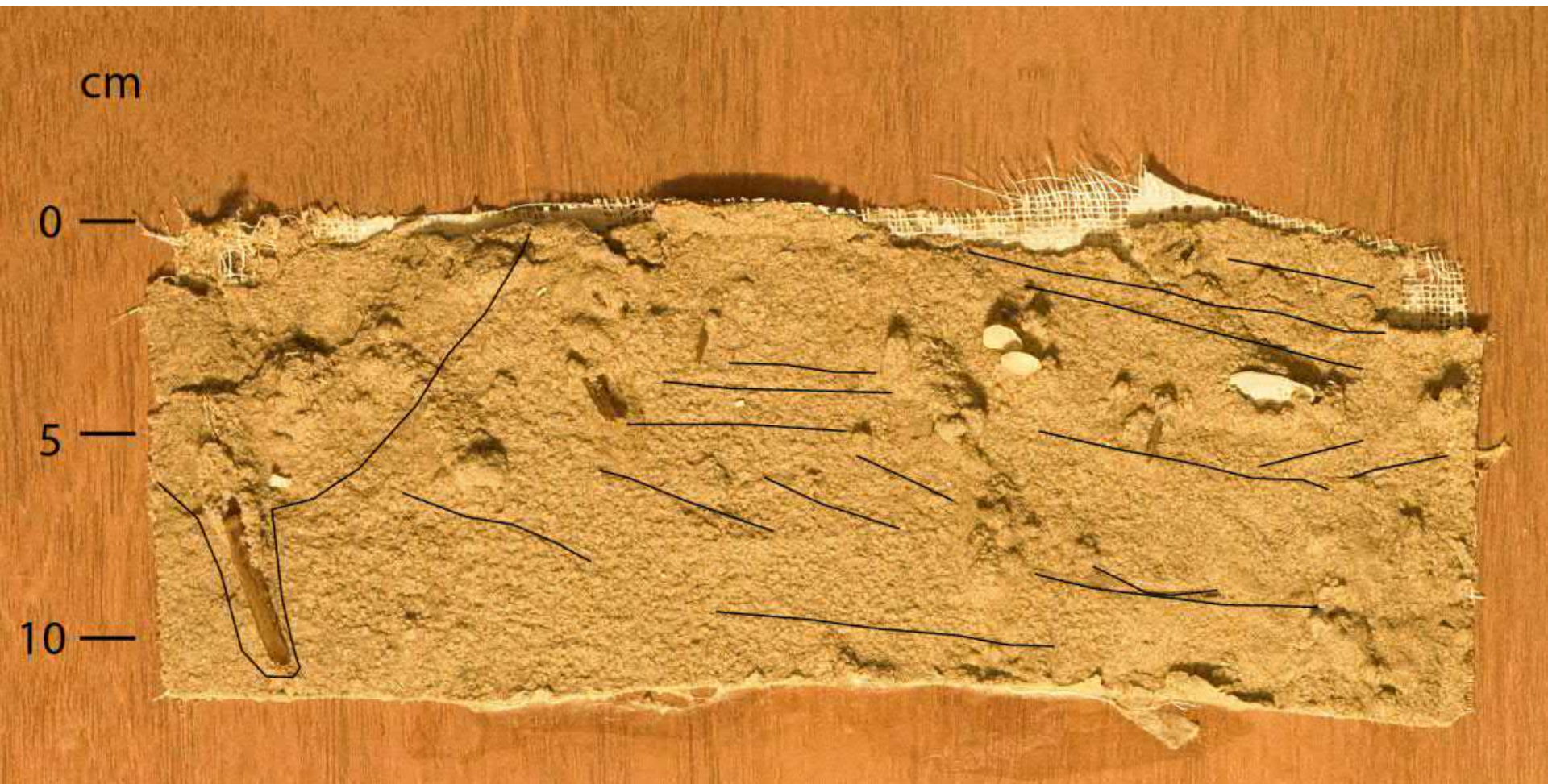
# Boxcore AM04



# Boxcore AM05



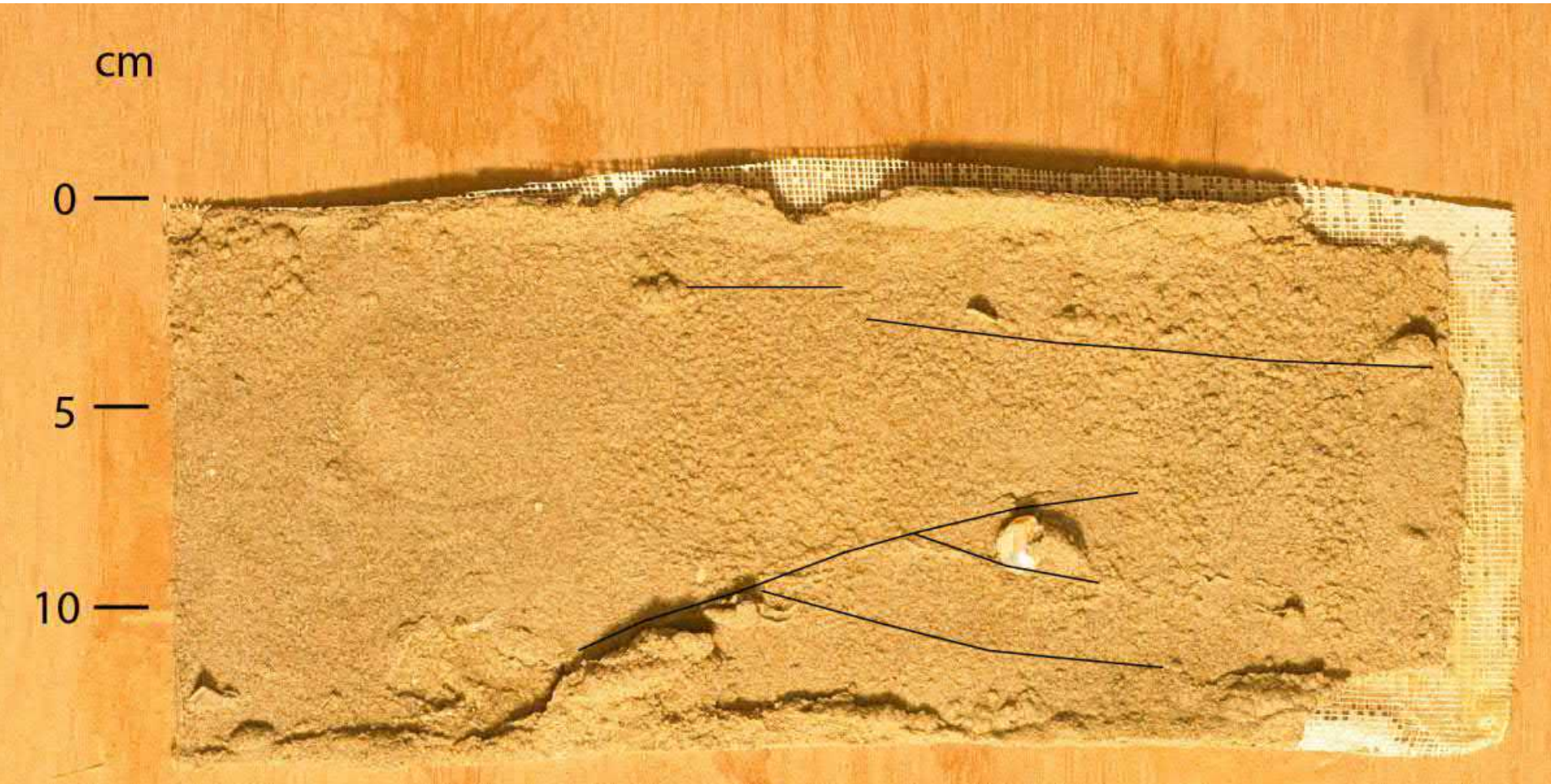
# Boxcore AM06



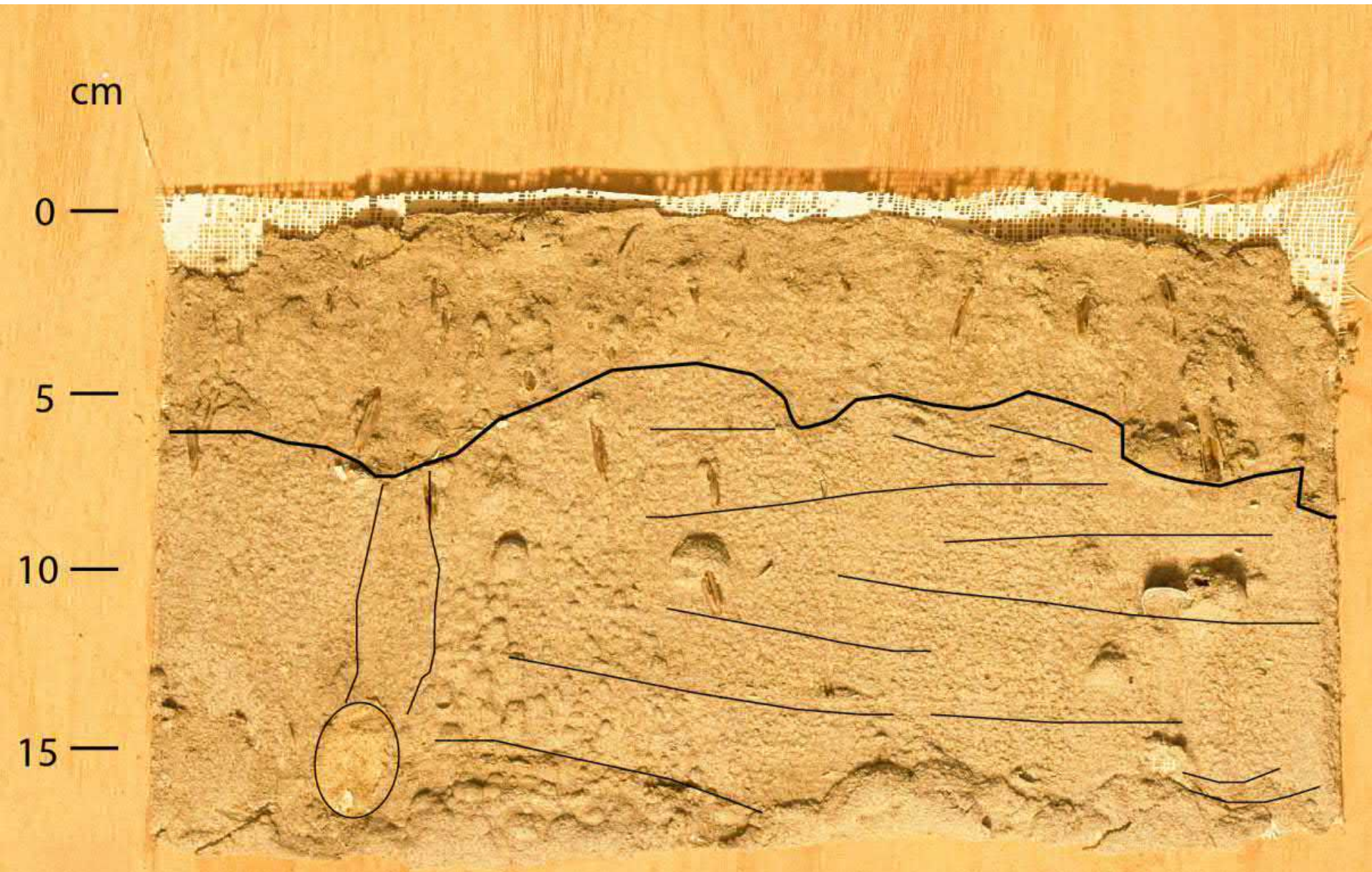
# Boxcore AM07



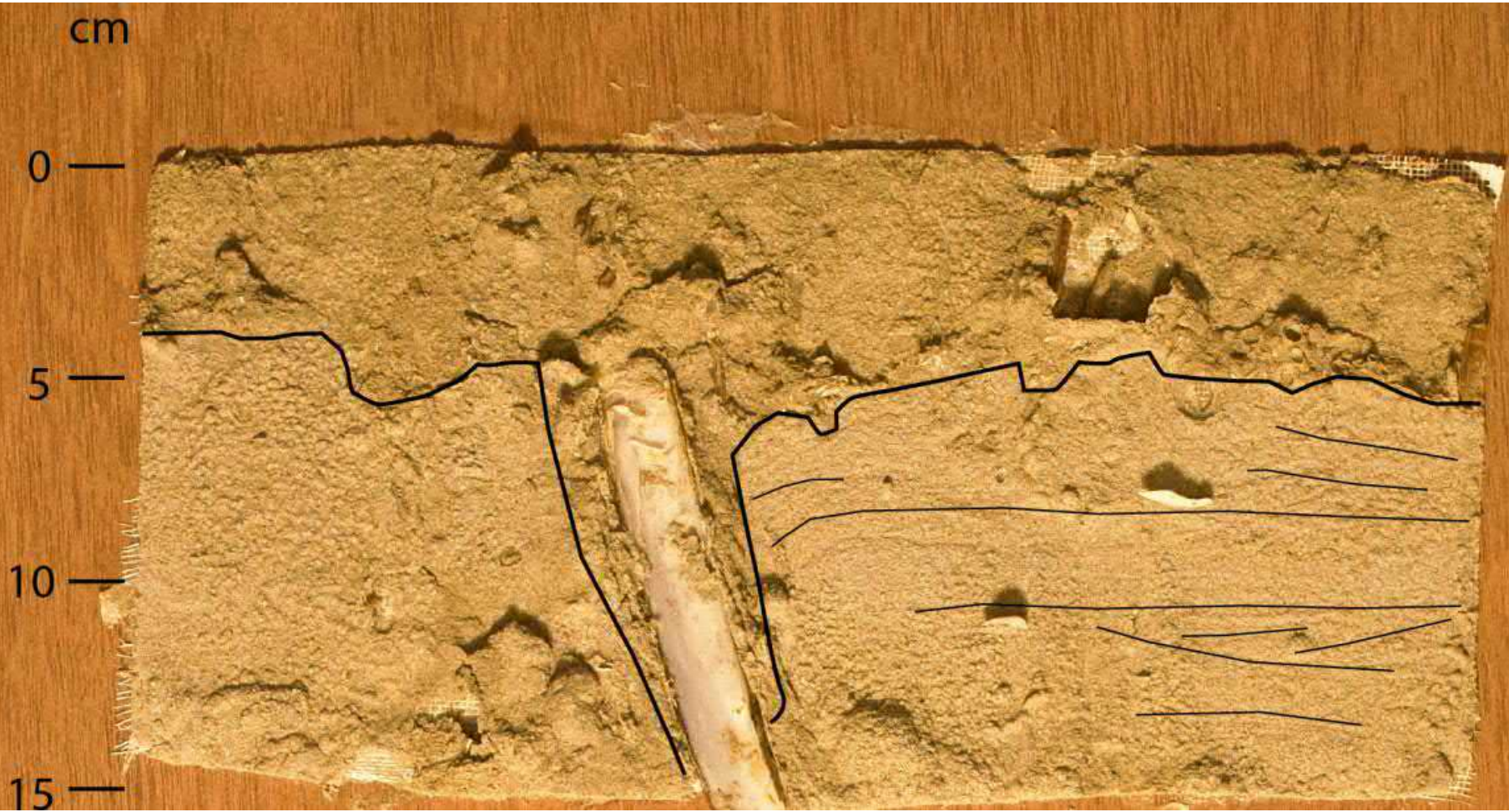
# Boxcore AM08



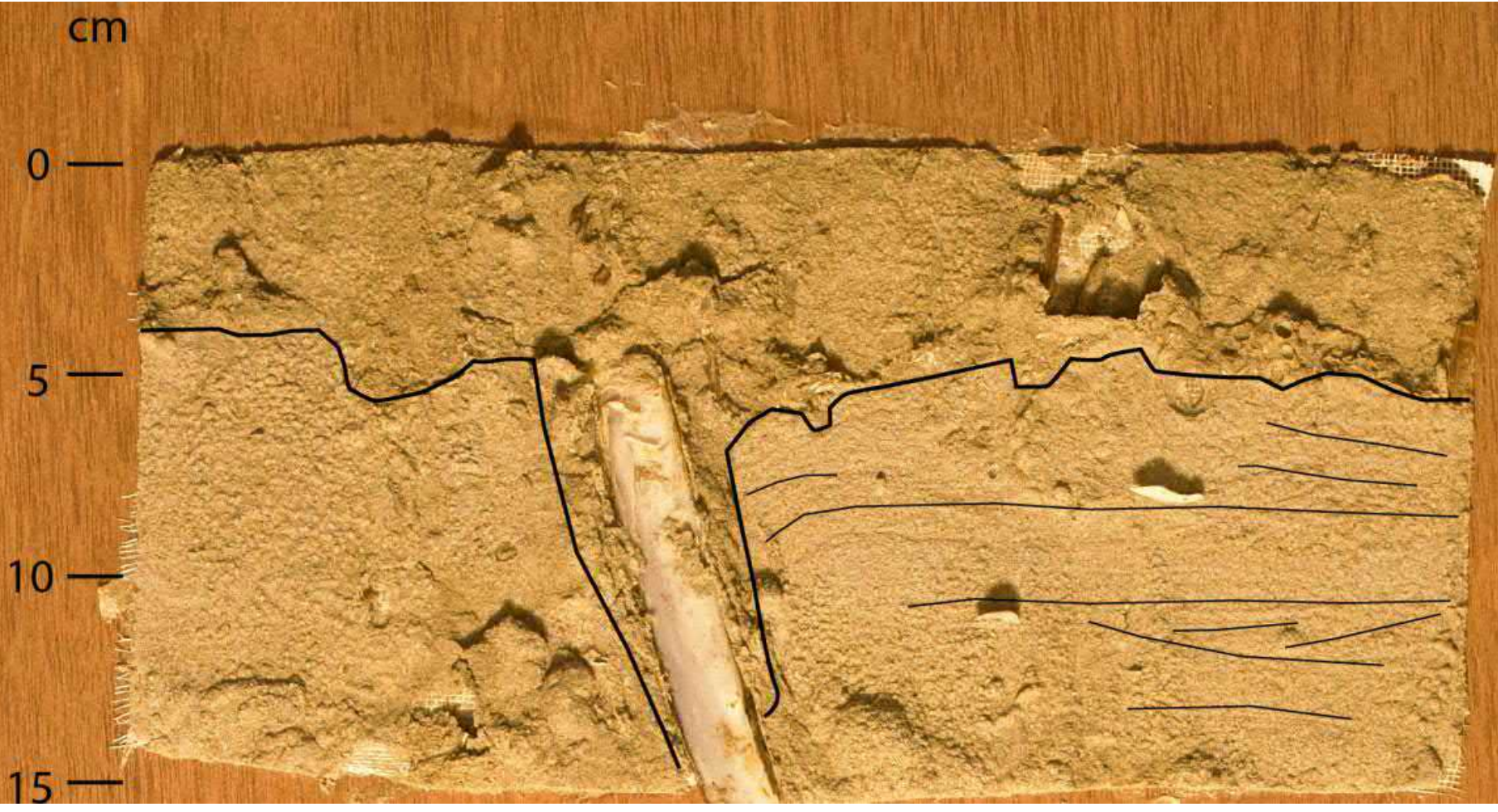
# Boxcore AM10



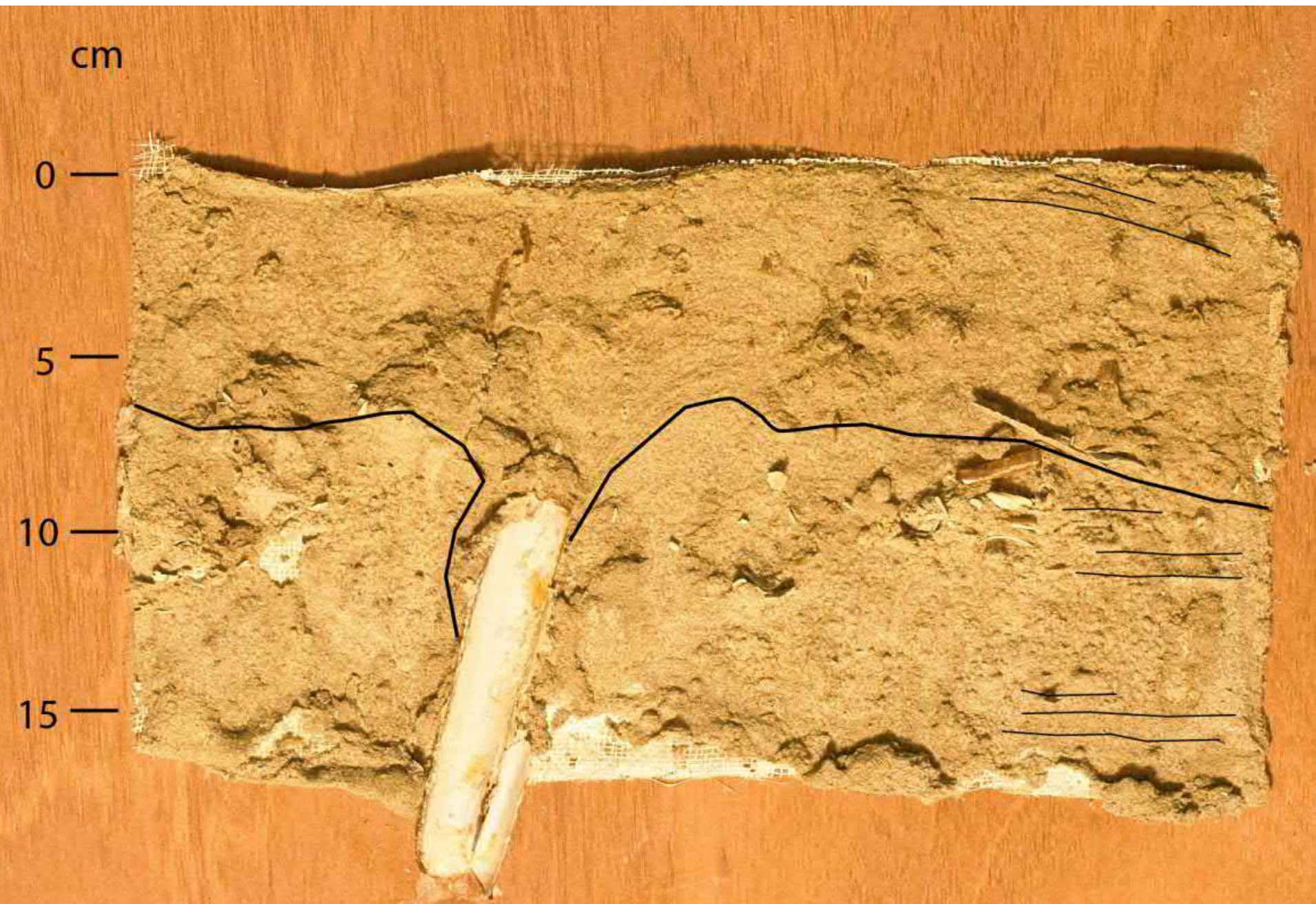
# Boxcore AM11



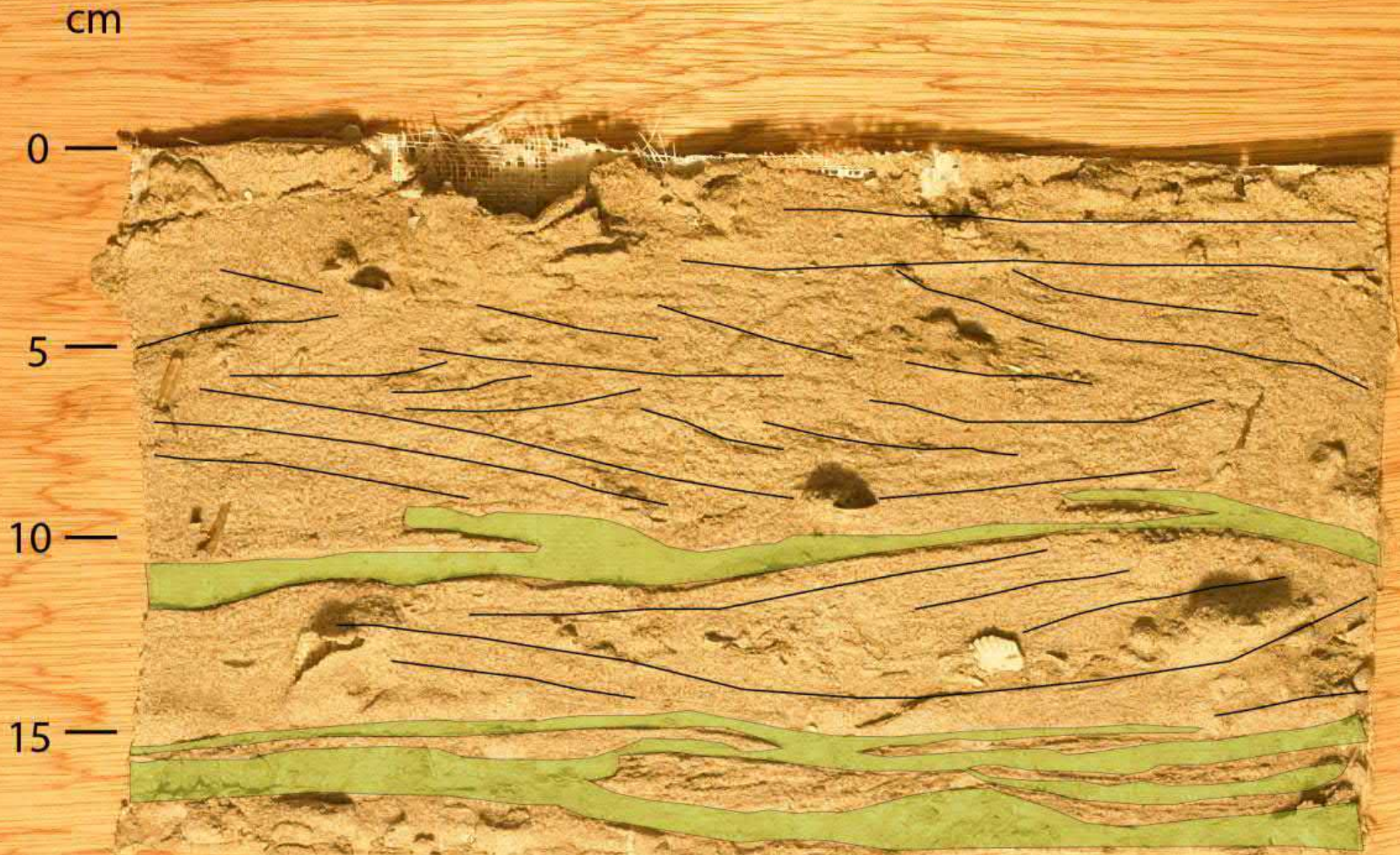
# Boxcore AM11



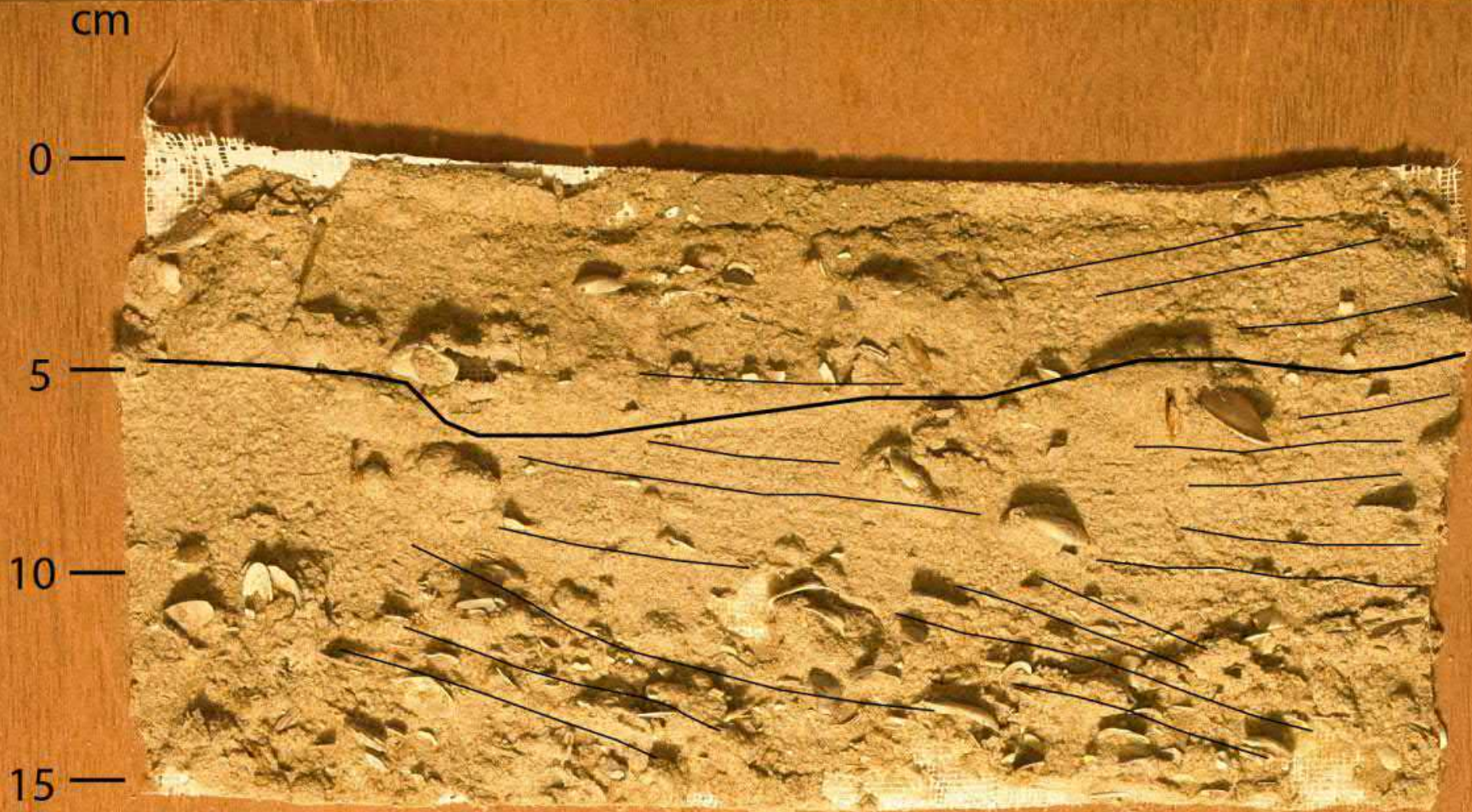
# Boxcore AM13



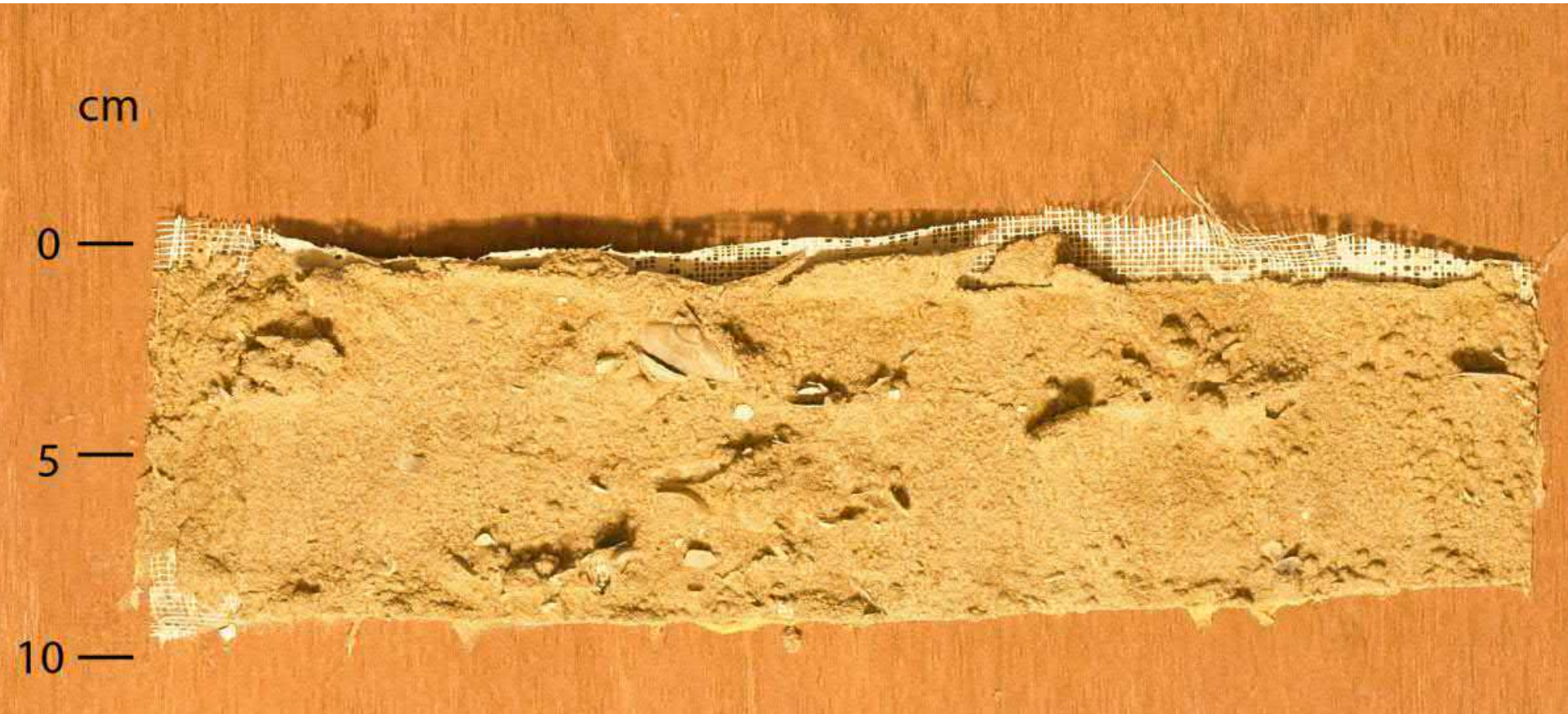
# Boxcore AM14



# Boxcore AM15



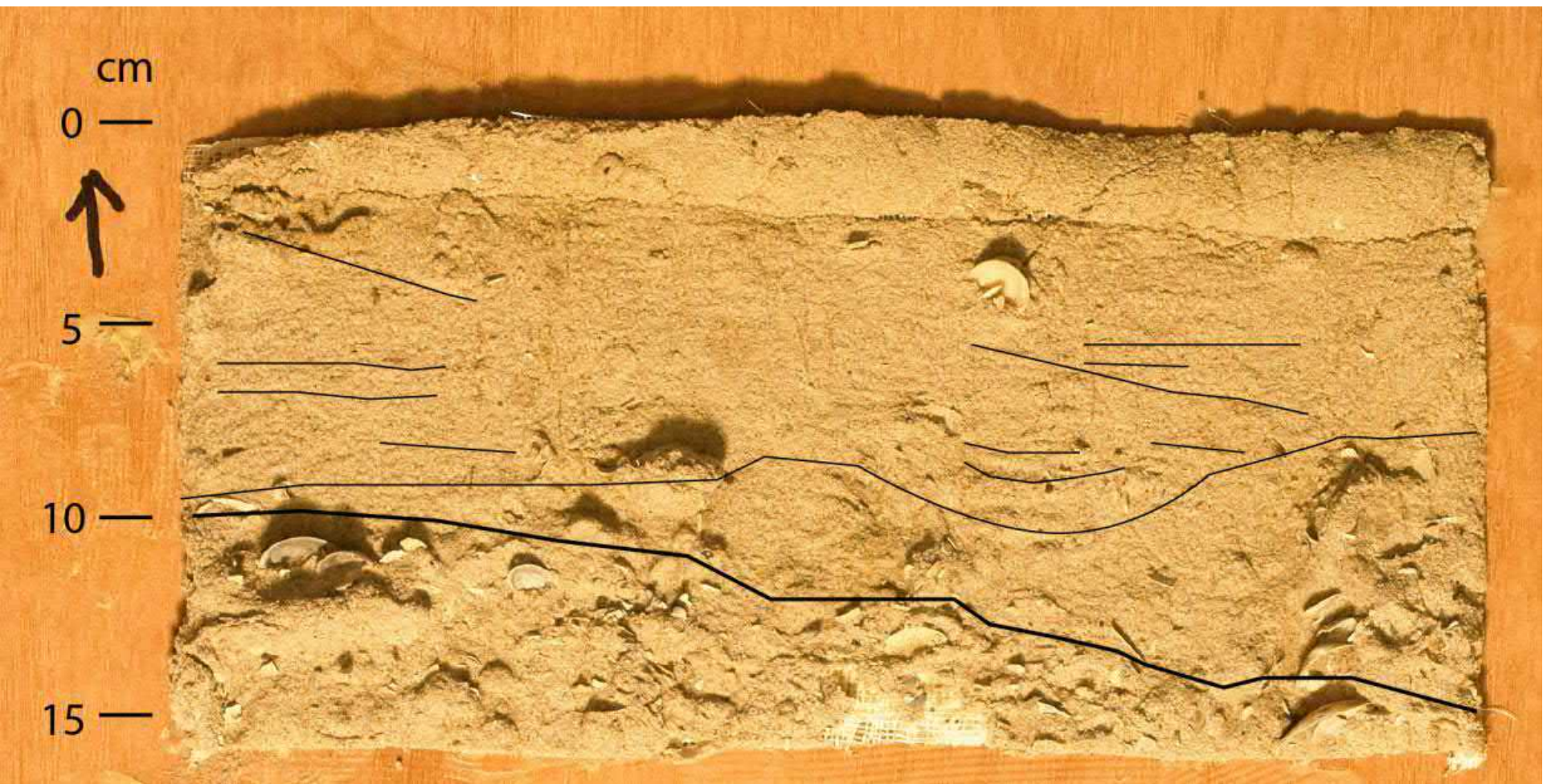
# Boxcore AM16



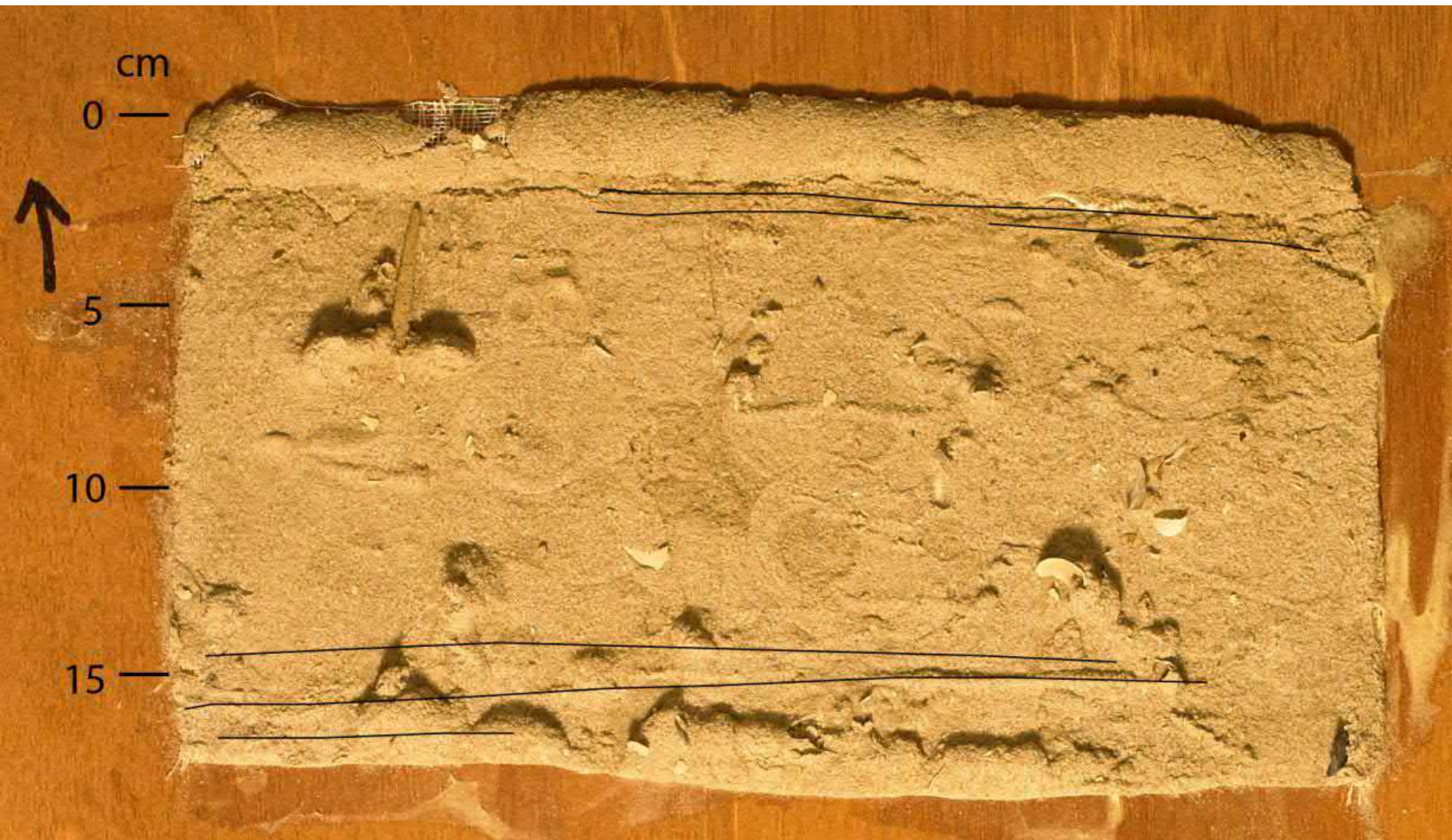
# Boxcore TS01



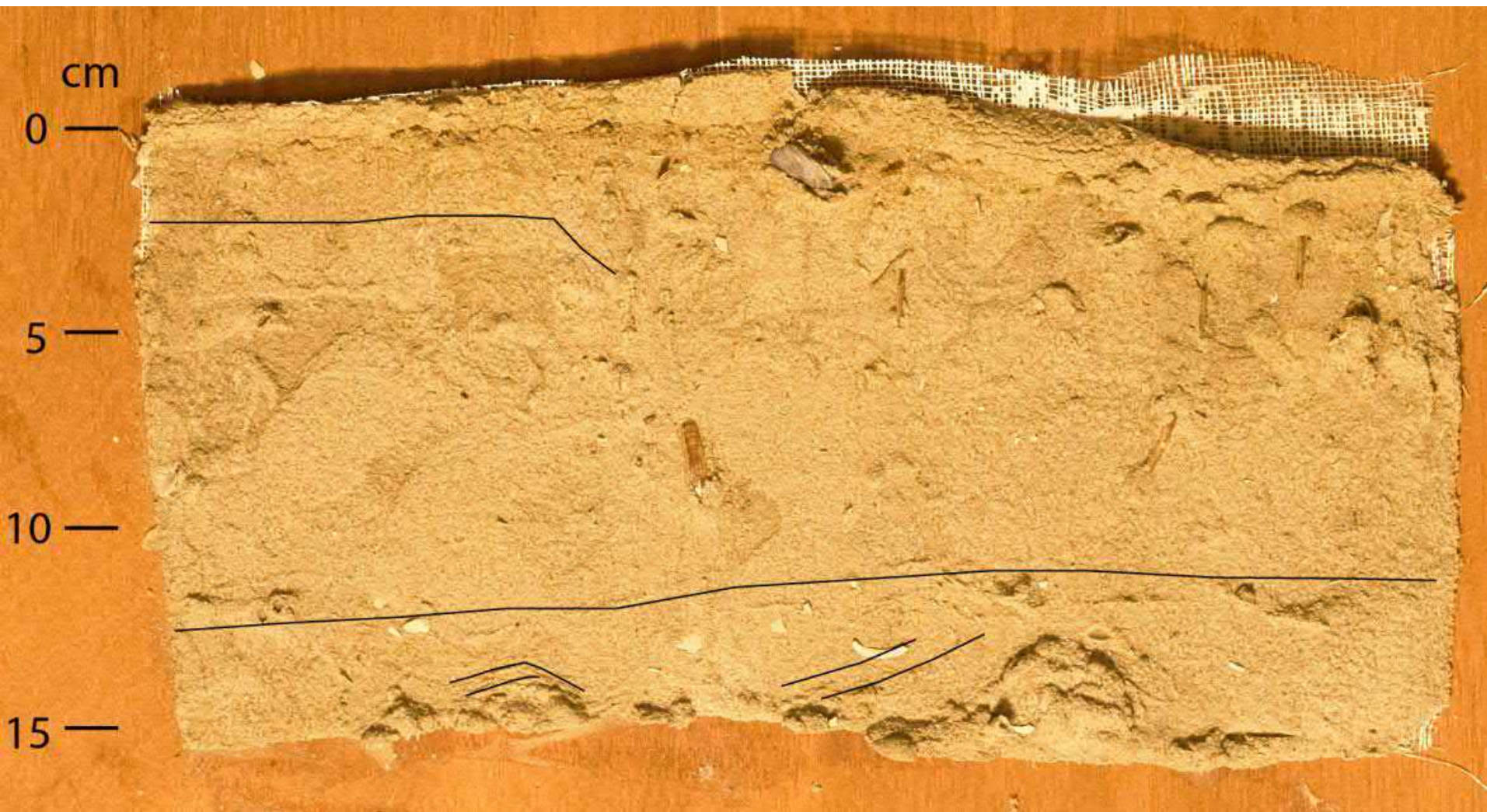
# Boxcore TS02



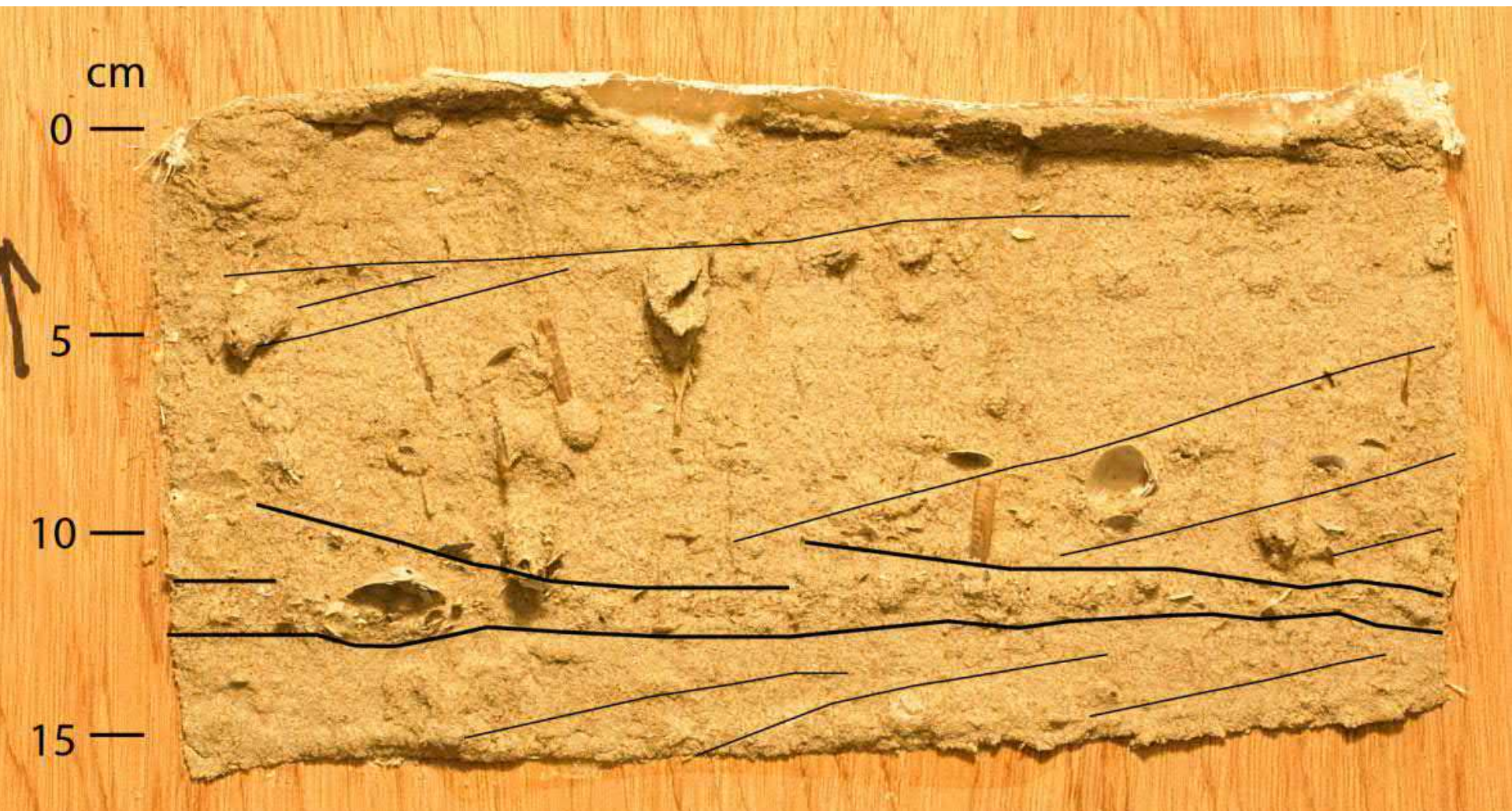
# Boxcore TS03



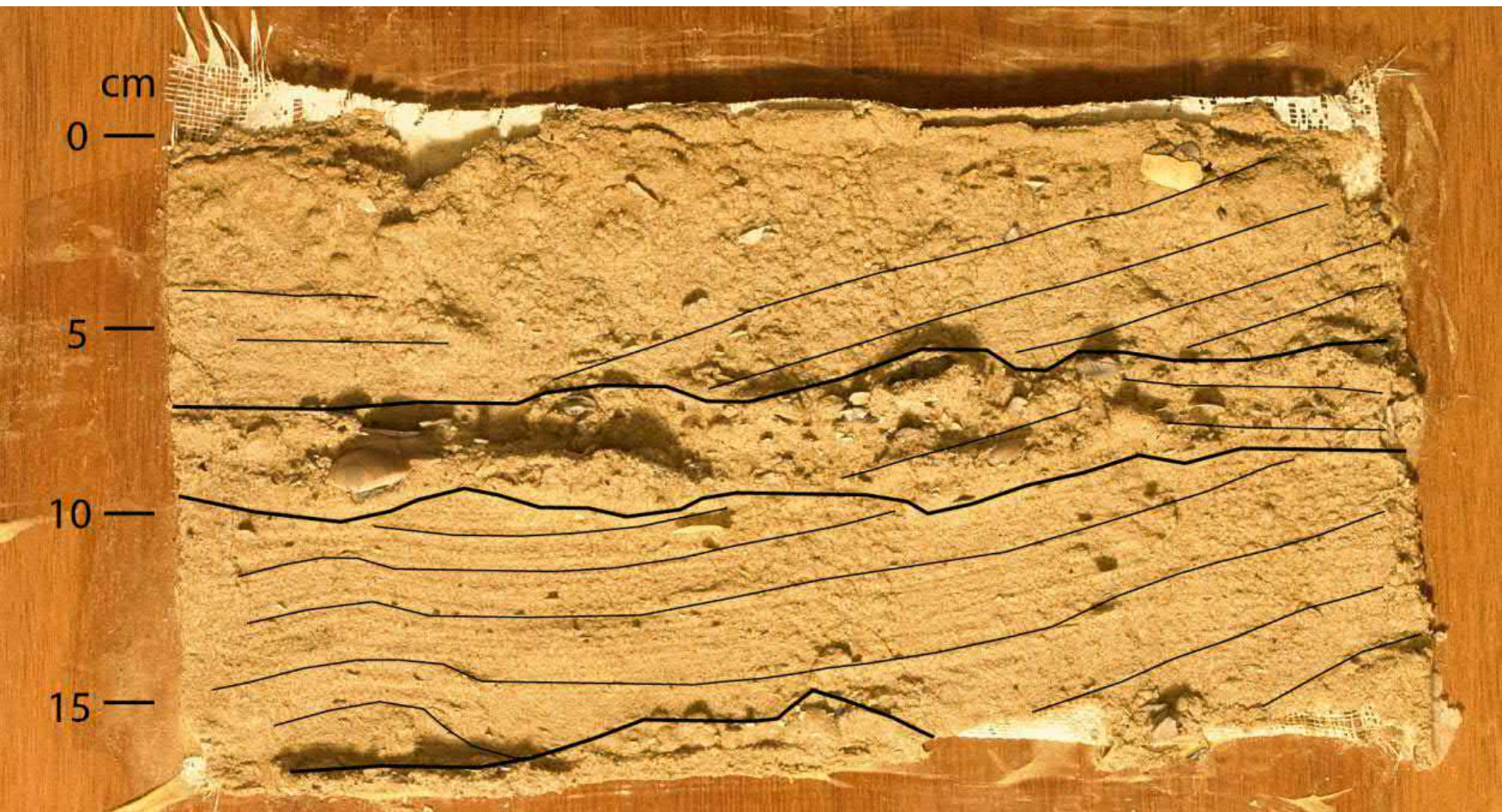
# Boxcore TS07



# Boxcore TS09



# Boxcore TS12



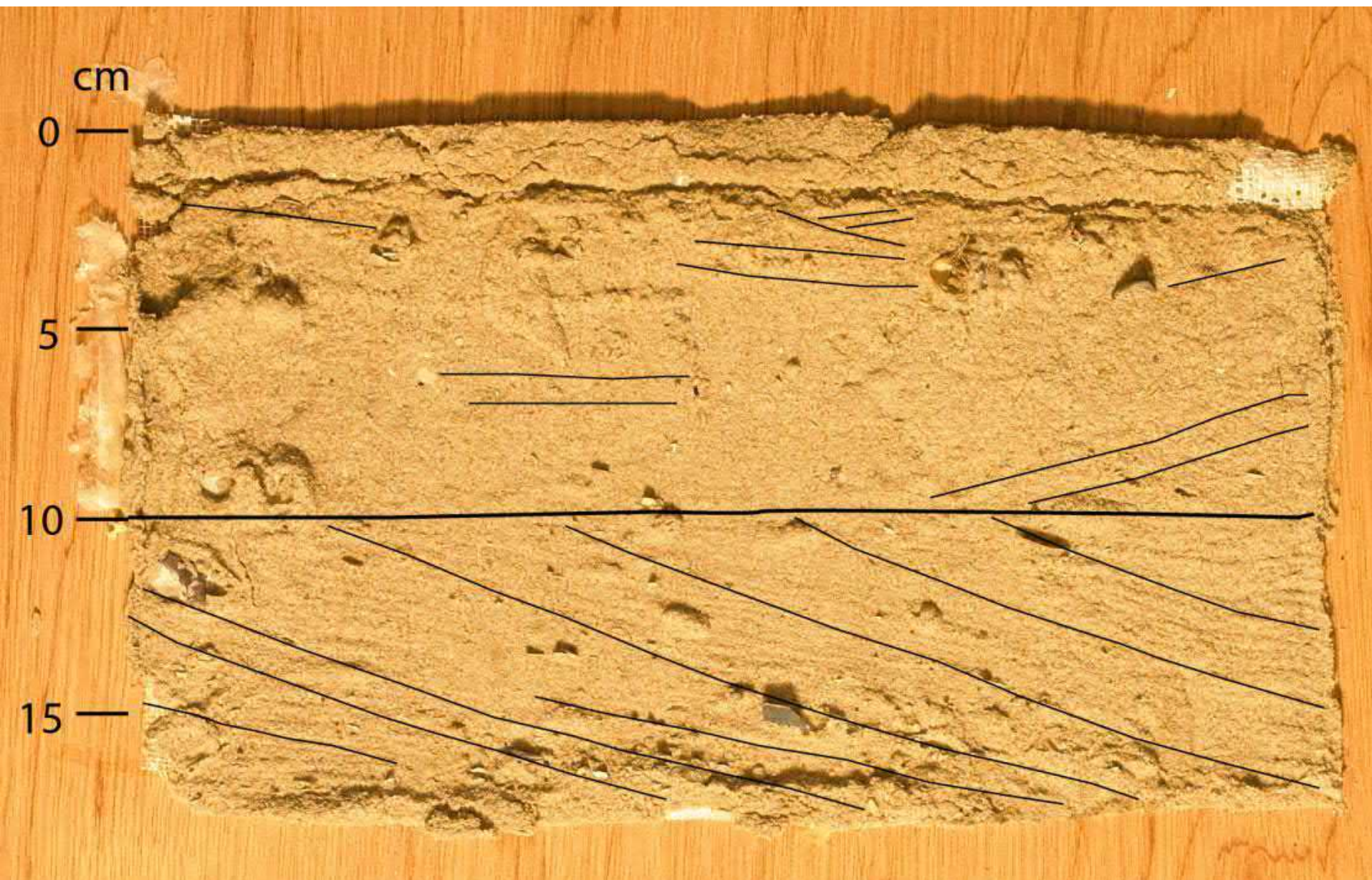
# Boxcore TS13



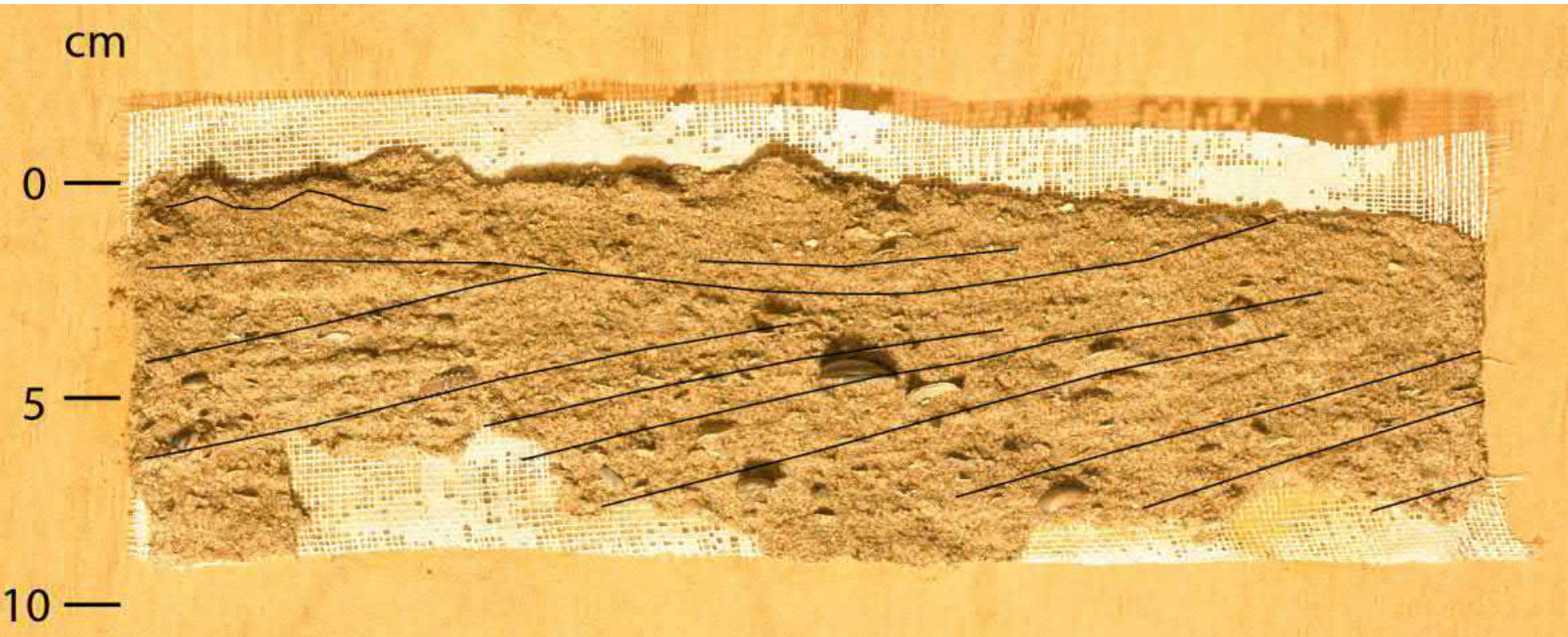
# Boxcore TS14



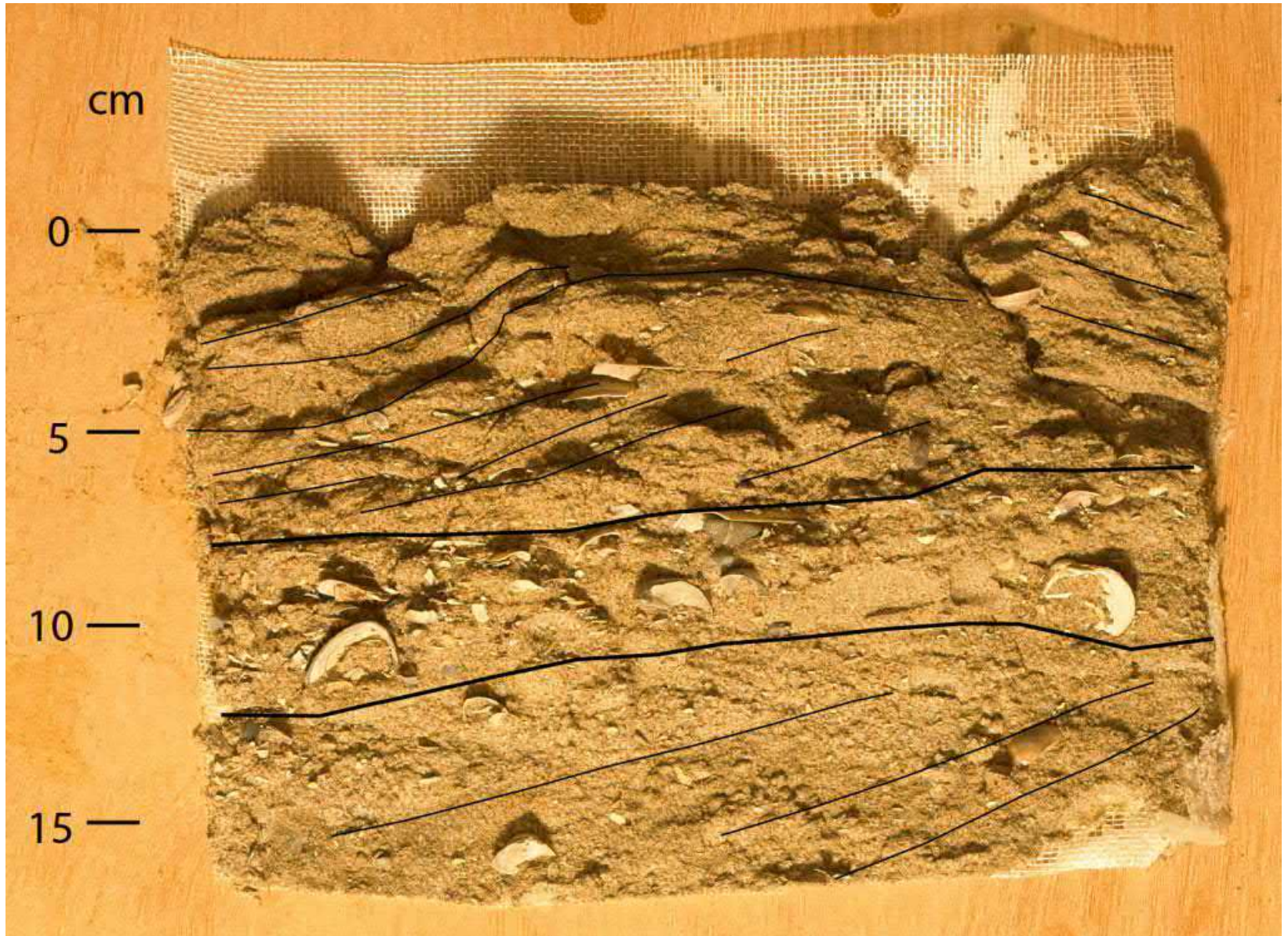
# Boxcore TS15



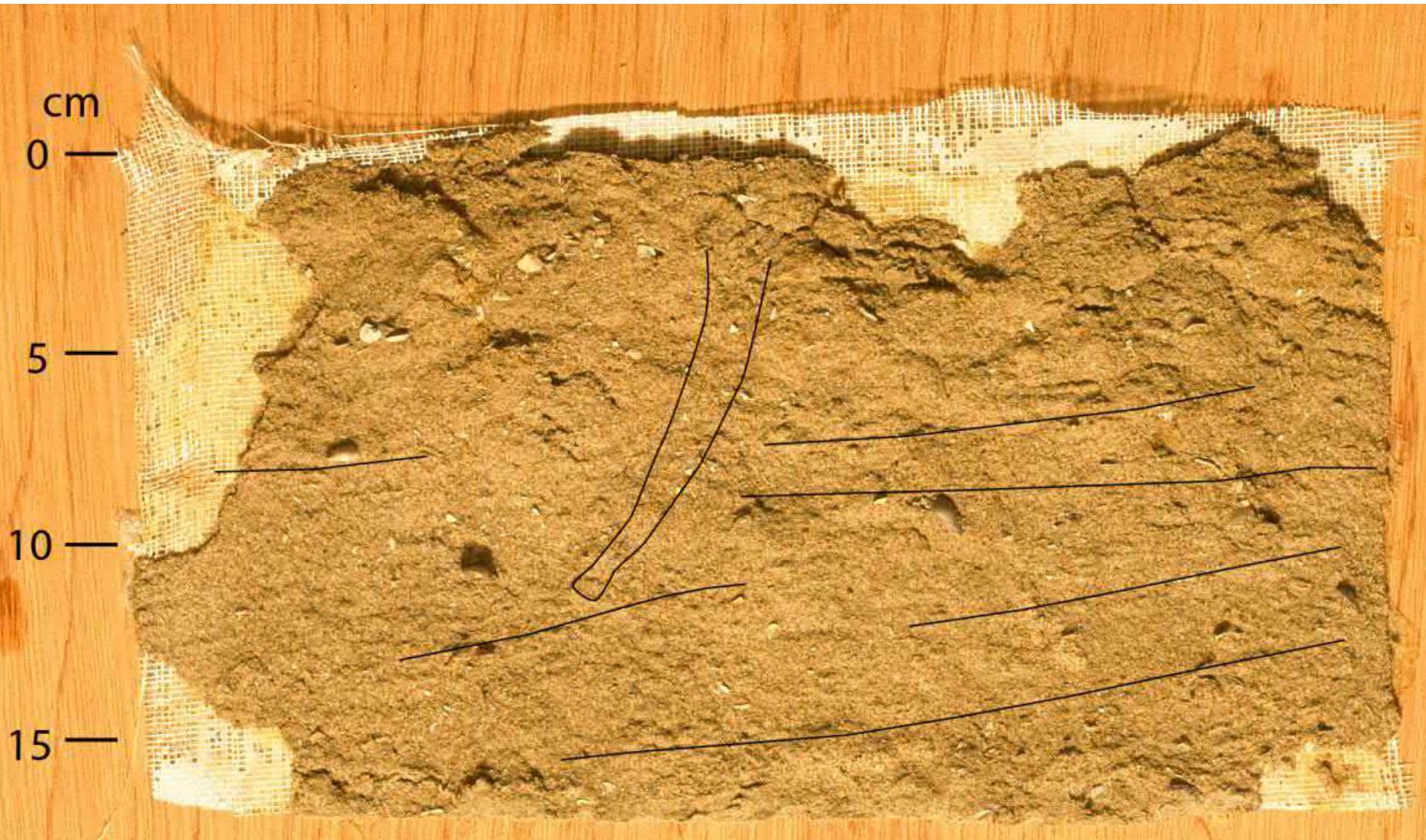
# Boxcore NW01



# Boxcore NW02



# Boxcore NW03



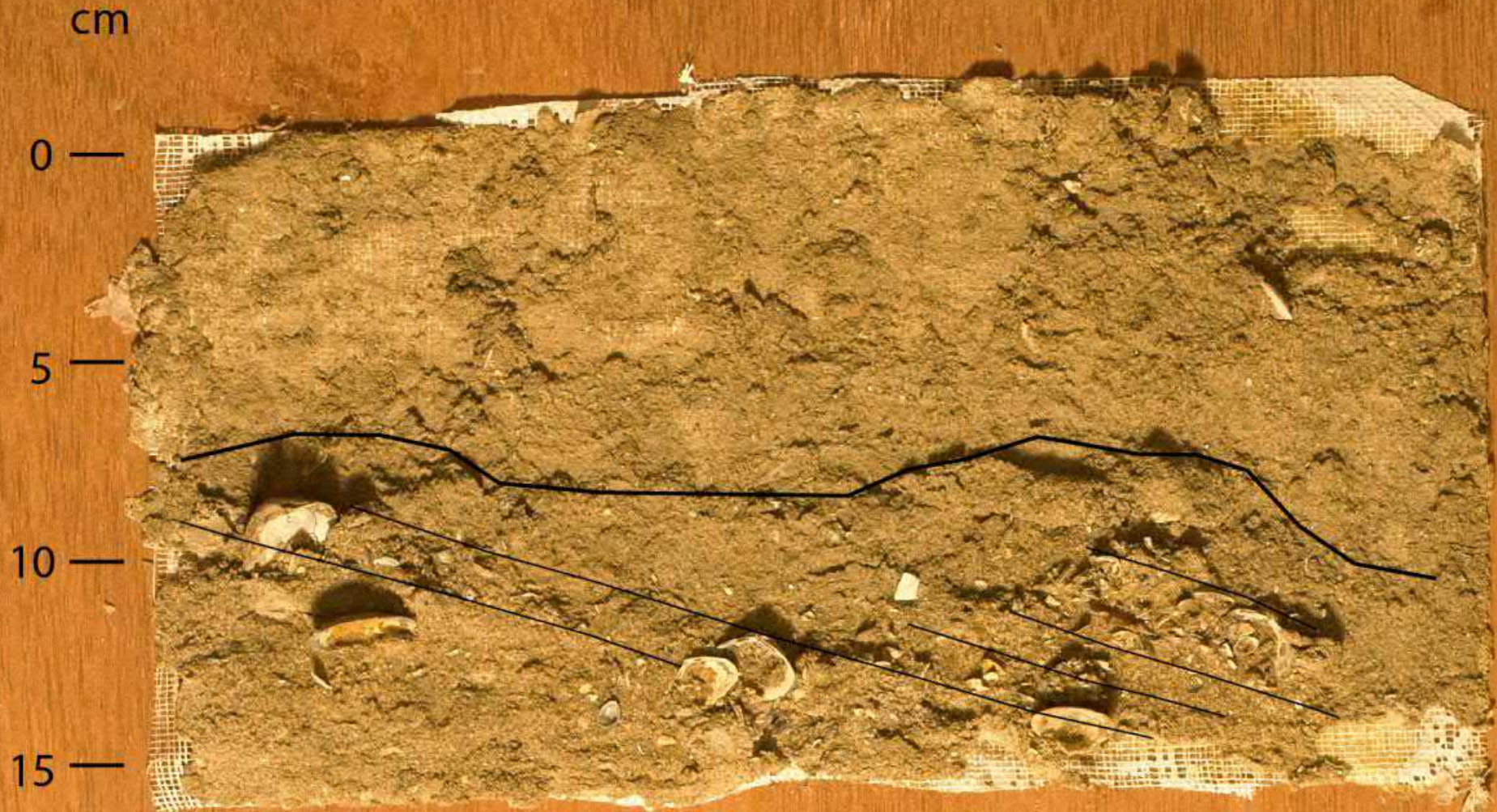
# Boxcore NW04



# Boxcore NW05



# Boxcore NW06



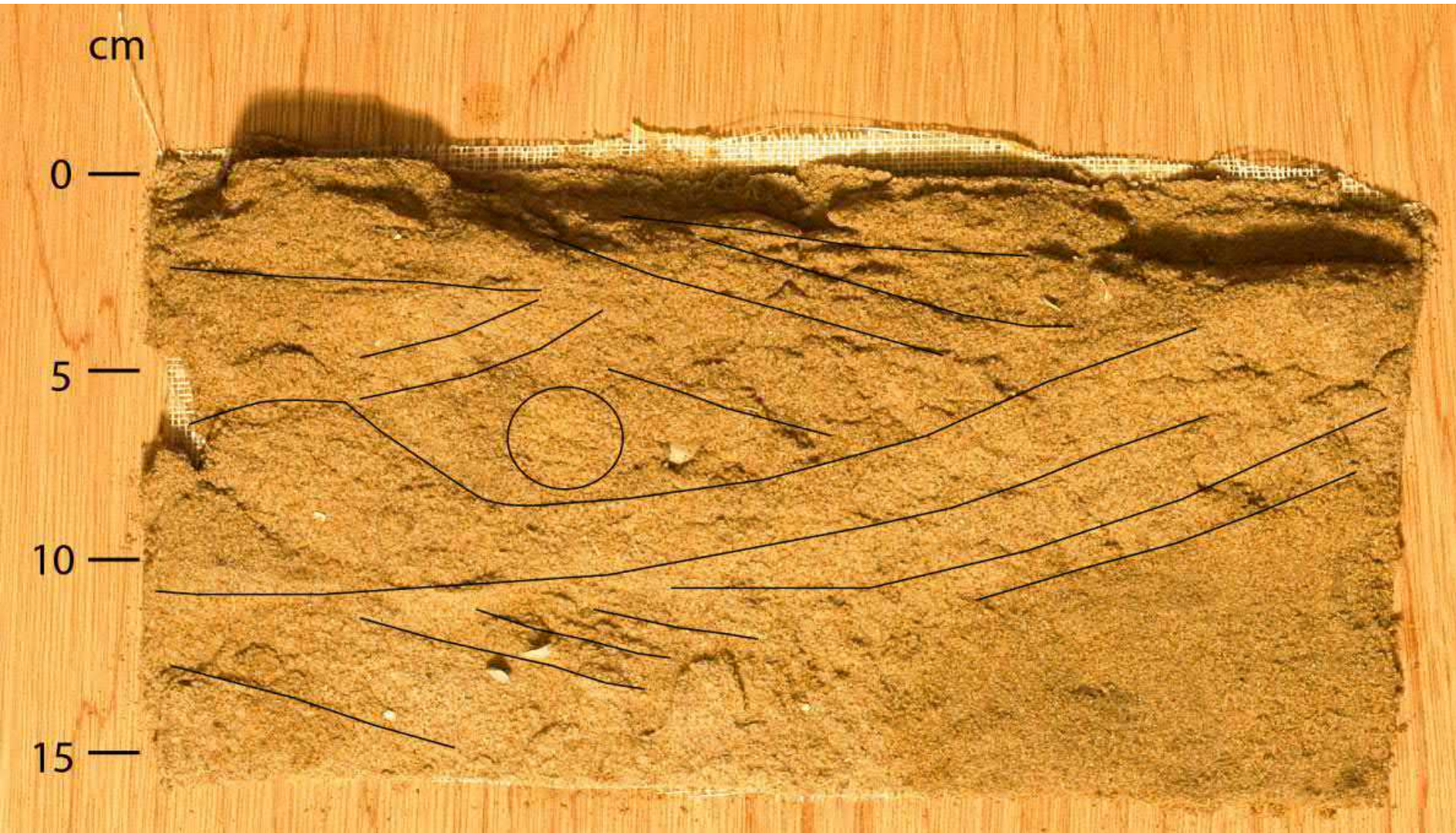
# Boxcore NW10



# Boxcore NW11



# Boxcore NW13



# Boxcore NW14



# Boxcore NW15

